Biological functionalization of polymer membranes

Inauguraldissertation zur

Erlangung der Würde eines Doktors der Philosophie

vorgelegt der

Philosophich-Naturwissenchaftlichen Fakultät

der Universität Basel

von

Caroline FRAYSSE-AILHAS

aus Toulouse, Frankreich

Basel, 2006

Genehmigt von der Philosophich-Naturwissenchaftlichen Fakultät

Auf Antrag der Herren

Prof. Dr. Wolfgang Meier (Universität Basel)

Prof. Dr. Ulrich Schwaneberg (Universität Bremen)

Prof. Dr. Hanspeter Huber (Universität Basel)

Basel, den 03.10.06

"Nanotechnology will bring changes as profond as the industrial revolution, antibiotics, and nuclear weapon all in one".

Eric Drexler, Science (*1991*), 1310.

Table of Contents

Abstract

In Nature, membranes play a crucial role. They maintain the cell integrity toward its environment, and they also separate the different organelles. Through the membranes, many functions are achieved. For example, transport is made through proteins embedded in the membrane; recognition takes also place via the molecules attached to the membrane.

The interest in mimicking membranes exist sine long time ago, with the outlook of taking advantage of membrane functionalities to create nanodevices. For that, different materials can be applied instead of lipids, which lack stability and are difficult to tailor.

In this work amphiphilic block copolymers were used as membrane mimic, to achieve high stability and functionalization. The goal of this thesis was to translate the Nature's compartmentalization and functionalization concept into synthetic nanometer scale objects. Their functionality was achieved by the use of membrane proteins and DNA.

Specifically, we developed a system to study the effect of polymers on the function and activity of a membrane protein essential for life. In the second case, we created and optimized a polymer-DNA based sensor to detect DNA hybridization.

General introduction

History of polymer science

People have had interest in polymers for centuries. It started with natural polymers and their first application, which was discovered in Central America in the sixteen century, where the Mayans are assumed to be the first users of a local rubber tree to make balls for children games. In 1839 Charles Goodyear discovered the vulcanization process, which comes from the heating of natural rubber with sulfur, leading to a substance much more resistant than the natural rubber. The interest in synthetic polymers has increased again during the first 20 years of the 20th century with the first synthetic plastic: bakelite, produced by Leo Baekeland. Staudinger's discovery of covalent bonds between different units of a polymer opened the development of the modern polymer theory. From the 1930s until early 1940s, a lot of new polymers like polystyrene (1930), nylon (1938) or polyethylene (1941) were synthesized, opening new perspectives in the textile and consumables industry (***Figure 1***).

At the beginning of the 70's, a new expansion in polymer synthesis arose with the creation of polymers like ekonol (1970) and kevlar (1971). Finally, in 1976 the polymer/plastic industry outstripped steel as the most widely used material per unit volume, and started the time were more plastics were used than steel, aluminum and copper combined [1, 2].
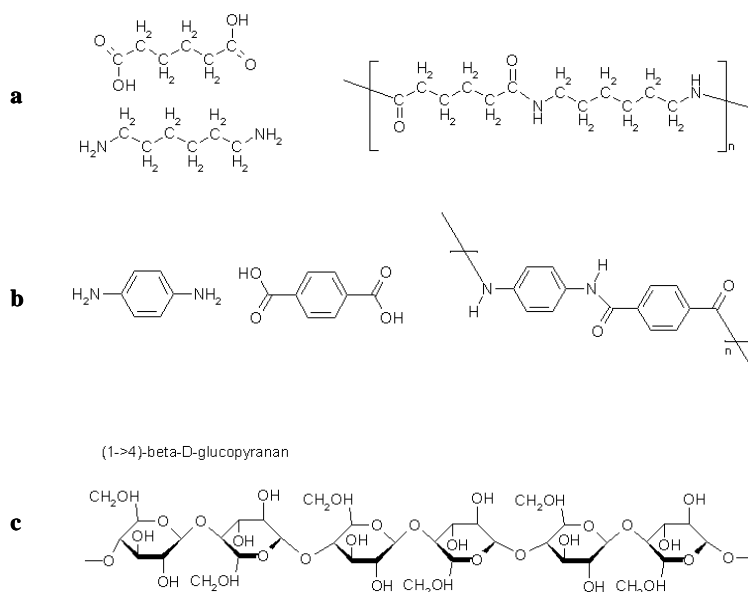
Figure 1: Examples of polymers (a). nylon, (b). kevlar, (c). cellulose. (a,b) are synthetic polymers, (c) is a natural one.[3]

Nowadays polymers are found and used everywhere around us, in agriculture, medicine, consumer science, sport, etc. This is mainly due to the fact that polymers and plastics have a wide range of properties (e.g. thermoresistance, elasticity) and they have a relatively low cost.

Biopolymers

The focus has not only been on synthetic polymers. A lot of work has been done on natural polymers, also called biopolymers, like starch, rubber or cellulose (*Figure 1*). In fact, a lot of biomolecules are polymers by nature. This comes from the definition of a polymer, which is *"a string of units covalently linked together either in linear form or with branching points. Polymers can be made of strings of different units. Proteins are made of 20 different amino acids; DNA and RNA are made of 4 different types of nucleotides"* [4]. Therefore, proteins, DNA molecules and polysaccharides are natural polymers.

From such consideration it seems interesting to work with natural and synthetic polymers. Taking advantages of both kinds of polymers could lead to some interesting hybrid materials, with biocompatibility of the natural polymers on one hand, and enhanced stability toward degradation of the synthetic polymers on the other hand. Moreover, biology offers a unique selection of building blocks that would be nearly impossible to achieve by synthesis in a laboratory.

Block copolymers: definition, properties and characteristics

The word 'polymer' comes from Greek where *poly* means 'many' and *meros* means 'parts'. In other words, a polymer is a high molecular weight macromolecule made up of multiple repeating units. The smallest repeating unit that could be found in a polymer is called a *monomer*.

When the polymer is made of only one kind of monomer, it is called a *homopolymer*. Different homopolymers could be found depending on the assembly of the monomers (***Figure 2***).

Linear homopolymer: A-A-A-A-A-A-A-A-A

Branched homopolymer: A-A-A-A-A-A-A-A-A
A   A‒A‒A
A‒A‒A

Stars homopolymer:
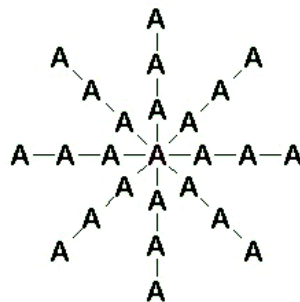
Figure 2: Different types of homopolymers.

When there are at least two different types of monomers (for example A and B), the polymer is called a *copolymer*. Depending on the block organization, different copolymers are found (***Figure 3***). When the different monomers A and B are attached in a random manner, the copolymer is called random or statistic copolymer. When the monomers are alternated in the chain, the resulting polymer is an alternating copolymer. When an A homopolymer is covalently grafted to a B homopolymer, the resulting molecule is called a diblock copolymer

(block copolymer in the *Figure 3*) in the case of a linear chain; and when the chains are not linear we have a grafted copolymer.

Statistic copolymer: A-A-B-A-B-B-B-A-A-B-B-A

Alternating copolymer: A-B-A-B-A-B-A-B-A-B-A-B

Block copolymer: A-A-A-A-A-A-B-B-B-B-B-B

```
Graft copolymer: A-A-A-A-A-A-A
                    |       |
                    B       B
                    |       |
                    B       B
                    |
                    B
```

Figure 3: Different types of copolymers

Another type of copolymer might be defined; it is the triblock copolymer where a B homopolymer is surrounded by two A homopolymers, this kind of copolymers are called symmetric copolymers. There are also asymmetric block copolymers where the three homopolymers forming the triblock copolymer are different (*Figure 4*).

Symmetric block copolymer: A-A-A-A-B-B-B-B-B-B-A-A-A-A

Asymmetric block copolymer: A-A-A-A-B-B-B-B-B-B-C-C-C

Figure 4: Different types of block copolymers.

The work that will be presented here focuses on ABA triblock copolymers and their ability to form vesicular structures. These polymers are composed of a hydrophobic middle block surrounded by two hydrophilic side blocks. This architecture results in amphiphilic behavior of the macromolecules, which are therefore able to self-assemble, leading to formation of different structures. Such structures are described in the next paragraphs.

Self-assembly principle

The definition of the self-assembly process is "a *method of integration in which the components spontaneously assemble, typically by bouncing around in a solution or gas phase until a stable structure of minimum energy is reached*" [5].

1. Natural polymers

In natural polymers, self-assembly is found everywhere. In fact, biopolymers have well defined structures. For example proteins have a primary, a secondary and a tertiary structure leading to the function of the protein. Another kind of self-assembly process is DNA hybridization. When two complementary strands are together, they self assemble to minimize the interactions with the surrounding media (*Figure 5*). These structures are provided by all the different interactions that can be found in Nature.
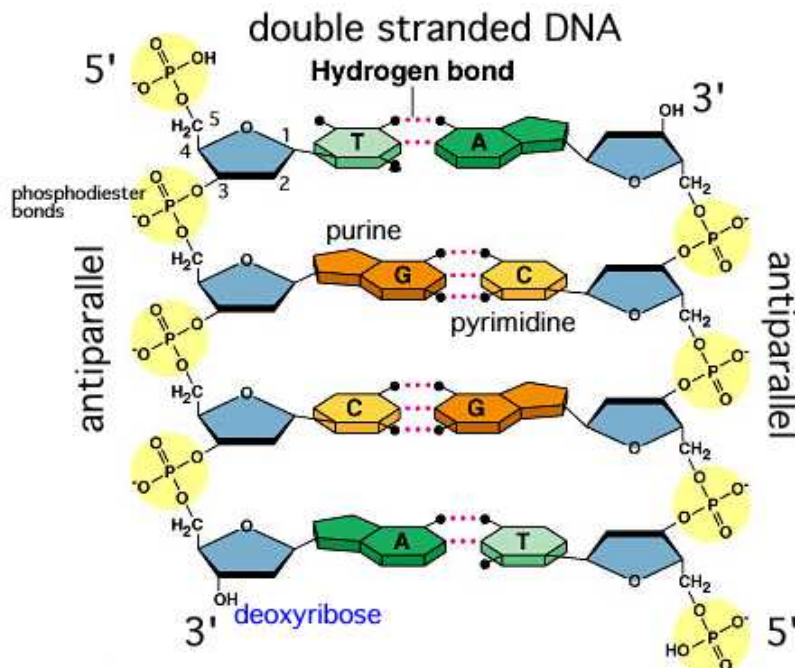
Figure 5: DNA helix obtained by self-assembly process. [6]

With lipids, self-assembly process is also occurring. This property comes from the amphiphilic nature of lipid molecules. There are different kinds of lipids, but the basic structure is shown in ***Figure 6***. Lipids are hydrophobic and insoluble in water. There are two important regions of a lipid molecule that render it amphiphilic. Each lipid molecule contains a hydrophilic region, also called a polar head region, and a hydrophobic (nonpolar) tail region (***Figure 6***).
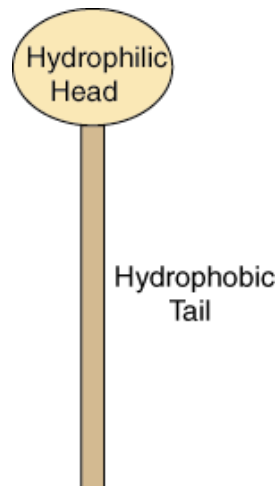
Figure 6: Schematic structure of a lipid molecule [7].

The most abundant class of lipid molecules found in cell membranes are phospholipids. A phospholipid molecule's polar head group contains a phosphate group. The molecule also carries two nonpolar fatty acid chain groups as its tail (***Figure 7***).
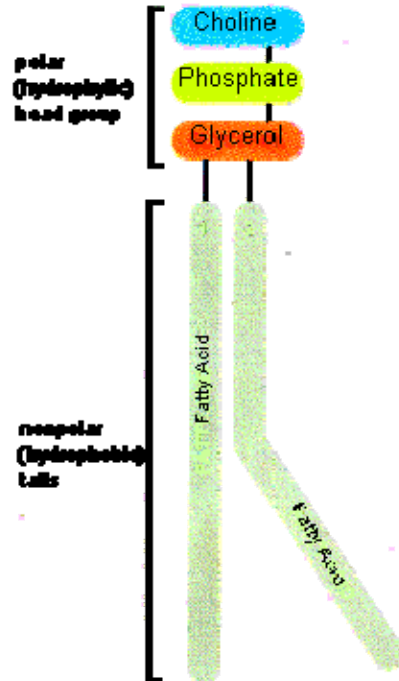
Figure 7: Phospholipid structure.[8].

Since lipid molecules contain both polar and nonpolar regions, they are called amphipathic molecules, and are able to self-assemble and form different structures. Micelles, nanotubes, vesicles and many more structures have been observed.

The geometry of amphiphilic molecules, such as surfactants, lipids, or copolymers, is currently believed to play a major role in defining their aggregation behavior [9]. In particular, surfactants that possess a conical shape are expected to maximize intermolecular hydrophobic interactions by organizing into spherical micelles; the ones that have cylindrical shape form planar bilayers. The geometry packing properties of different lipids may be expressed in terms of the packing parameter.
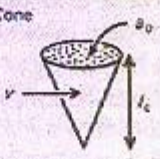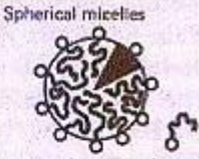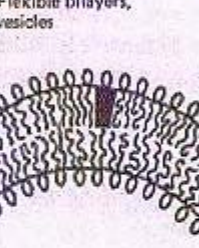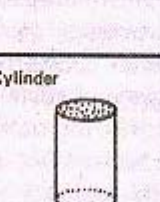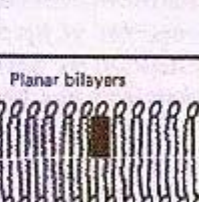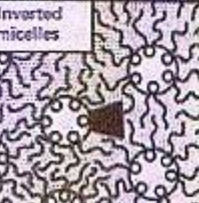
$$v/a_0 l_c$$

Where v is the volume and l_c the length of a (hydrophobic) chain, a_0 is the (hydrophilic) head group area (*Figure 8*).
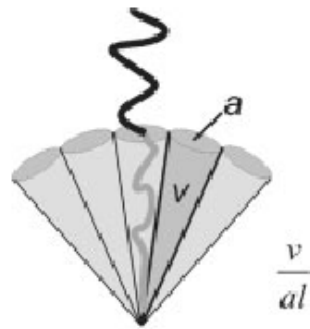
Figure 8: Amphiphile shape in terms of surfactant packing parameter v/a [10].

The surfactant packing parameter is characteristic for each lipid in a given solution environment; its value determines the type of aggregates. *Table 1* shows the structures formed by some common lipids, and how this can be modified by the ionic environment, temperature, chain unsaturation, etc [11].

Lipid	Critical packing parameter $v/a_0 l_c$	Critical packing shape	Structures formed
Single-chained lipids (surfactants) with large head-group areas: *SDS in low salt*	< 1/3	Cone	Spherical micelles
Single-chained lipids with small head-group areas: *SDS and CTAB in high salt, nonionic lipids*	1/3-1/2	Truncated cone	Cylindrical micelles
Double-chained lipids with large head-group areas, fluid chains: *Phosphatidyl choline (lecithin), phosphatidyl serine, phosphatidyl glycerol, phosphatidyl inositol, phosphatidic acid, sphingomyelin, DGDG[a], dihexadecyl phosphate, dialkyl dimethyl ammonium salts*	1/2-1	Truncated cone	Flexible bilayers, vesicles
Double-chained lipids with small head-group areas, anionic lipids in high salt, saturated frozen chains: *phosphatidyl ethanolamine, phosphatidyl serine + Ca^{2+}*	~1	Cylinder	Planar bilayers
Double-chained lipids with small head-group areas, nonionic lipids, poly (cis) unsaturated chains, high T: *unsat, phosphatidyl ethanolamine, cardiolipin + Ca^{2+} phosphatidic acid + Ca^{2+} cholesterol, MGDG[b]*	> 1	Inverted truncated cone or wedge	Inverted micelles

[a] DGDG, digalactosyl diglyceride, diglucosyl diglyceride.
[b] MGDG, monogalactosyl diglyceride, monoglucosyl diglyceride.

Table 1: Mean dynamic packing shapes of lipids and the structures they form [11].

Moreover, *Table 1* shows that the size of the (hydrophilic) head group is an important factor: large sizes favor spherical shape whereas small sizes favor planar bilayers. The vesicle formation process was reviewed for a lot for lipids as well as for polymers [10, 12-15], and it appears that the vesicle formation can be seen as a two-step self-assembly process. The amphiphile forms first a bilayer, which in a second step closes to achieve a vesicle (**Figure 9**).
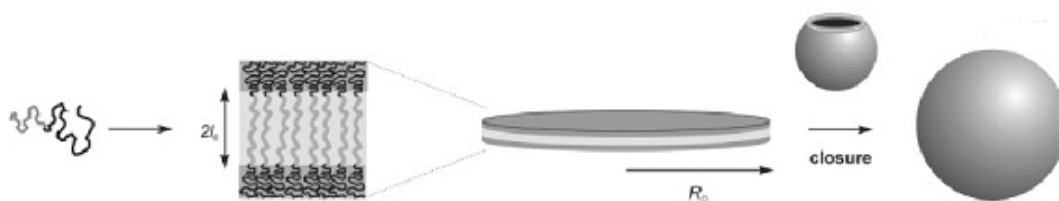
Figure 9: A schematic illustration of bilayer formation and its closure to a vesicle [10].

2. Block copolymers

Like their low molecular weight analogues (lipids), block copolymers are able to self assemble in aqueous media [16] and a lot of work has been done on the chemistry of these molecules in order to give them this property [17]. Various structures can be obtained depending on different factors like block length, temperature, and concentration or preparation method of the sample [18, 19]. The self-assembly behavior of block copolymers is driven by the incompatible nature of the blocks with respect to each other and the surrounding solvent. Indeed, the structural specificity of these molecules allows the aggregation of the hydrophobic fragments in a selective polar solvent, whereas the hydrophilic groups will have high affinity to that polar (aqueous) media. [20]. Consequently in a block copolymer solution, macrophase separation cannot occur since the blocks are covalently bound. As a result, only microphase separation can occur in such systems, leading to different structures [21].

A representative phase diagram of ABA triblock copolymer is shown on *Figure 10*. These polymers are able to form nanostructured hydrogels in concentrated solution or to self assemble into nanovesicles in dilute aqueous solution [22].
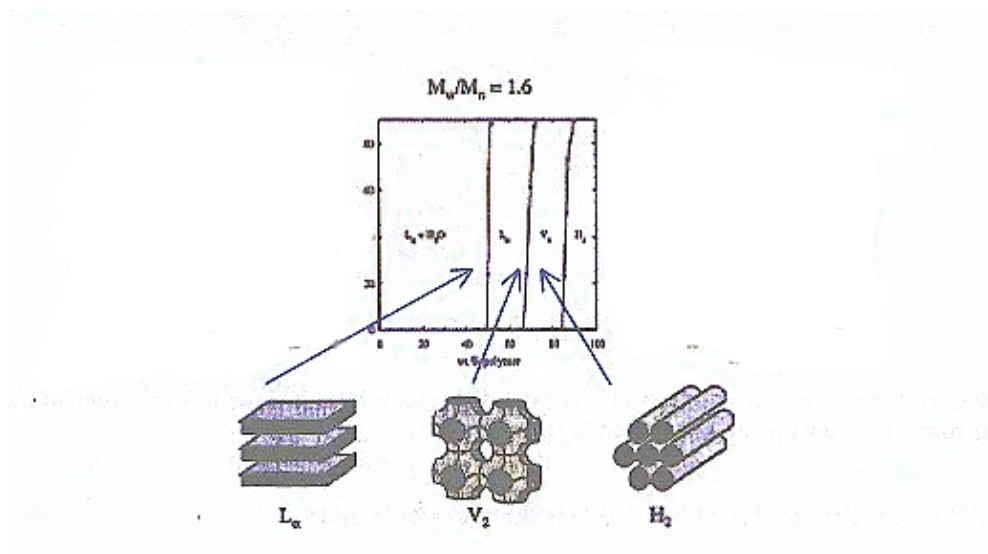
Figure 10: A phase diagram of ABA triblock copolymer in water [22].

The aggregate morphology is given by the volume fraction of each component of the polymer. For example, a volume-symmetric block copolymer, with equal volume of the hydrophobic and hydrophilic parts, will lead to a lamellar structure. Cylindrical, spherical and other more complex morphologies are achieved by volume-asymmetric block copolymers, like our ABA triblock copolymer. Moreover, the thermodynamic tendency to lower the surface area at the interfaces between the domains will curve interfaces, which is preferred in case of highly volume-asymmetric block copolymers.

As an example, a series of poly (butadiene)-*b*-poly (ethylene oxide), PB-PEO block copolymers are shown in Figure 11. In these polymers there is a decrease of the hydrophobic to hydrophilic ratio, and the interfacial area increases in proportion to the hydrophilic block length. This leads to shape changes from spherical to cylindrical micelles and finally to vesicles [10].
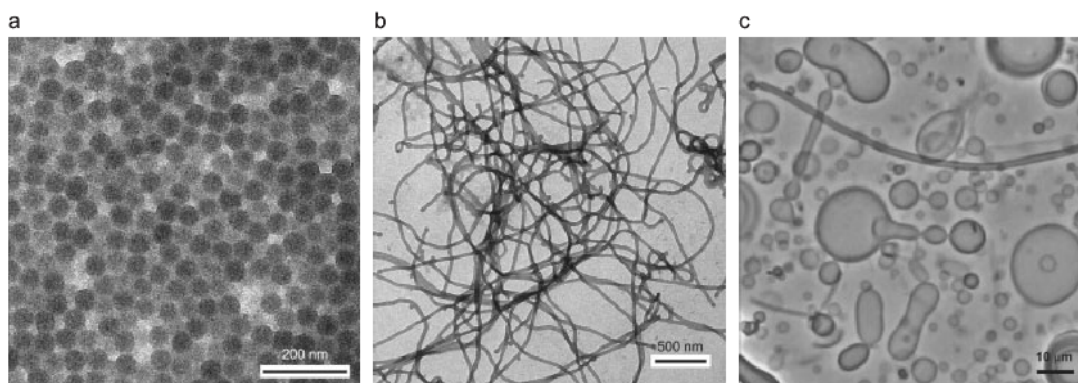
Figure 11: TEM images (a, b) and optical micrograph (c) of different shapes of aggregate structures in a series of PB-PEO block copolymers; from spherical micelles (PB_{200}-PEO_{360}) via cylindrical micelles (PB_{125}-PEO_{155}) to vesicles (PB_{37}-PEO_{40}) [10].

Another interesting feature is the size achieved via self-assembly of polymers. Indeed, amphiphilic polymers can form defined structures depending on the concentration of the polymer and on the preparation method. The resulting structures are interesting because of their typical nanometer size range. This property makes them useful for a lot of applications, which integrates polymer science in the promising application field of nanotechnology. In fact, the interest in such structures comes from Nature where there is an abundance of structures with nanoscale dimensions. Moreover, the functionality of most biological structures is a direct consequence of their dimensions. A few examples of nanoscale materials in biology are lipid cellular membranes, ion channels, spider silk and so forth.

The polymers used in this work were ABA triblock copolymers made of two hydrophilic PMOXA blocks and one hydrophobic middle block made of PDMS. They are able to nanometer scale vesicle sin aqueous media. I will now present the various applications of block copolymer vesicles.

Applications of block copolymer vesicles

Lipid vesicles (liposomes) found various applications, i.e. in drug delivery [23-30]. However, lipid membrane are unstable aver time and as such not applicable in many fields were membrane "toughness" is required. Therefore, a lot of work was done on stabilization of liposomes [17-22, 29, 31-35] as shown on *Figure 12*. But even if some improvements were made, they were still not sufficient for the applications that required long-term stability. The next step was then to create purely polymeric vesicles and verify their biocompatibility for further applications in biological sciences.
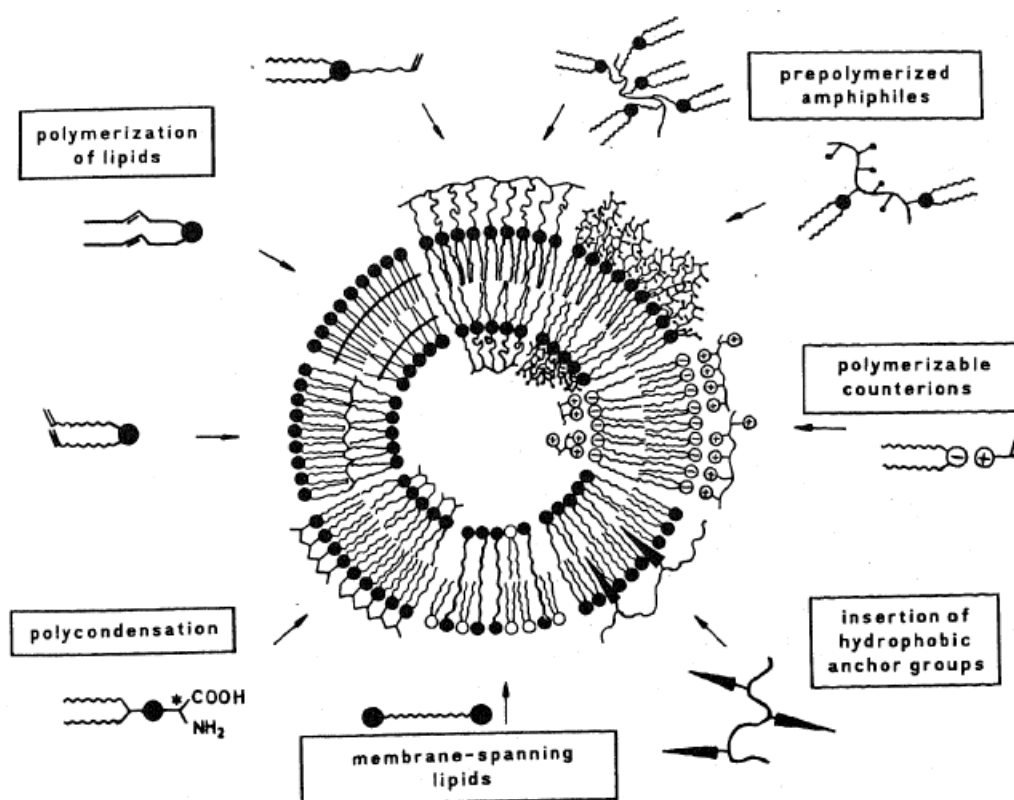
Figure 12: Strategies for lipid bilayer membranes stabilization [36].

Indeed polymer membranes have the advantage of a higher stability and toughness than liposomes. Moreover, they offer numerous possibilities of tailoring physical, chemical, and biological properties by variation of block lengths, chemical structure, and conjugation

with biomolecules. A lot of different functions can be obtained either in a single polymer chain or by mixing another polymer into the bilayer. This opens extremely broad fields where functionalized polymer vesicles can be used for applications ranging from electronics, optics, agro chemistry and sensor; to biology and more particularly pharmacy, where they can be used for drug delivery, gene therapy or even tissue engineering [31].

It is possible to encapsulate various substances in polymer vesicles (***Figure 13***b).
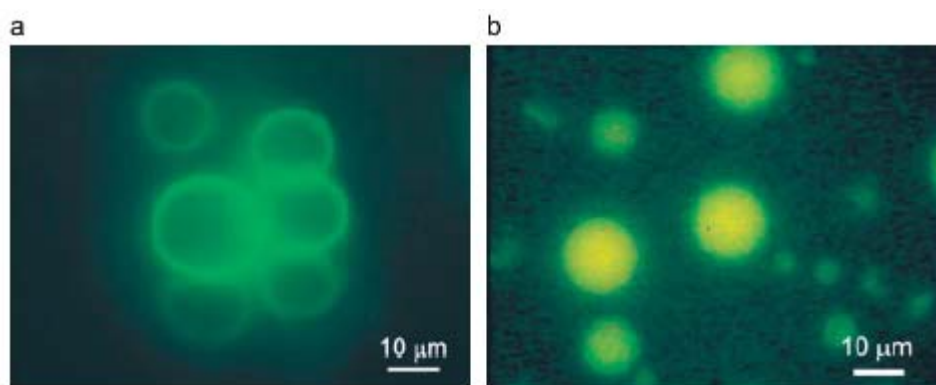
Figure 13: Vesicles with luminescent CdTe quantum dots solubilized into the vesicle bilayer (a) and encapsulated fluorescein in the interior (b) [10].

Hydrophilic molecules can be encapsulated by dissolving the block copolymer and the molecule of interest in the aqueous solution. Removal and recycling of non-encapsulated molecules is possible by ultra-filtration, gel filtration or dialysis, and expensive substances can be reused. Polymer vesicles can retain encapsulated molecules over period of days to week. The encapsulation of hydrophobic molecules was also widely studied [37-42].

In every system (liposomes or polymeric vesicles), a loss of encapsulated substance will occur via permeation through the vesicle membrane [32]. This phenomenon is related to two characteristics of the vesicles: the membrane thickness and the vesicle radius. As a result, release rates can be tailored via these two factors, which themselves can be controlled by polymer block length and vesicle preparation. Due to the larger thickness of polymer membranes (5-20 nm) compared to the liposomes (3-5 nm), the permeation of molecules in polymeric vesicles can be slower.

Another release mode has to be considered: special vesicles are able to interact with their environment: the solution conditions can trigger a spontaneous structural rearrangement,

leading to a release of the encapsulated molecules (***Figure 14***). Therefore it is interesting to synthesize block copolymers responding to pH, temperature or ionic strength.
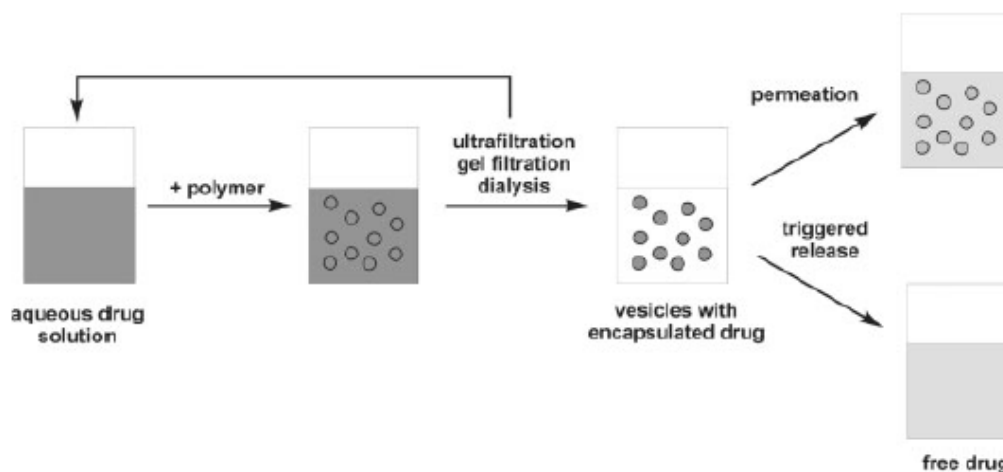
Figure 14: Scheme for encapsulation and release of hydrophilic substances [10].

Some other biological functions were achieved by using different polymers. Nolte et *al.* described the synthesis and use of a new amphiphile forming vesicles with biological activity. This amphiphilic molecule was a thiophene-containing rod-coil block copolymer composed of 40 styrene and 50 3-(isocyano-$_L$-alanyl-amino-ethyl)-thiophene (PS-PIAT) units. The amphiphilic behavior of this PS-PIAT molecule enables the formation of vesicles in either aqueous or organic solvents. The authors have then formed microreactors via encapsulation of *Candida antartica* Lipase B (Cal B) enzyme in the vesicles. The activity of the entrapped enzyme was tested by addition of the substrate, 6,8-difluoro-4-methylumbelliferyl octanoate (DiFMU octanoate) to the vesicles solution. This experiment shows that the substrate can permeate through the vesicles membrane, and its hydrolysis proves that the enzyme was still active in the vesicles. Moreover, the thiophene groups located in the outer layer of the membranes can be coupled to give polymerized vesicles. This way, the resulting polymerizable vesicles from diblock copolymers, with the inclusion of enzymes, open the possibility to create stable micrometer-sized reaction vessels [33].

Another level of functionalization can be achieved after insertion of membrane protein, with remaining of the activity. So various proteins were reconstituted, some examples are given:

- ✓ Alamethicin was used to performed biomineralization in vesicles [43, 44].
- ✓ OmpF could make DNA transfer inside the proteovesicles [39].

There are different parameters that render polymeric vesicles extremely attractive. The first one is their stability toward lysis with classical surfactants, which is much higher than with lipid vesicles. The second important property of polymer vesicles is found in the possibilities they offer in terms of functionalization and modification of their surface. Indeed, the surface of polymer vesicles can be functionalized by molecules such as DNA or sugar, but also by incorporation of proteins in the membrane.

Polymer vesicles surface functionalization

The overall properties of polymer vesicles give them a great potential for a lot of various applications. All these functions can be achieved by functionalization of the particles. Several studies have been made on the functionalization of nanoparticles surface [45-49], and nearly everything can be attached at nanoparticles surface, like antibodies, sugars and various others ligands. For example, Torchilin and coworkers proved that as much as 60 to 100 antibody molecules can be attached to a single 200nm diameter liposome, which once again provides multi-point liposome binding with a target [26-30].
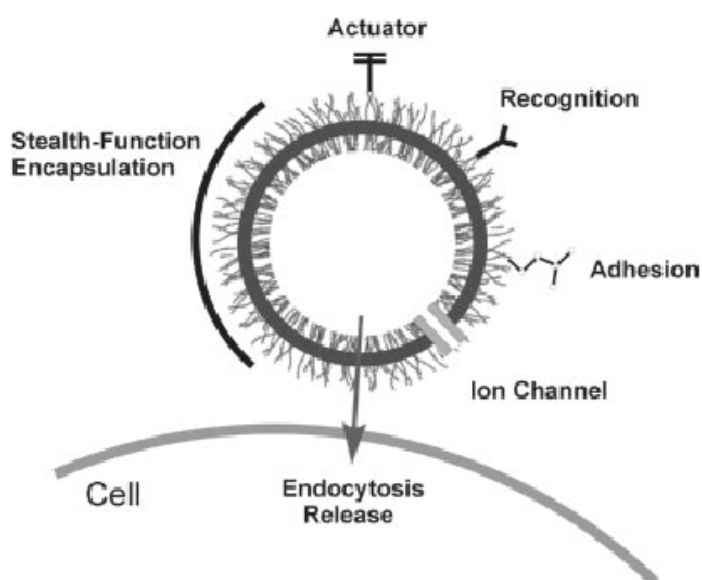
Figure 15: Biological functions of vesicles trough attachment of ligands [10].

In fact, functionalization of nanovesicles' surfaces comes from two main interests. The first one is compartmentalization offered by nanovesicles. In fact, compartments are found everywhere in cells, they separate cells from each other, but they also define organelles inside a cell. The second point comes from the fact that all life processes require an interface. A good example is energy conversion systems. As mentioned before, membrane proteins need

to be stabilized; consequently their reconstitution in polymer is studied as an alternative to liposomes this will be discussed in the following part of this work.

Functionalized vesicles can also be used for vaccine administration or for diagnosis imaging [23, 24]. In this last case, nanoparticles used are most of the time magnetic particles, because detection by magnetic resonance imaging is possible. Functionalization of the surface is necessary to provide a specific label to these molecules. Josephson et *al.* first used superparamagnetic iron oxide nanoparticles derivatized with a part of the tat-peptide to image cell trafficking, but also to make magnetic separation of in vivo homed cells (***Figure 16)***. Due to its transmembrane translocation function, tat-peptide was often used [25, 50, 51].
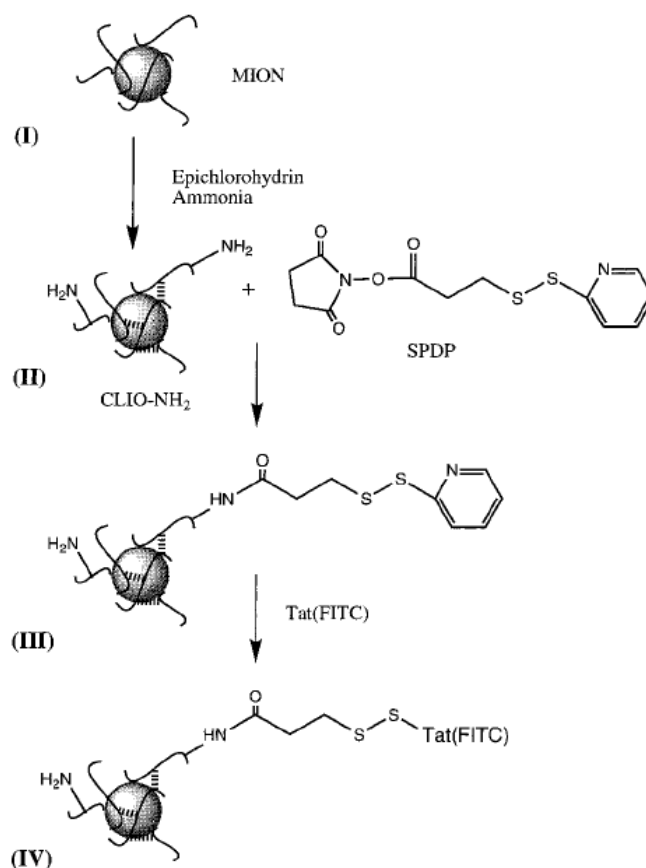
Figure 16: Synthetic scheme of superparamagnetic iron oxide–Tat peptide conjugate [25].

Some studies were also done on functionalization of nanoparticles with oligonucleotides [52-56]. This will be discussed in more details in the second part of this thesis.

We decided to study surface functionalization via two kinds of experiments. The first study was related to compartmentalization of processes. To achieve that, we inserted and characterized a membrane protein, with an important function for cell life, in ABA triblock copolymer vesicles. Next, we used this molecular machine to create a miniaturized electron transfer device, to achieve energy conversion.

In the second case, we used the molecular recognition system occurring in every cell, to develop a nanometer-sized DNA sensor. This work included the design of new carriers enabling us to work in solution. We investigated the ability of the system to hybridize its complementary sequence.

Finally, these studies allowed us to mimic a key mechanism of Nature by using specific recognition taking place at an interface but also by using compartmentalization. This last point is reached via the structure of the particles (vesicles and core-shell particles) to achieve spatial and (perhaps) also temporal separation of the individual steps involved.

Insertion of membrane proteins in polymeric vesicles

Introduction

Biological membranes have crucial importance to life because a cell must separate itself from the outside environment for two major reasons. The first one is to keep its molecules of life (DNA, RNA) from dissipating away. The second point is to keep out foreign molecules that damage or destroy its components and molecules. If a cell has to always fulfill these two principles, it has also to communicate with its environment and to continuously monitor the external conditions and adapt to them. Each cell in our tissues communicates with dozens if not hundreds of other types of cells about a variety of important issues; when it should grow or differentiate or die, when it should release certain protein products or metabolites needed by other cells at distant sites in the body, and what other cells it should associate with to build complex tissue architectures.

Ironically, the intrinsic structure of cells creates a formidable obstacle to these important processes of intercellular communication. The cell shields itself behind its membrane, which is relatively impermeable to most types of molecules. This barrier enables the cell to create its own intracellular environment that is distinct and very different from the world around it. But this arrangement also creates a problem, in that it prevents the free interchange of material between inside and outside. This barrier must be breached somehow in order for a cell to inform itself on what is happening in the world outside (*Figure 17*). For this purpose Nature has used highly specialized and optimized proteins. These proteins are divided in two types:

- Integral (or intrinsic) membrane proteins
- Peripheral (or extrinsic) membrane proteins
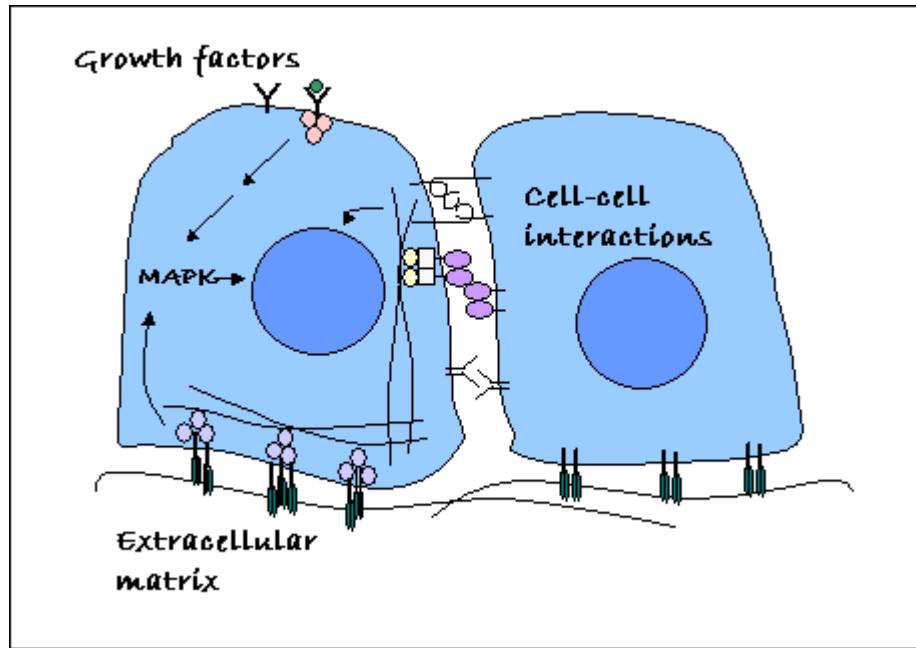
Figure 17: Cell-cell interactions.

The peripheral proteins are usually globular proteins bound to the bilayer surface via ionic interactions with other proteins, by the hydrophobic part of an α helix or via a lipid anchor (**Figure 18**: 4-8).
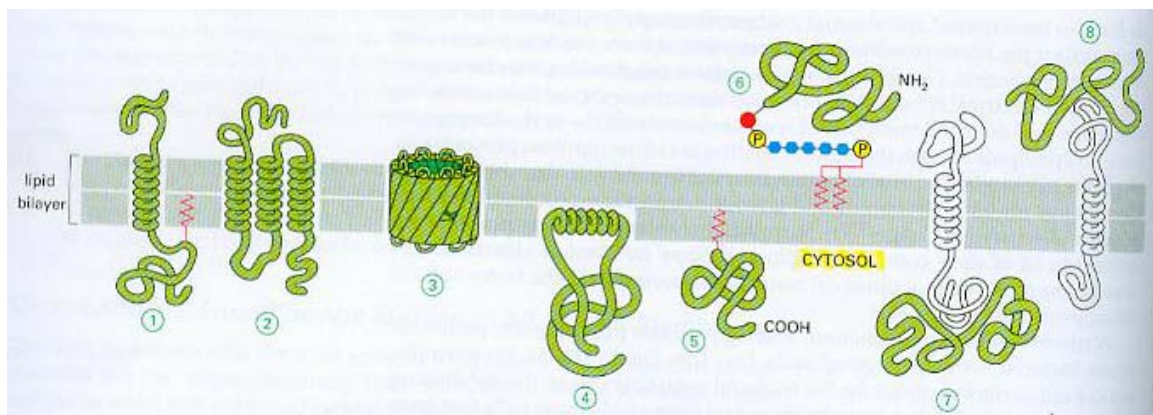
Figure 18: Various possibilities for membrane protein association with lipid bilayer [57].

The integral membrane proteins expose hydrophobic side groups at their surface, which allow them to be located within the hydrophobic environment of the lipid bilayer.

These membrane proteins span the entire thickness of the bilayer and they are called transmembrane proteins. They are usually involved in the transport of polar molecules across the membrane. The crossing of the membrane is achieved with a single α helix, multiple α helices or a β barrel form of the protein (**Figure 18**: 1-3).

Proteins not involved in the transport of polar solutes usually have different functions like anchoring the cytoskeleton or other cells (linkers), signal transduction (receptors) or performing enzymatic reaction (enzymes). Therefore, it takes many different membrane proteins to enable a cell to function and interact with its environment (*Figure 19*). It is estimated that about 30 % of the proteins are encoded in an animal genome are membrane proteins.
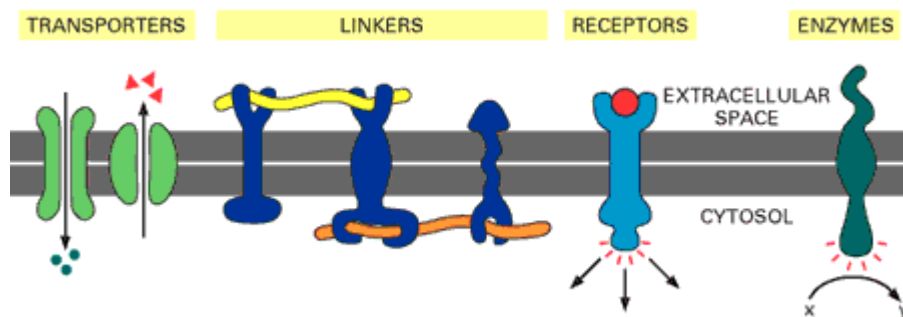
Figure 19: Different types of membrane protein [58].

When membrane proteins are studied in vitro, they need to be extracted from the membrane. But membrane proteins cannot "survive" in an aqueous solution because of their hydrophobic part. They need to be stabilized. To this aim they are reconstituted in liposomes, which are membrane mimickers [59-61]. This process enables to study structure and functions of proteins that are not so easy to handle. Indeed, membrane proteins can be extracted from the membrane by the use of detergents or apolar solvent or mechanical forces, which disrupt the membrane (*Figure 20*). These harsh methods are necessary due to the strong interactions between the alkyl chains of the lipids and the hydrophobic domains of proteins [62-64].
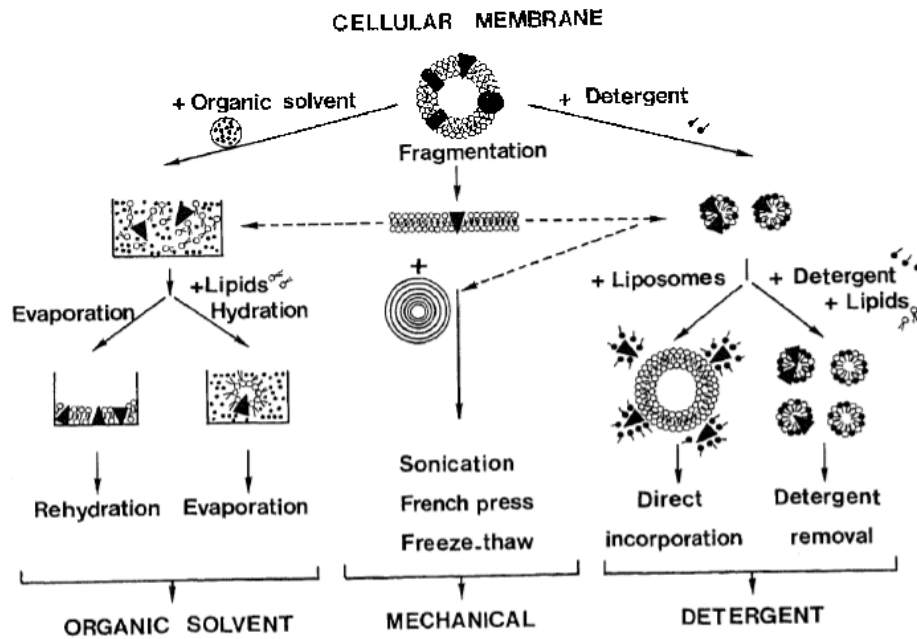
Figure 20: Different strategies for the functional reassembly of membrane proteins into liposomes. (A) represents the membrane fragmentation, (B) represents the various methods for reconstitution of membrane proteins [64].

When detergents are mixed with protein-containing membranes, their hydrophobic moiety will bind to the hydrophobic regions of the protein, thereby displacing the lipids (*Figure 21*).
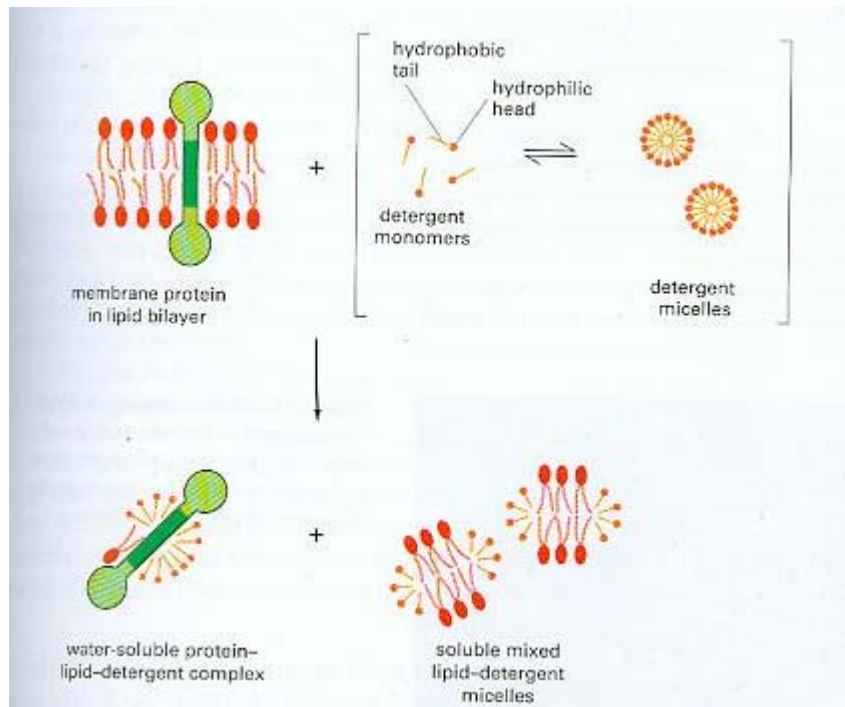
Figure 21: Solubilization of membrane protein with detergent [57].

A problem arises from such a process; that is protein unfolding. Nevertheless, this can be avoided by detergent removal. In the standard procedure, proteins are first cosolubilized with phospholipids in the appropriate detergent in order to form a solution containing lipid-protein-detergent and lipid-detergent micelles. Next, the detergent is removed resulting in the progressive formation of bilayer vesicles with incorporated proteins. An example of such a process is described in *Figure 22* with the reconstitution of the Na^+/K^+ ATPase pump. For the detergent removal, different techniques can be used depending on the type of protein and detergent used for the solubilization (*Figure 23*). For detergents, the important parameters are critical micelle concentration (CMC), micelle size, and the hydrophilic-lipophilic balance.
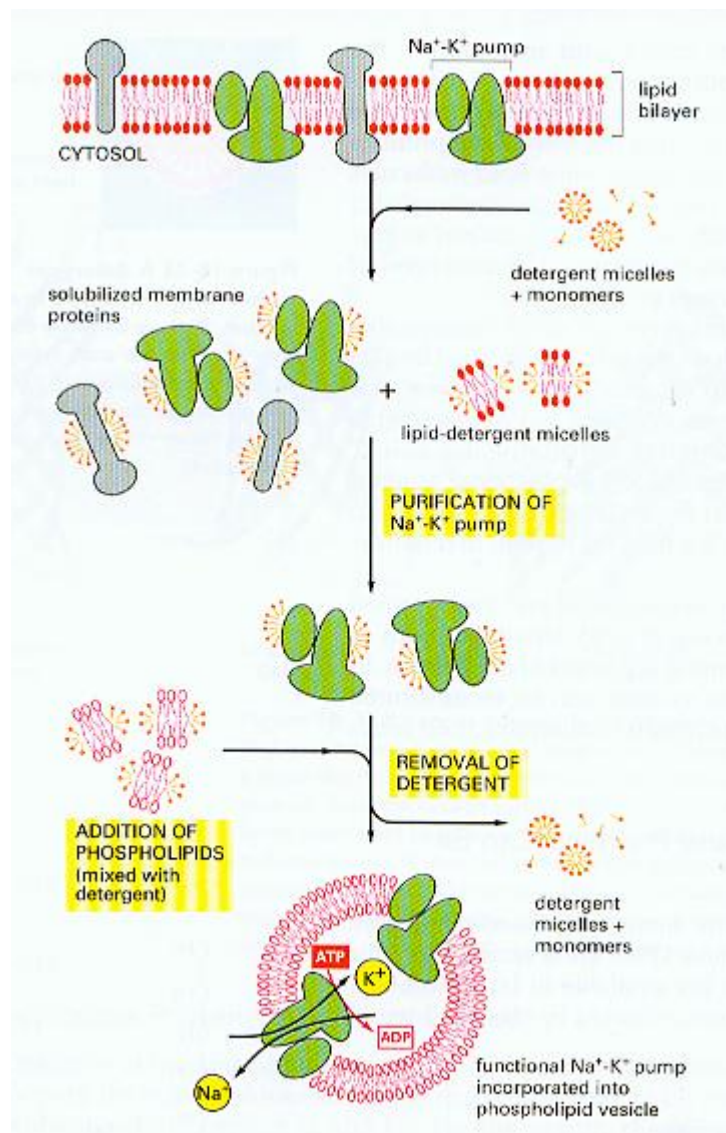
Figure 22: Reconstitution of membrane proteins is lipids vesicles [57].

From various studies on protein insertion, several methods have been developed for the reconstitution (***Figure 23***). Dialysis is widely used in 2D-crystallization trials and is reviewed for a lot of detergent used with various proteins [65]. This method was applied to many proteins, but it is not suitable for detergents with low cmc's, which would require very long dialysis time, incompatible with low stability of membrane proteins. Another technique to remove detergents with high cmc's is gel filtration techniques. In this case, the micellar mixture is eluted through a size exclusion chromatography gel: as the mixture passes through the resin, the protein is integrated into liposomes that elute from the column before the

detergent. The most significant advantage of this technique is its rapidity, avoiding long periods of contact between detergents and proteins. However, this might turn into disadvantages in terms of incomplete protein incorporation [66].

The third procedure to obtain proteoliposomes from lipid-detergent-micellar solutions consists of diluting the reconstitution mixture [67]. Dilution lowers the detergent concentration below its cmc and proteoliposomes form spontaneously; this technique, however, has failed in many cases [ref].

The last detergent removing method is adsorption on hydrophobic resins (SM$_2$ Bio-Beads or Amberlite XAD). These are mainly used in the case of low cmc's detergents, but it was demonstrated that this method is also efficient with high cmc's detergents. This method is the one we decided to use in membrane proteins insertion experiments.
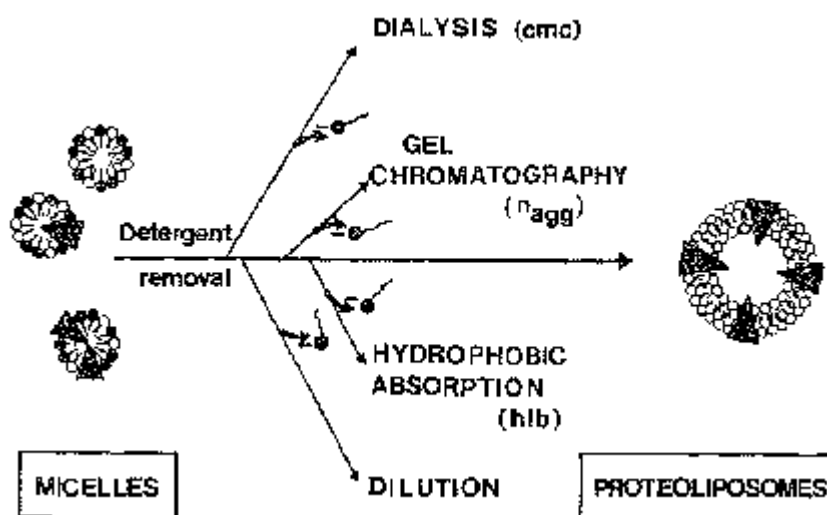
Figure 23: Different strategies for detergent-mediated reconstitution of membrane proteins. Black triangles represent membrane proteins, open circles represent phospholipids and black circles represent detergent [64].

Block copolymer-protein hybrid systems

As discussed previously, the incorporation of membrane proteins in liposomes has been used for long time. Many different proteins have been reconstituted, and their function studied via the use of liposomes [64, 68]. However, the lack of stability of those structures brought some groups to use another kind of a system made of polymers, to develop nanoscale hybrid protein-polymer devices. The use of block copolymer-protein hybrid systems is quite a new application in polymer science. It started in 2000 when Meier and coworkers proved that amphiphilic ABA block copolymers were suitable for membrane proteins reconstitution [69]. They also proved that the membrane protein OmpF can be incorporated in the polymer membrane and remain active. This has drawn much attention to the self-assembling, amphiphilic ABA triblock copolymers as a potential building material in the fabrication of biosensors and nanocontainers [70]. These ABA copolymers, composed of a hydrophobic layer (B) set between two hydrophilic layers (A), are analogous to typical lipid bilayers. For the reconstitution of membrane proteins in functional form, thin walled vesicles are normally required to be compatible with the transmembrane protein size, provide sufficient stability, and exhibit biologically useful properties. Obviously, the ABA triblock copolymer membranes are much thicker than a lipid bilayer, but still the incorporated proteins remain active despite of the 2-3 fold higher thickness of the polymeric membrane compared to natural membranes [71]. Furthermore, the size of the synthetic membrane does not match with the hydrophobic–hydrophilic pattern of natural membrane proteins, but on the other hand polymer's hydrophobic chains possess higher vertical flexibility than lipids. Indeed, the chains might be able to adapt to the specific geometry of the membrane proteins (discussed in the second paper) to assure the functionality of the incorporated proteins. This way the design of polymer-protein hybrids opens the possibility to combine the mechanical and chemical stability of polymers with the specificity of membrane proteins. Such block copolymer-protein hybrid systems are of big interest in areas like pharmacy or biotechnology because they enable stabilization of proteins against proteolysis and self-denaturation [69, 72]. Moreover, due to their high stability, polymer vesicles provide a constant environment for encapsulated molecules. This point is crucial in technical applications where storage for long periods of time is required.

As mentioned before, the first protein-polymer hybrid was produced with the membrane protein OmpF [41, 42, 69, 73]. Later, other symmetric membrane proteins were reconstituted in polymeric vesicles (FhuA, LamB, and Aquaporin 0). In the case of LamB, the β-barrel protein was inserted in ABA vesicles and its activity was recorded [39]. This protein is the receptor for the phage λ, which binds to the protein and eject its DNA into the cytoplasm of the target cell. Graff et *al.* showed that the phage is able to attach to its receptor reconstituted in polymer membranes and next send the DNA into the vesicles.

Furthermore, in the last two years some other groups started to incorporate membrane proteins in polymer vesicles. For example some studies were done on genetically modified proteins like FhuA to create some nanocompartment systems with biotechnological applications [40]. Such studies were also done on symmetric proteins.

Montemagno and coworkers started to work on the incorporation of two membrane proteins at the same time. They were interested in functionalization of biopolymer vesicles with energy transduction proteins. This system employed the emerging concept of synthetic biology towards the production of practical devices based on inherent molecular function. In this case they used bacteriorhodopsin (BR) and cytochrome oxidase c (COX). In *Figure 24* the fabrication scheme of the two protein-polymer hybrids is shown. In this system bacteriorhodopsin is the element that confers light-dependence to the system. COX is the electron-producing element; the polymer membrane serves as a matrix for protein reconstitution and also facilitates oxidation-reduction reactions between proteins, cytochrome c mediator and the electrodes. Here the system used BR's unidirectional transport of protons, after light illumination, to the vesicle exterior. This vectorial catalysis of BR was then utilized to drive COX in a partially reversed reaction, altering its normal proton pumping mechanism, to become a source of electron release. To enable electron transport to the electrodes, a cytochrome c mediator was used. Finally, the assembled system demonstrated successful light-dependent current generation through protein coupling with no applied voltage, satisfying the anodic component requirements for potential integration into a bioenergy source [37, 73].
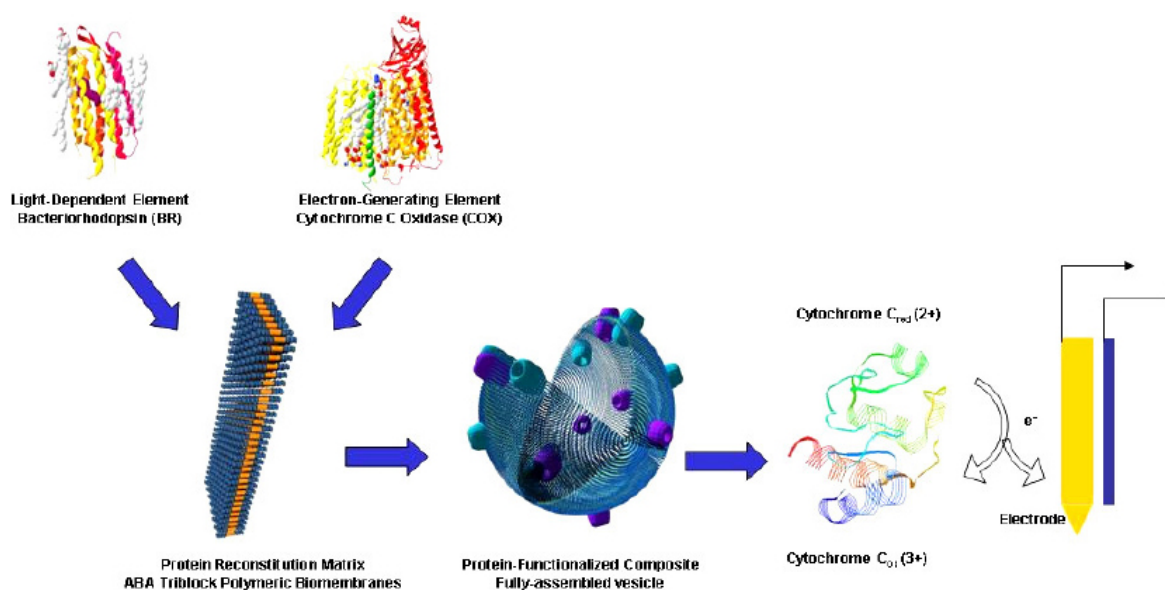
Figure 24: Fabrication scheme of composite vesicles (BR/COX/cytochrome c) [73].

Finally, Montemagno et al. worked with another class of membrane proteins, the proteins that 'catalyze' vectorial transport. For these studies, they used F_0F_1-ATP synthase motor protein [38, 74, 75]. The hybrid developed in this case is shown in ***Figure 25***, BR is also present and like in the previous system it is the starting point of the reaction mechanism via light illumination. In this system, the ATP synthase used the electrochemical proton gradient generated by BR to synthesize ATP from ADP and inorganic phosphate (Pi), by using its rotating activity. Such a hybrid system did not only represent the first successful biosynthesis through coupled reactions between reconstituted transmembrane proteins in single proteopolymersomes, but also demonstrated the molecular motor functionality in a polymer membrane.
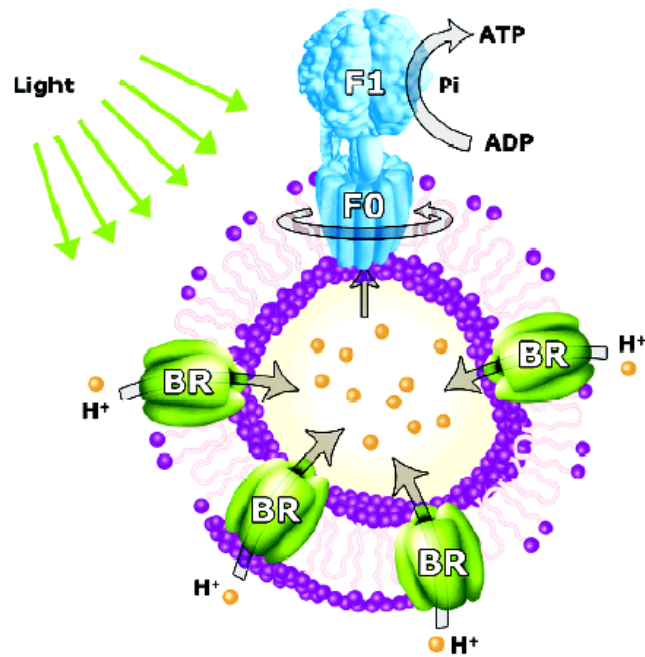
Figure 25: Proteopolymersomes reconstituted with BR and F0F1-ATP synthase [38].

In all these studies, the possible presence and the role of remaining lipids, after purification, around the protein of interest were never studied. Therefore, we decided to study this problem by using a membrane protein that 'catalyzes' a vectorial transport, NADH: ubiquinone oxidoreductase.

A model membrane protein: Complex I

In our attempt to nanoparticles functionalized with a highly asymmetric protein, we decided to incorporate one of the oxidative phosphorylation pathway proteins. The protein of interest is the NADH: ubiquinone oxidoreductase also called Complex I, which is the first enzyme of the mitochondrial electron transfer chain (***Figure 26***). We worked with Complex I purified from *Escherichia coli*, which together with Complex I from *Klebsiella pneumoniae* are the only bacterial enzymes that could be purified in intact form [76, 77]. The function of the enzyme in the oxidative phosphorylation pathway is to link electron transfer to proton translocation out of the mitochondrion. By doing so, it generates a transmembrane proton motive force, from the inside to the outside of the membrane, which subsequently drives ATP synthesis by the H^+-ATPase (Complex V in ***Figure 26***) [78].
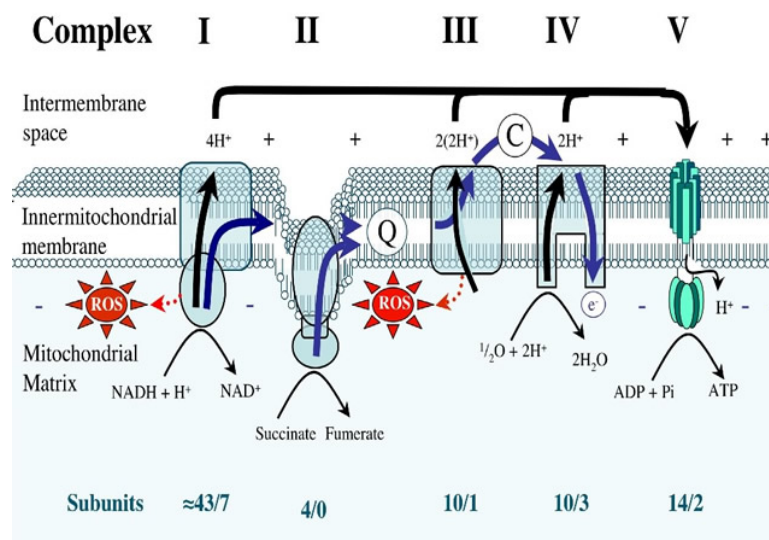
Figure 26: Representation of the oxidative phosphorylation pathway [79].

Complex I is by far the largest and most complex protein among the proton translocating enzymes of mitochondria. It is comprised of some 30 different subunits with little variations depending on the species. Electron microscopy pictures of Complex I [ref] revealed that it is composed of two subunits: one is hydrophilic and protruded from the membrane. The second part is highly hydrophobic and inserted in the mitochondria

membrane. These two parts form an 'L'-shape in the membrane of bacteria and in mitochondria (*Figure 27*). In other words, Complex I can be dissociated into two main sub-complexes, corresponding to the 'ankle' of the boot, and the 'foot' of the boot (*Figure 27*). The reaction mechanism of Complex I is known and couples the oxidation of NADH to NAD$^+$ in the mitochondrial matrix and the reduction of ubiquinone in the inner mitochondrial membrane, leading to the generation of a proton gradient across the membrane [80]. In fact, the ankle, which is predominantly in the aqueous phase, contains the binding site for NADH and the input electron transfer chain. The foot contains a catalytic site at which ubiquinone is reduced, and inhibitors bind, and several iron and sulfur centers. There is a second catalytic site for ubiquinone reaction on the ankle, but this is seen as separate activity only in the dissociated complex (*Figure 27*) [81].
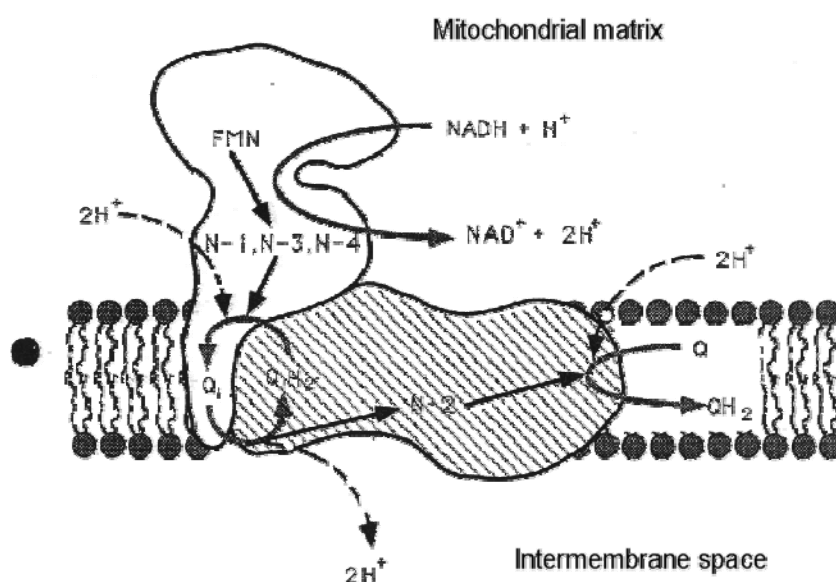
Figure 27: Schematic representation of Complex I mechanism [82].

The orientation of Complex I is essential for its mechanism, as shown in *Figure 28*. The NADH used by Complex I comes from the citric acid cycle. As the acceptor site for NADH is only present in one part of the protein, the orientation has to be accurate to allow the mechanism to start.
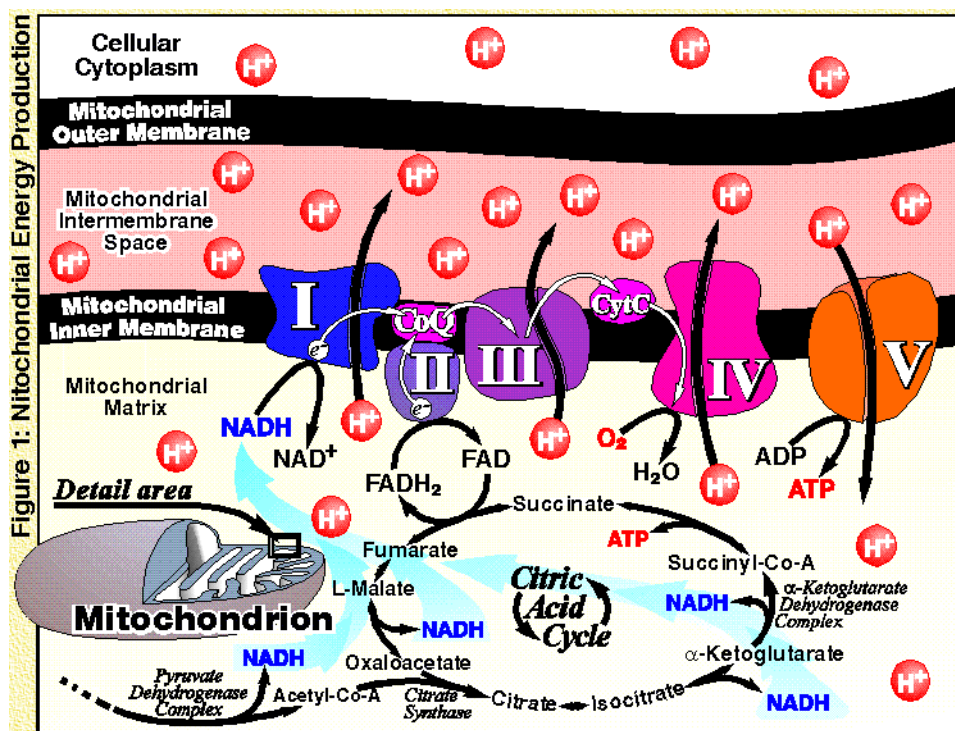
Figure 28: Mitochondrial energy production [83].

Our interest in Complex I was based on the experiments we made to produce a nanometer-sized energy converter. For that purpose we wanted to have a closer look at electron transfer through Complex I, which can be recorded by EPR (Electron Paramagnetic Resonance) [46, 49]. We wanted to investigate the reduced species obtained from NADH oxidation. To complete our study we investigated the H^+ transfer coupled with NADH oxidation. In the first paper, we focused on the potential uses of a new hybrid protein-polymer system.

On the other hand, we were interested in the property of Complex I to be switched on and off by addition or depletion of lipids [45, 47, 48, 84]. In fact, several studies showed specific lipid requirements for structural integrity and proper function of membrane proteins [85, 86]. In the case of membrane proteins incorporated in polymeric membranes it was never proved that there were no remaining lipids around the protein, inducing the activity of the protein studied [39]. Our interest, shown in the following paper, was to look at the activity of Complex I in a completely synthetic environment and to prove the ability of a polymer to switch on and off the protein as it would be done be lipids.

Protein insertion: conclusions

From different experiments we made, we demonstrated that Complex I can be incorporated in polymer membranes. Via EPR and fluorescence measurements we were able to prove that the electron transfer was occurring from the media to Complex I. Unfortunately, we were not able to prove that this transfer was reaching the interior of the nanoreactor. This is mainly due to the use of the improper electron acceptor encapsulated in the vesicles. We were also able to prove that the observed electron transfer was linked to proton translocation, meaning that the protein was entirely in the membrane and still active. We also proved that the incorporation of Complex I in vesicles is efficient but we did not get any information on the orientation of the protein in the membrane.

In the second paper we demonstrated that polymers are able to activate the completely dilapidated Complex I. We also saw the influence from both blocks of the polymer. We concluded that the thickness of the hydrophobic part makes stress on the protein, which increases the protein activity. We were also able to prove that the hydrophobic part of the polymer can limit the access to the NADH binding site of Complex I to NADH, leading to a decrease of the activity of the protein.

Finally, all these studies showed that integration of more complex proteins than β−barrels in polymeric membranes is feasible. We also proved that the enhanced activity of the protein after incorporation is not due to remaining lipids, which could be found around the protein, but to the polymer alone.

Biosensors

Summary

In this second part I am going to introduce a new DNA biosensor. In short, we have decided to develop a sensor that could be used in solution, enabling us to recover the sample after the measurement. The sensor is based on core-shell particles grafted with DNA oligonucleotides. The detection system we took for the DNA hybridization to its complementary strand was with a fluorescent dye. The complementary strand was labeled and the detection was made via Fluorescence Correlation Spectroscopy (FCS) measurements.

Introduction

Biosensor development began with Professor Leland C. Clark Junior in 1956, with the production of an oxygen electrode coupled to enzymes for glucose quantification. Since then a lot of modifications were made to enhance sensor sensibility, selectivity, and specificity, but also the fields of application. The definition of a biosensor is the following: "*it is a device for the detection of an analyte that combines a biological component with a physicochemical detector component*". It consists of 3 parts (***Figure 29***):

✓ The *sensitive biological element*: biological material (e.g. tissue, microorganisms, organelles, cell receptors, enzymes, antibodies, nucleic acids etc), a biologically derived material or biomimetic material. The sensitive elements can be created by biological engineering (number 1 in ***Figure 29***).

✓ The *transducer* which associates the biological and detector components (number 2 in ***Figure 29***).

✓ The *detector element* works in a physicochemical way; optical, piezoelectric, electrochemical, thermometric, or magnetic.

In ***Figure 29***, the principle of a biosensor is detailed. One compound (black circles) of a mixture specifically interacts with the sensor. The resulting biological signal is then converted into a physical signal (e.g., electric or optical) by a transducer (upper part of ***Figure 29***). Substances that are not able to interact with the biological component will not produce any signal (bottom part of ***Figure 29***).
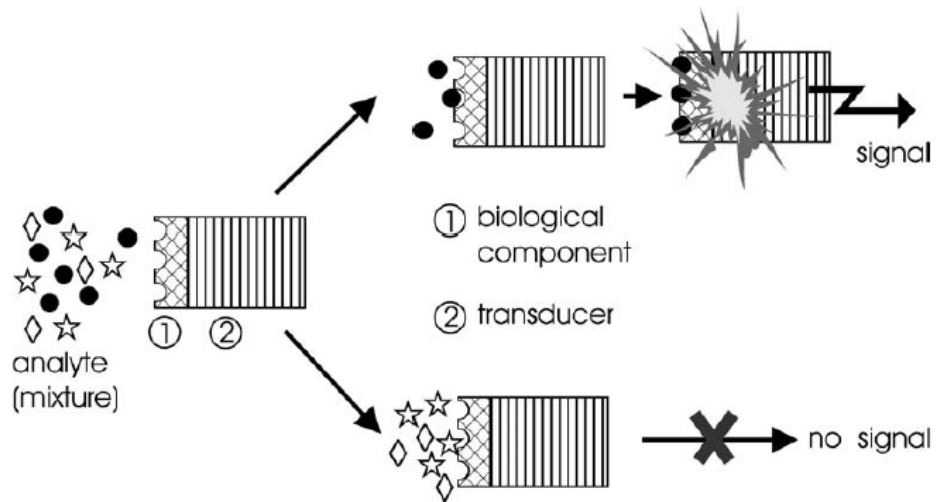
Figure 29: Principle of the function of a biosensor [87].

The development of biosensors was made first for clinical diagnosis, e.g. glucose quantification in the blood (***Figure 30***).
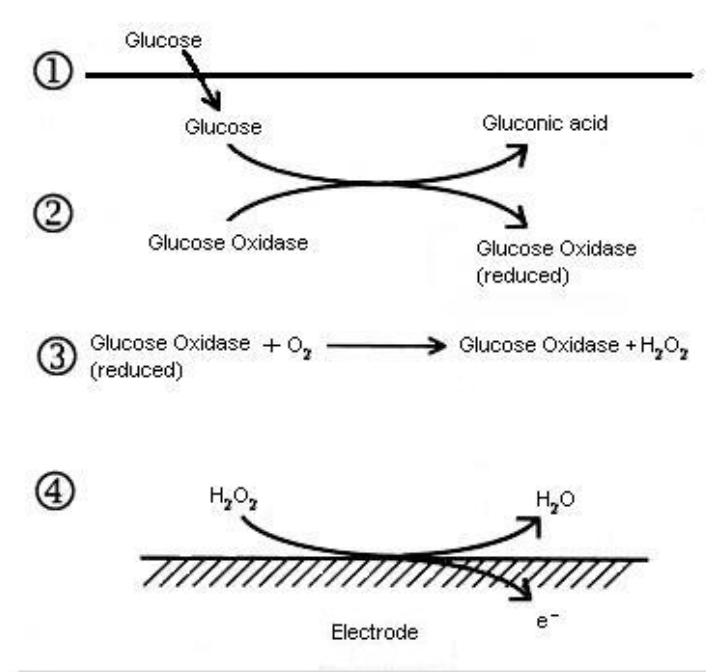
Figure 30: Reactions used for glucose quantification in blood [88].

The glucose quantification is achieved by the production of hydrogen peroxide (H_2O_2) via the glucose oxidase. An electron flux is then produced by the degradation of H_2O_2 and is recorded (*Figure 31*).
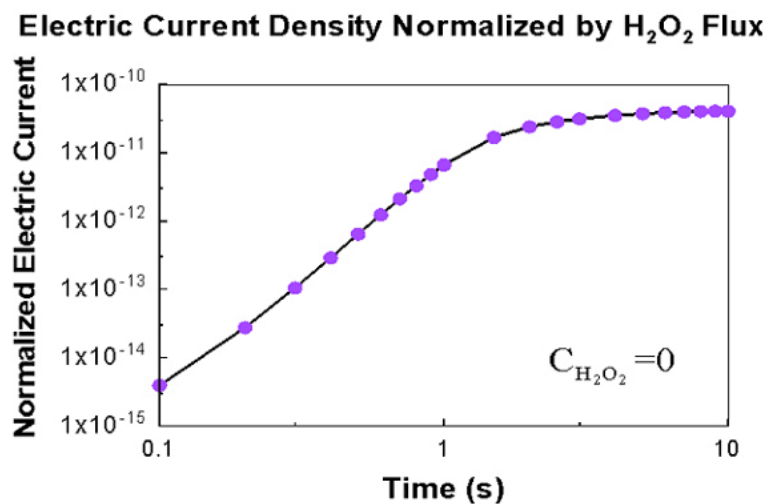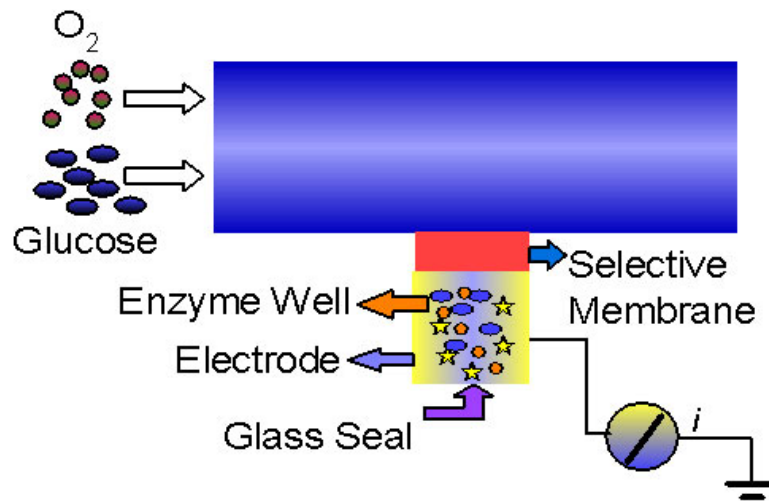
Figure 31: Principle of a glucose based sensor (upper part) and curve obtained when the reaction occurs (down part) [89].

Nowadays, biosensors are used in five other areas than medical diagnosis: pharmaceutical research, forensics, transplantation, identity testing, water and environmental testing.

There are two main types of biosensors, based on the nature of the recognition event. The first one is the bioaffinity device that relies on selective binding of the target analyte to a surface-confined ligand partner (e.g. antibody or oligonucleotide). The second one is

biocatalytic device, where immobilized enzymes are used to recognize the target substrate (the best example is the immobilized glucose oxidase for diabetes monitoring).

In *Figure 32* an example of a bioaffinity biosensor is presented. This is a DNA biosensor and it functions through the hybridization of DNA on the chip and the complementary fluorescent DNA added. Here, the signal of hybridization is produced by a fluorescent dye.
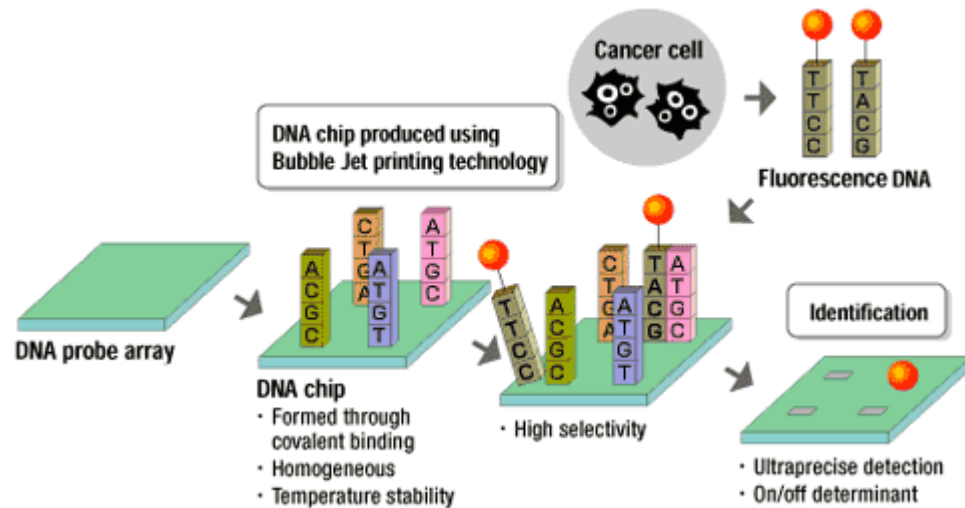
Figure 32: Example of a bioaffinity biosensor [90].

In *Figure 33*, an example of a biocatalytic biosensor is shown. Here, protein A is bound to the sensor, and then the antibody Anti-Cholera toxin is added. Following the cholera toxin and liposome bearing Horse Radish Peroxidase (HRP) are added on the sensor. Finally, the substrate of the enzyme is added to the reaction and a colored product appears.
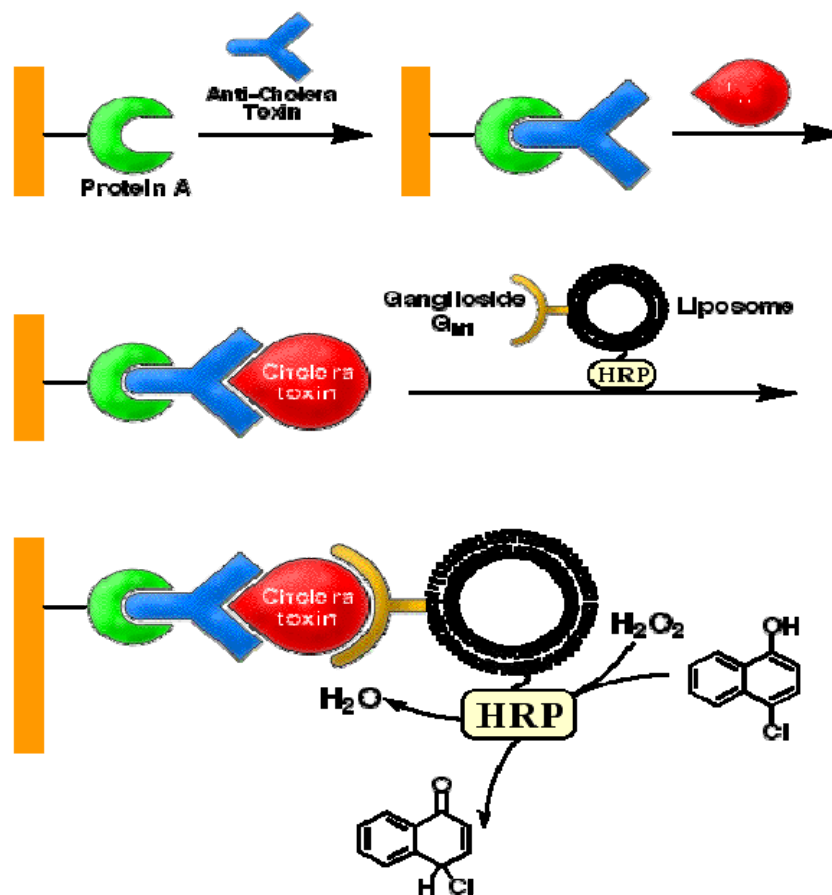
Figure 33: Example of a biocatalytic biosensor [91].

In this chapter we will focus on bioaffinity biosensors, and more particularly on DNA biosensors also called DNA microarrays.

The number of DNA biosensors has exploded with the completion of human genome analysis, characterization and deciphering. The information obtained from the project has opened the door to tremendous analytical opportunities ranging from diagnostics tests for mutations to the assessment of medical treatment, because it dramatically speeds up DNA analysis. Indeed, traditional methods for detecting DNA hybridization, such as gel electrophoresis or membrane blots, are too slow and labor-intensive for high throughput screening. To the contrary, DNA biosensors offer a promising alternative for faster, cheaper, and simpler nucleic acid assays [92].

DNA microarrays
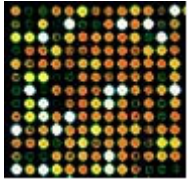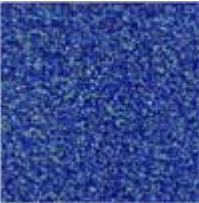
The definition of a DNA microarray (also called a DNA chip) could be the following*: "a collection of microscopic DNA spots attached to a solid surface, such as glass, plastic or silicon chip, forming an array for the purpose of expression profiling, monitoring expression levels for thousands of genes simultaneously [93] ".* For example, DNA microarrays can be used to identify disease genes by comparing gene expression in disease affected and normal cells [94].

For DNA biosensors, specific nomenclature has been created, to allow people to understand each other. The oligonucleotide attached to the chip, which has to be tested, is called the probe and the complementary strand is the target (***Figure 34***).
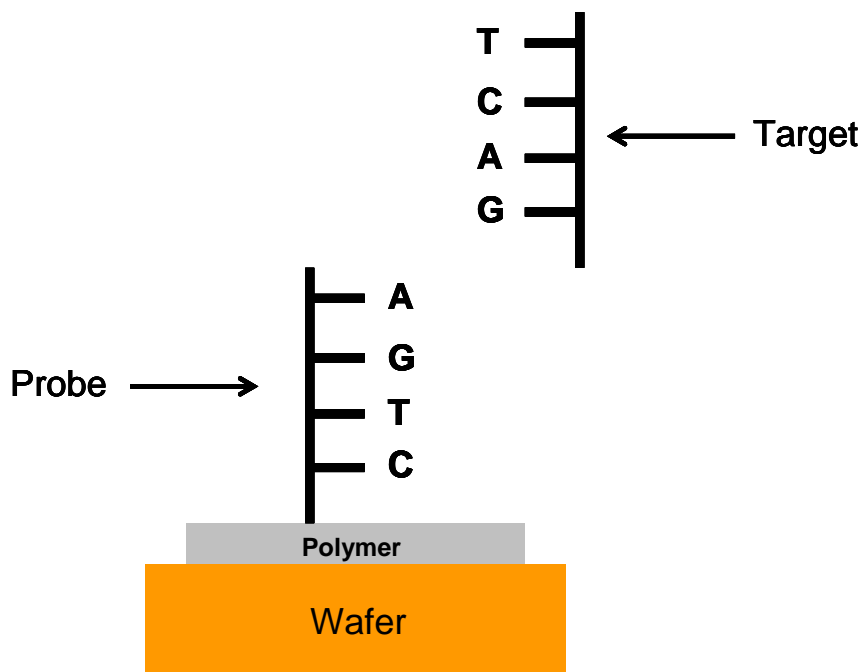
Figure 34: Side view of a DNA biosensor.

As mentioned before, several types of DNA biosensors exist. They have different sizes and can carry different quantities of DNA. ***Table 2*** contains two examples of DNA biosensors with their typical size and loading capacity.

Glass microarray	Chip
Size: 5.4cm x 0.9 cm	Size: 1.28 cm x 1.28 cm
10000 genes per array	300000 oligonucleotides per chip
Fluorescent label	Fluorescent label
2 experimental conditions per array	1 experimental condition per chip

Table 2: Principal characteristics of two kinds of DNA biosensors.

Various technologies exist to produce DNA microarrays. There is photolithography with pre-made masks, ink-jet printing, electrochemistry and even printing with fine-pointed pins onto glass slides.

Another way to prepare DNA microarrays is the direct printing of genes on the chip, for this purpose cells are grown in certain conditions and their DNA is used after amplification and purification. With such production conditions, it becomes possible to get samples with specific characteristics depending on the time, temperature, or growth

conditions of the cells where the genes are expressed (*Figure 35*). cDNA is first amplified by PCR. The purified aliquots (~ 5 nl) are printed on coated glass microscope slides by a robot. The target used for the hybridization is RNA. Two different RNA's are used; one is referred as the test and the second as the reference. Usually, the detection is made via fluorescence measurements (see below).
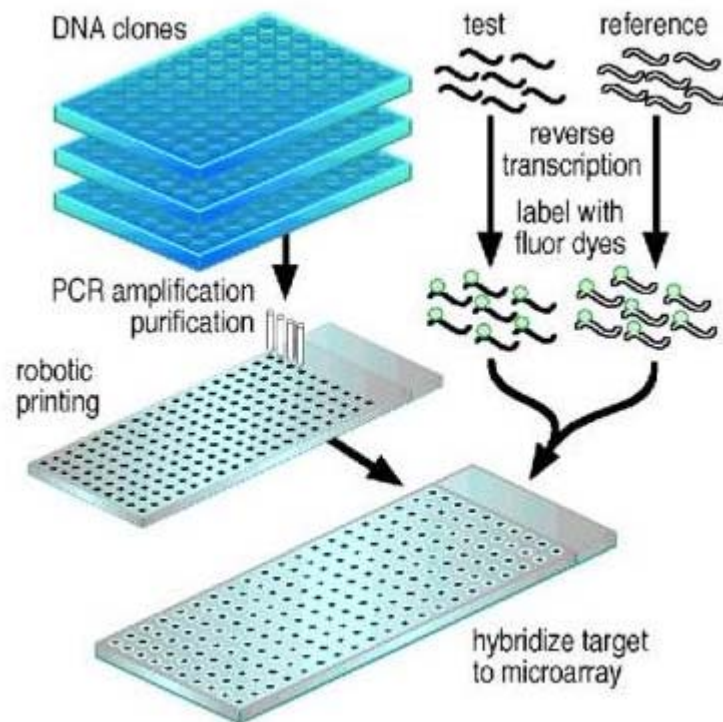
Figure 35: Scheme of a cDNA microarray [95].

Detection methods for DNA biosensor

After the hybridization has been performed, the result has to be read. In DNA biosensors there are only three ways to get signal transduction: by optical, electrochemical, or microgravimetric devices [92, 96-98].

Figure 36 shows the mechanism of an electrochemical device. First, the target is added to the probe DNA and the hybridization occurs. Then the indicator is added and its oxidation occurs, releasing some electrons. The resulting current leads to signal transduction to the detector [99, 100]. Of course, there are many other electrochemical components that can be used, like DNA intercalators, direct oxidation of nucleotides, or amplification of the signal via enzymatic processes.
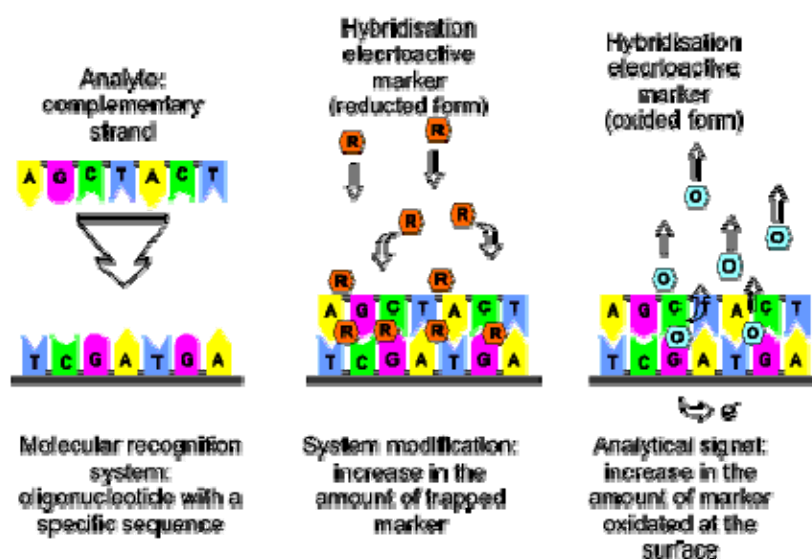
Figure 36: Electrochemical DNA biosensors using oxidation process [101].

In the case of optical detection, the target DNA must carry fluorescent labels, which emit a signal. As shown in *Figure 37*, two fluorescent dyes (Cy3 and Cy5 here) are grafted to two different batches of target DNA: sample A and B. These fluorescent targets are next deposited on the chip and the hybridization process is checked via excitation of the dyes by a

laser (step 5). The resulting emission of the dyes gives different colors that are seen at the bottom part of *Figure 37*, the color variation is due to the hybridization process occurring on the plate. If there is no hybridization, corresponding to no target present, there is only a black dot. If there is hybridization, one can have green or red dots, depending on the expressed gene.
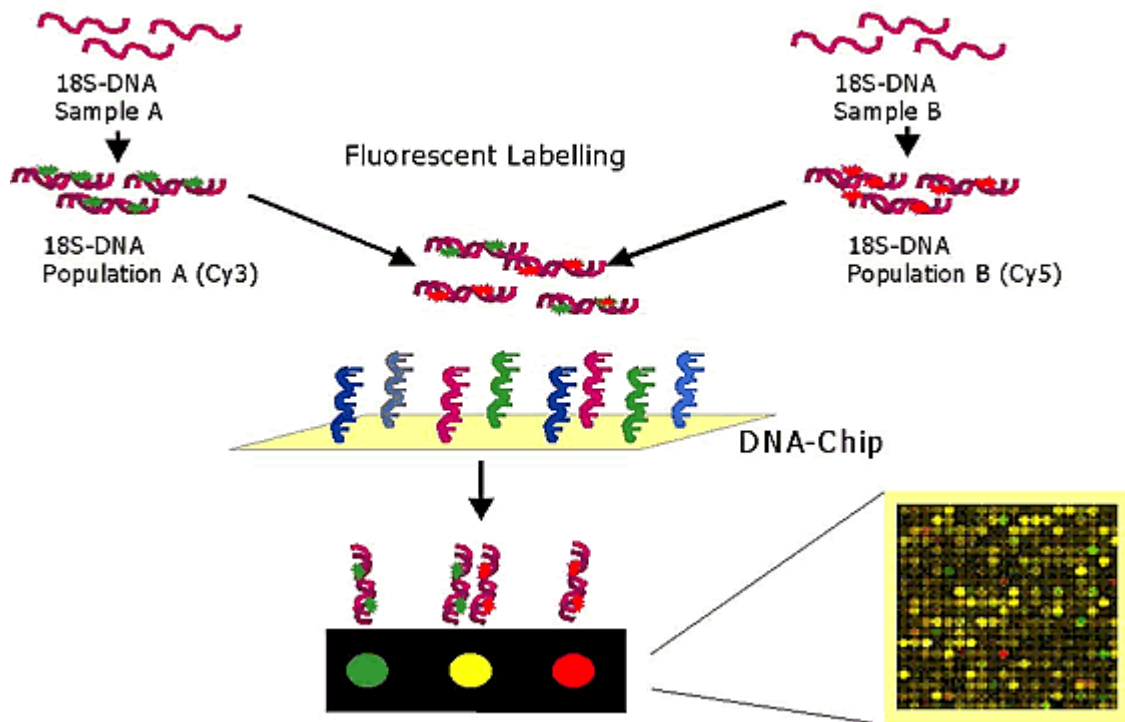
Figure 37: Optical detection in DNA biosensor.

The use of such systems allows the user to learn exactly which gene or sequence is present on the array and at which position. It is also easy to compare samples for which only the incubation time or the temperature were different. Such a system is useful to compare the gene expression in certain cells or tissues. One disadvantage of DNA microarrays is the loss of the sample. It is not possible to retrieve the sample after the measurements.

Use of nanoparticles in DNA biosensors

As shown in the first part of this dissertation, nanoparticles can be conjugated with a variety of biomolecules, and particularly with proteins. The conjugation of DNA to nanoparticles can lead to new devices with interesting properties. Here, the goal after combining DNA with nanoparticles was to use them in solution. There were two reasons for this: the first one is to design a nanometer scale DNA biosensor; the second one is to produce an analytical tool able to separate DNA from the rest of the solution, then allowing us to recover the targets DNA and study them in more details if needed.

First of all, some advances will be introduced concerning different kinds of nanoparticles and then our approach to this topic will be discussed.

1. Gold nanoparticles

The advances in DNA biosensors field are mainly from the miniaturization of the detection methods [102]. In many detection assays, the reaction volume ranges is between micro- and nanoliters. This immediately shows that the detection of biological samples at such extremely low amounts is a major challenge for clinical diagnosis and detection. Most biochemical assays require secondary detection of a label, because biomolecules lack intrinsic properties that are useful for direct highly sensitive detection. Label detection is then a key determinant of sensitivity, and the use of metal or semiconductor nanoparticles offer interesting opportunities in this direction.

Gold particles or other nanoparticles (like quantum dots) enable scientists to decrease the setup size and increase the detection sensitivity. The first use of gold nanoparticles for biosensors was made to enhance the signal in electrochemical devices [103] on solid surfaces.

In the sensor developed by Steel et al., the DNA-modified electrode is placed in a low-ionic strength electrolyte containing a cationic redox marker. The redox cations will be exchanged for native counterions associated with the nucleotide phosphate residue of the probe. Finally, the redox marker, "electrostatically trapped" at the DNA-modified electrode, is determined using chronocoulometry. Anyway this approach is insensitive to both the base composition and chain order (single-stranded vs. duplex). But the measured redox marker is

directly proportional to the number of phosphate groups present at the surface. The authors were then able to quantify the surface density of the probe as a function of the deposition procedure and the hybridization of target to those surfaces, based on electrostatic attraction between the cationic marker and the anionic DNA phosphate backbone (*Figure 38*).
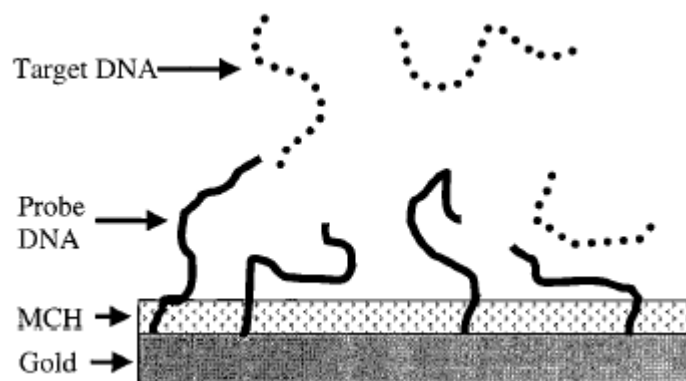
Figure 38: Scheme of a mixed probe-DNA/MCH monolayer in solution containing single-stranded target DNA [103].

The work of Mirkin et al. substantially contributed to application of gold nanoparticles for DNA biosensors. The Mirkin group, as well as other groups, have used inorganic nanoparticles as building blocks and chemically modified duplex DNA as the molecules interconnecting the particles [104-106], which led to a DNA/nanoparticles network. The interesting point was that gold nanoparticles provided a powerful tool to measure environmental changes in the sample. The behavior of gold particles is very sensitive to their environment (*Figure 39*). All those studies were motivated by the fact that gold nanoparticles could be surface-functionalized with thiolated oligonucleotides and then stabilized in aqueous biological buffers [107].

Figure 39 shows the first published example of DNA-functionalized gold nanoparticles [104]. A mixture of gold nanoparticles with surface-immobilized non-complementary DNA sequences (a, b) appears in red (strong absorbance at 520nm). When a complementary sequence (a', b') is added to the solution, the particles reversibly aggregate causing a red shift of the absorbance to 574 nm, thus appearing purple in the tube. This behavior comes from the DNA hybridization occurring between the probe and the target present in the tube. With this system it was also possible to make structural characterization of the DNA-gold nanoparticles networks, formed by DNA hybridization [98, 108].
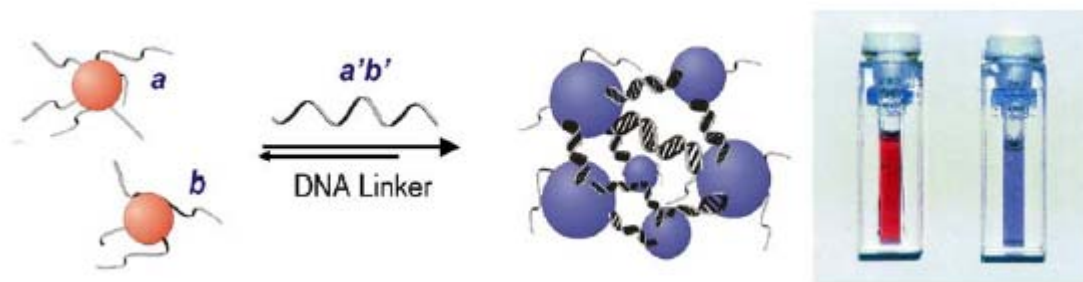
Figure 39: Optical properties of DNA-functionalized gold nanoparticles [104].

This group also developed a detector based on gold and silver nanoparticles [52]. The use of two different labels allowed a two-color-change-based method for Single Nucleotide Polymorphism (SNP) detection (***Figure 41***). A SNP is a DNA sequence variation occurring when a single nucleotide differs between members of a species (or between paired chromosomes in an individual). With this system it became possible to find out if there was a SNP present in the sample studied.

First of all, the oligonucleotide probes (a and b in ***Figure 40***) were functionalized with both Ag/Au core-shell particles and pure Au particles (B and C, respectively, in ***Figure 40***). In the presence of the complementary target, the nanoparticles formed aggregate structures. But no distinct color changes were observable by naked eye for Ag/Au core-shells, while a red-to-purple change was observed for pure Au nanoparticles. The aggregates obtained were investigated under TEM. The solutions were also spotted on C_{18} reverse-phase alumina TLC plate. With the core-shell particles, a distinct yellow to dark brown color change was observed upon particle assembly in the presence of the complementary target (***Figure 40***, parts EI and II). The same behavior was shown with the pure Au particles, with a color change going from red to dark purple (***Figure 40***, parts GI and II).

Target
5' TAG-GAA-TAG-TTA-TAA-ATT-GTT-ATT-AGG-GAG 3'
HS-$(CH_2)_6$-$(A)_{20}$-ATC-CTT-ATC-AAT-ATT TAA-CAA-TAA-TCC-CTC-$(A)_{20}$-$(CH_2)_3$-SH
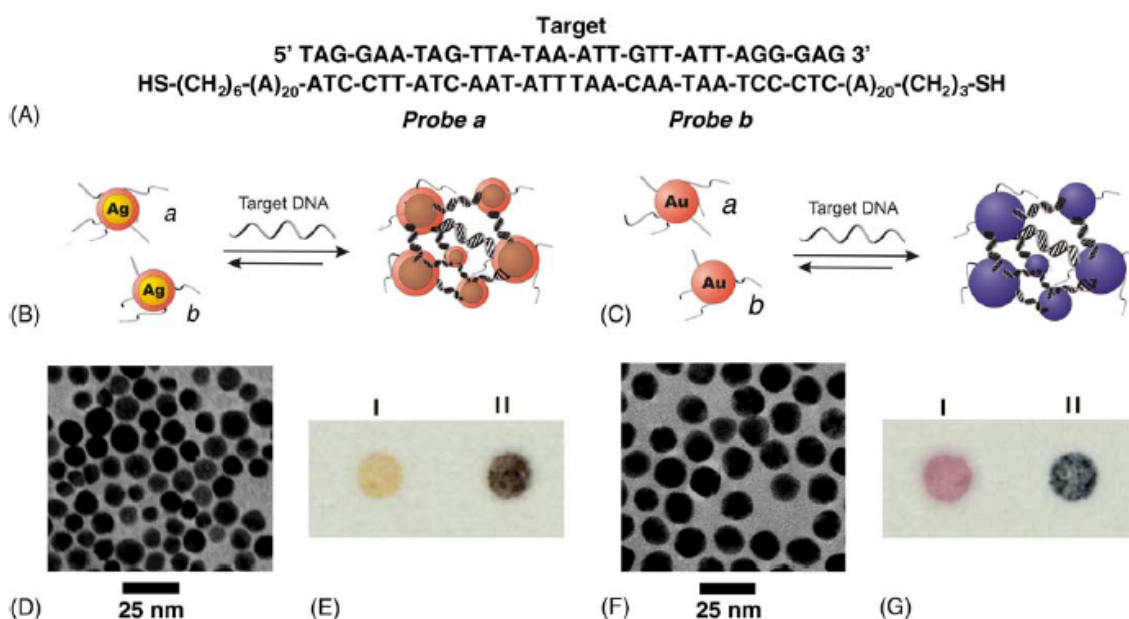
Figure 40: Two-color-change labeling for DNA detection. The experiment principle is the following, (A) are the mercaptoalkyl-capped oligonucleotide probes and a oligonucleotide target. On (B, C) are shown respectively the Ag/Au core-shell nanoparticles and pure gold nanoparticles-based detection system. The TEM pictures are showing (D) Ag/Au nanoparticles and (F) Au nanoparticles. Finally, the coloring reactions for each type of nanoparticles are shown. (E) represents the Ag/Au nanoparticles without and with target (respectively I and II). The same is shown in (G) with pure gold nanoparticles [52].

The use of two-color change particles was made to detect the presence of SNP's (*Figure 41*). In this case, two target strands were used: one span the wild type and the other one span a single nucleotide mutation in the beta-globin gene. Oligonucleotides perfectly complementary to the normal gene were used to modify the Au particles, and those perfectly complementary to the mutation target were functionalized with Ag/Au core-shell nanoparticles (*Figure 41* A). Two experiments were carried out to evaluate the suitability of the system. In the first experiment, the normal target was added to solutions containing the pure gold and Ag/Au core-shell nanoparticles probe systems, respectively. The particles were aggregated in the pure Au system with a higher melting temperature compared to the core-shell-particle system (*Figure 41* B and C). In this case the wild type was perfectly complementary to the Au probes, but there is a single mismatch with the core-shell system (*Figure 41*A). In the second experience, the mutant target was added to the same two probes

systems, and the opposite result was obtained (**Figure 41** E). In this case the core-shell particle system exhibited a higher melting temperature than the pure gold system.
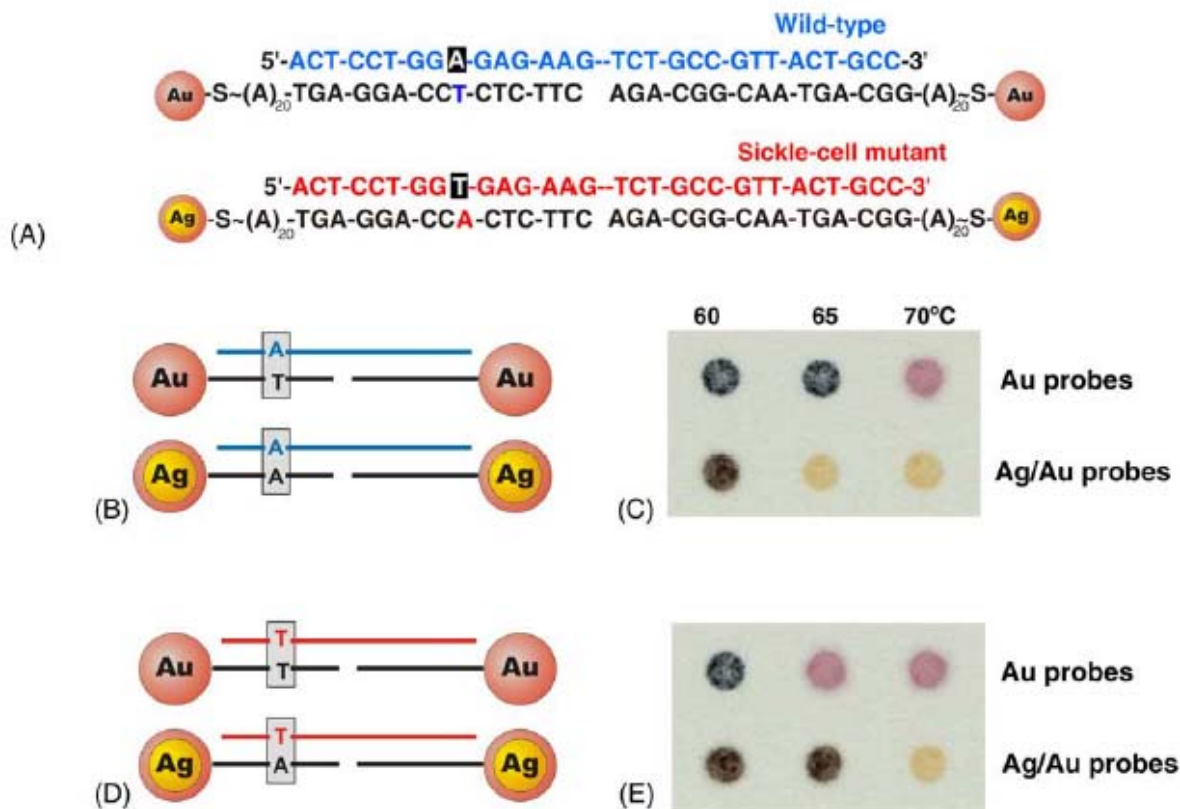
Figure 41: Evaluation of suitability of a two-color-change labeling system for SNP detection. *(A) represents the modified oligonucleotides and the targets. The parallel detection experiments in presence of wild-type targets (B) or mutant targets (D) are represented. Finally, the spot-test results are shown (C) in presence of wild-type target and (E) in presence of the mutant targets [52].*

The results of these experiments showed an easy way to distinguish the SNP targets by just observing different patterns in the TLC spot test.

Mirkin and coworkers also studied the behavior of diblock and triblock copolymers grafted with DNA oligonucleotides [109, 110]. The polymers used were ferrocene derivatives (**Figure 42**). The use of such polymers was made because of their high amplification capabilities. Other groups have also worked on the coating of gold, for example gold nanoparticles have been coated with silica core-shell particles [111].
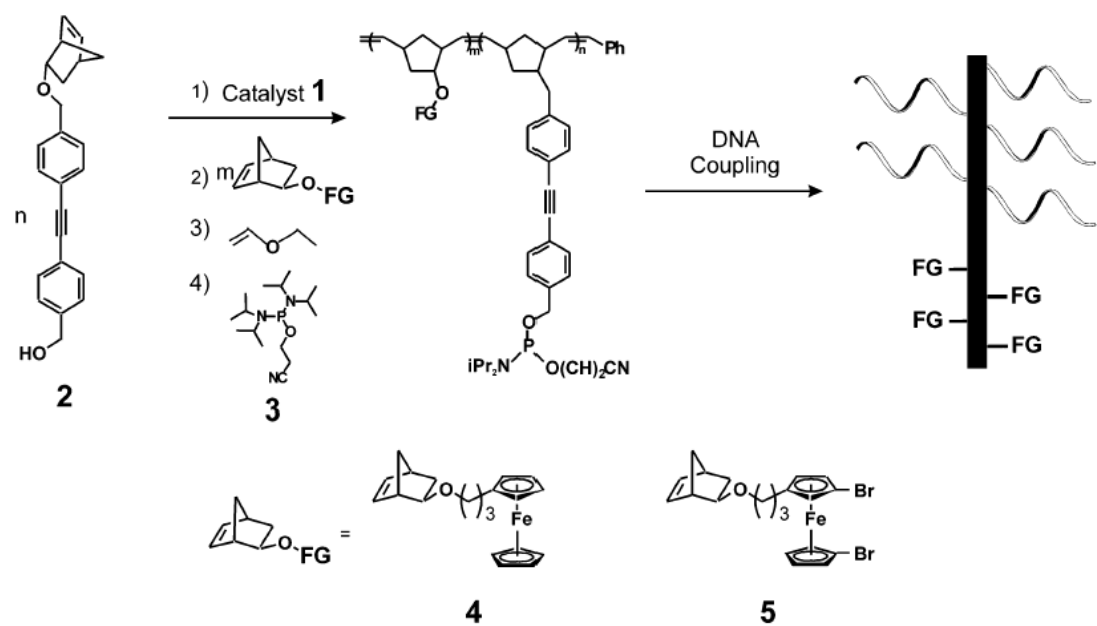
Figure 42: Synthesis of polymer-DNA hybrids [109].

Polymer-DNA hybrids were used in a three-component sandwich type electrochemical detection strategy [112, 113]. In all these systems, the third element was a gold electrode modified with the DNA probe (*Figure 43*).

a 3'-CCT AAT AAC AAT-5'
b 3'-TTA TAA CTA TTC CTA T₃-5'
a'b' 5'-GGA TTA TTG TTA AAT ATT GAT AAG GAT-3'
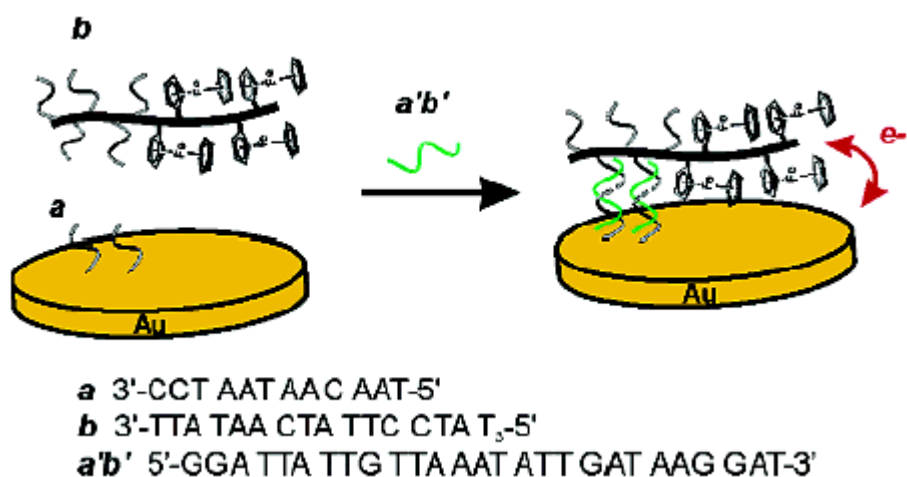
Figure 43: DNA detection based on polymer-DNA hybrids [109].

Diblock copolymers were successfully used to detect picomolar levels of oligonucleotides, where the presence of an electrochemical signal after DNA hybridization verifies the presence of a target strand. Furthermore, with two different diblock copolymer-DNA probes, small differences in DNA sequence mismatches (single base pair) can be reliably distinguished.

From all this work done so far it is obvious that gold particles are useful in both heterogeneous (e.g. microarrays) and in homogeneous solution detection formats in a lot of applications. On the other hand, this type of sensors can only be used with UV spectroscopy and in electrochemical sensors.

2. Quantum Dots

Other kinds of nanoparticles were developed for optical devices and solution. These particles are semiconductor nanocrystals, have a typical size between 2 and 10 nanometers and contain from a few hundred to a few thousand atoms of a semiconductor material. Usually, they are made of cadmium mixed with selenium or tellurium; this layer is then coated with an additional semiconductor shell (often ZnS) to improve the optical properties of the material. The structure of such a particle is shown in *Figure 44*.
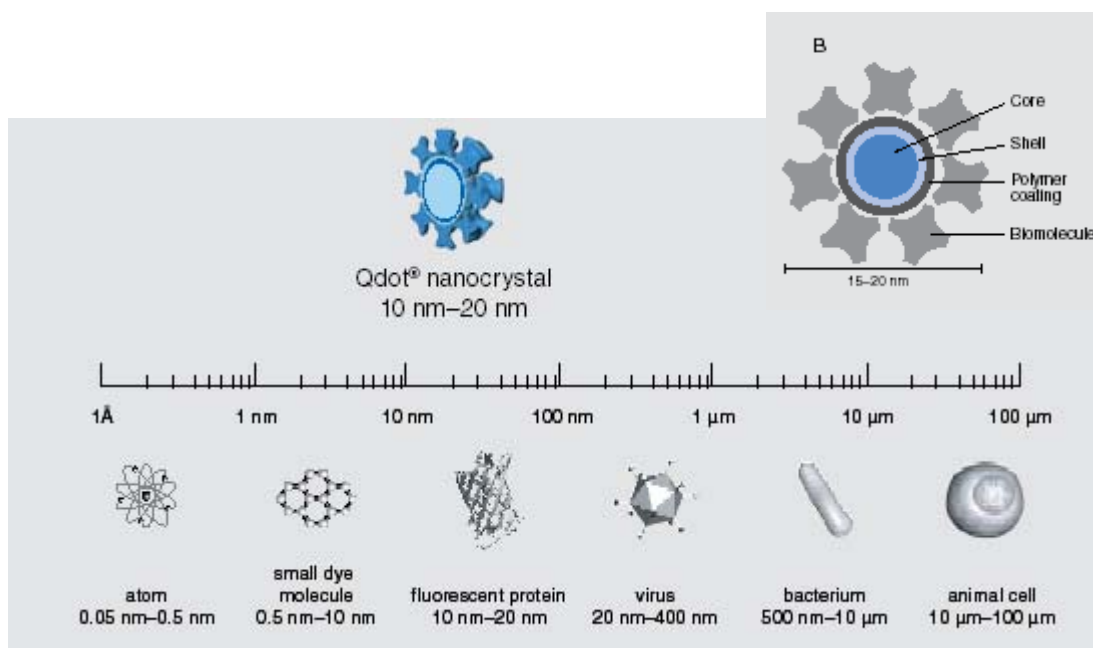
Figure 44: Typical size and structure of Quantum dots [114].

These particles are very attractive because, in contrary to classical organic dyes, they possess many properties attractive for biolabelling [115-118]. They have a broad excitation spectrum but narrow and precisely tunable emission by simply varying the size of the nanoparticles, negligible photobleaching, fairly high quantum yields and stability (***Figure 45***, ***Figure 46***).
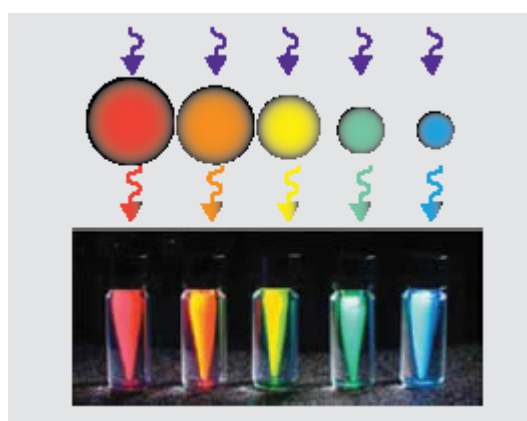
Figure 45: Fluorescence induced by exposure to ultraviolet light in vials containing various sized cadmium selenide (CdSe) quantum dots [114].
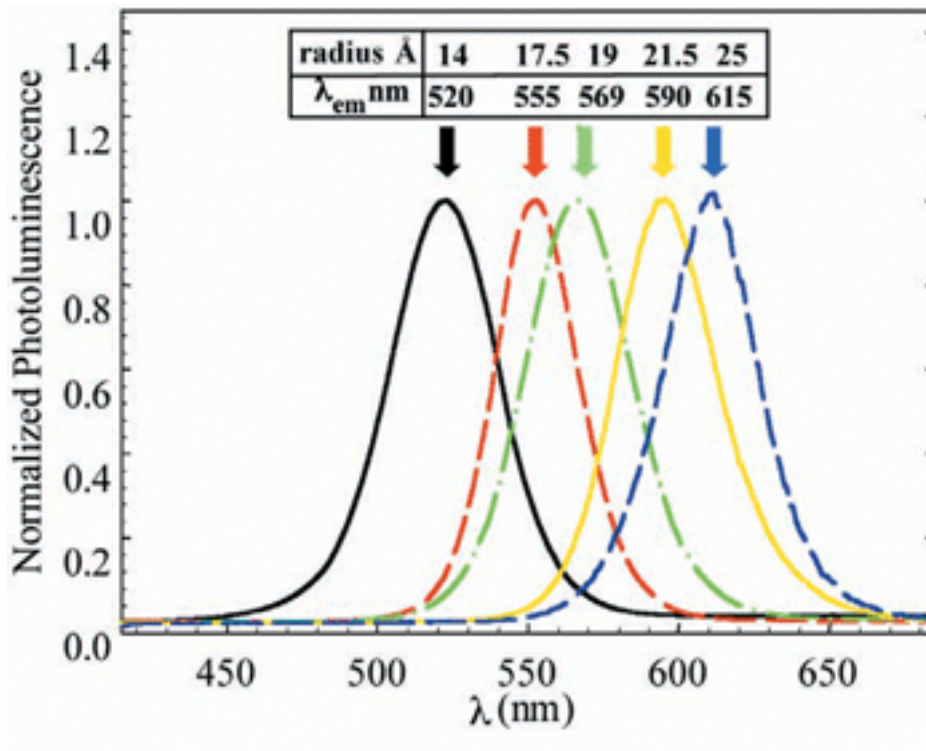
Figure 46: Emission spectra of several CdSe-ZnS quantum dots. The excitation is at 350 nm in all cases. The table gives the size of each QD and the maximum wavelength emission [119].

Quantum dots have a main drawback, because they are not soluble in water and are then not suitable for biological applications [120, 121]. The first possibility to overcome it, is to make them water soluble by reaction with an acid, like mercaptoacetic acid. The mercapto moiety binds to zinc atoms and the polar carboxylic acid group renders the QD's water soluble (*Figure 47*). In a paper from Letsinger and al [122], the third layer was made with trioctylphosphine oxide (TOPO) and trioctylphosphine (TOP). The resulting QD's were water insoluble, but this was overcome by the grafting of single stranded DNA onto the polymer shell (*Figure 47*), after a treatment with mercaptoacetic acid.
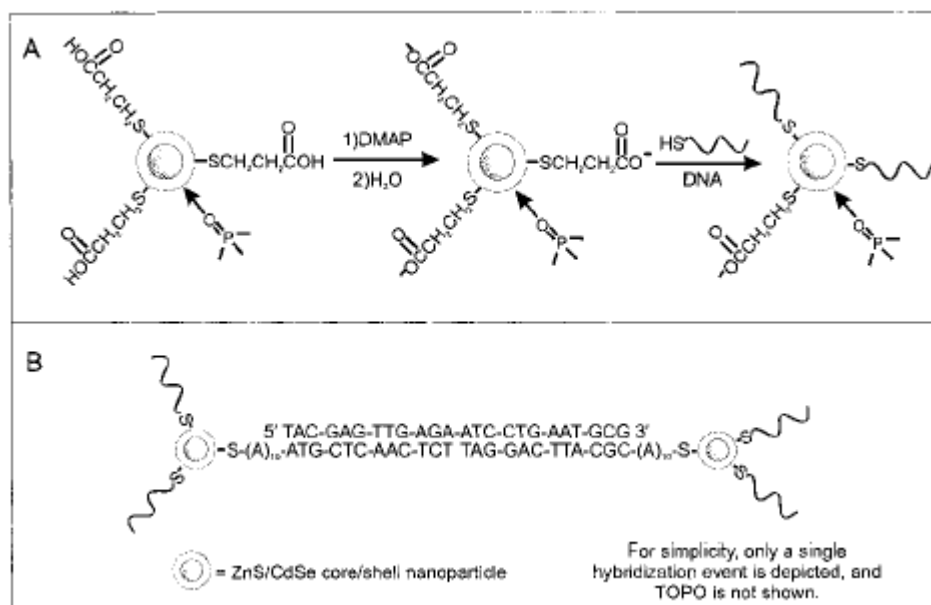
Figure 47: Scheme of DNA grafting method onto QD's nanoparticles (A), and oligonucleotide sequence (B) [122].

The second possibility is to form a third, polymer layer that is synthesized around the nanocrystals, then producing water soluble core-shell particles. The polymer used might be poly(ethylene glycol) (PEG), and even silica can be used [120, 123-125]. This strategy has numerous advantages compared to strategies that use a single direct bond to the surface of the nanocrystals: the polymerized layer ensures that the nanocrystals stay soluble in spite of a loss of the bound thiol. Afterwards, the modification of silica surface with different groups can be used to control the interactions with the biological sample.

Another possibility to add a polymer around QD's is to encapsulate them in core-shell particles (*Figure 48*). The group of Nie [126, 127] has incorporated QD's into polystyrene (PS) microbeads for multiplexed optical encoding. In this system, they have a triple-color encoded bead. In order to detect a signal, the target DNA molecules are directly labeled with a fluorescent dye or with a biotin (for binding to fluorescently tagged avidin). Then optical spectroscopy at the single-bead level yields both the coding and the target signals. The coding signals identify the DNA sequence, whereas the target signal indicates the presence and the abundance of that sequence.
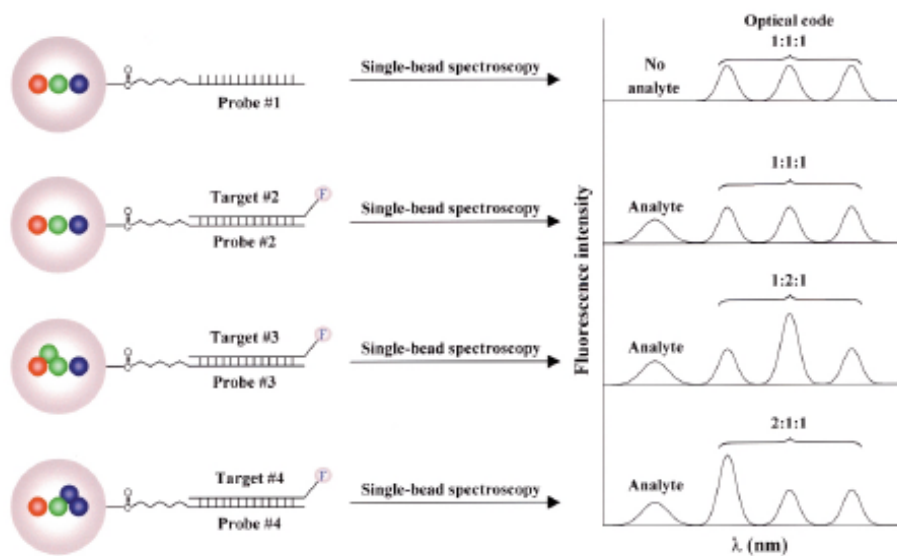
Figure 48: Illustration of DNA hybridization assays using QD's-tagged beads [126].

In ***Figure 49***, various signals obtained from the triple-color beads are shown. It is seen clearly that when control oligonucleotides (non-complementary sequences) are added, there is no signal detected (A, ***Figure 49***); whereas when a complementary sequence is added, there is a clear signal (B-D, ***Figure 49***).
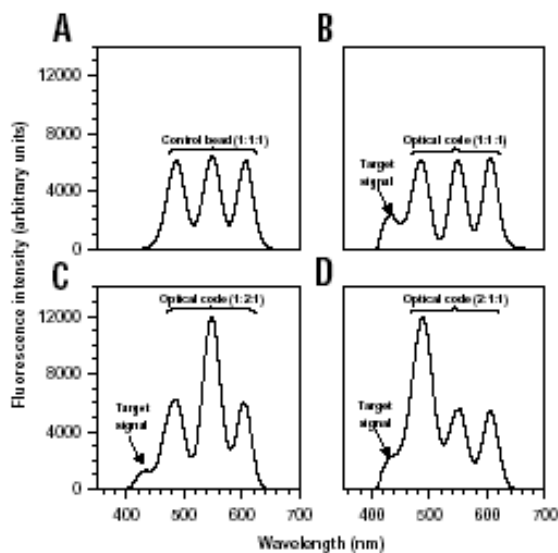
Figure 49: DNA hybridization assay using multicolor encoded beads. *(A) fluorescence signal with non-complementary target, (B-D) hybridization with different optical codes and different targets [126].*

Caruso et al. [128] produced QD's-labeled polystyrene beads via layer-by-layer (LbL) deposition process (*Figure 50*). This approach permits the formation of a new class of QD-beads bioconjugates for application in biotechnology. The interest in such a method is due to the fact that the number of layers, and then the quantity of QD's incorporated, is exactly defined. Other groups also worked on such polymer deposition on QD's [129].
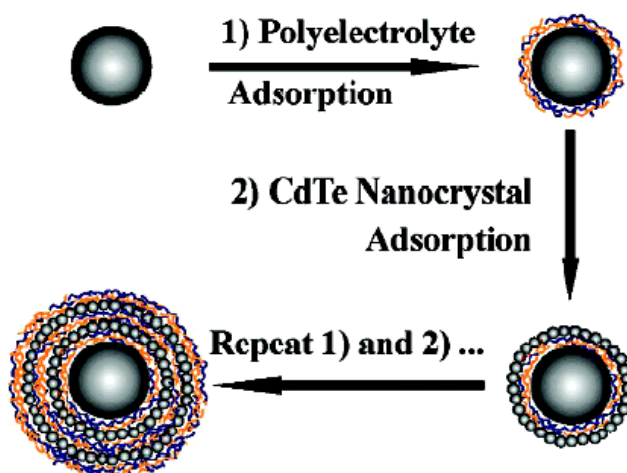
Figure 50: Illustration of the procedure used to prepare CdTe QD-microspheres via LbL assembly [128, 129].

The literature on that topic proves that nanoparticles attracted a lot of scientific interest, mainly because when put in solution, they allow easier handling than solid supports. Still, with these two kinds of nanoparticles a problem arises, concerning their modifications. In fact, QD's need to be modified before use for biological applications, and in the case of gold the thiol group could not be suitable for such experiments. We have thus searched for other nanoparticles, which could fulfill all the requirements we had for our system.

3. *Other nanoparticles*

3.1. Silica particles

Silica-based nanoparticles can be very useful in biological applications because they can be conjugated with biomolecules. This is due to the fact that the silica surface can be quite easily modified to contain sulphide, amine or carboxylate groups. Then, after appropriate surface modification, the nanoparticles can be directly used in bioanalytical applications [130].

Recently, some studies were made on DNA immobilized onto silica nanoparticles. Tan et al. prepared DNA-silica nanoparticles via disulfide bond [131]. **Figure 51** shows the principle of their system. First, silica nanoparticles are synthesized and then modified to end up with -SH groups at the particles surface. In the second step, disulfide modified oligonucleotides are attached to the silica nanoparticles, via a thiol - disulfide exchange reaction. Finally, the target DNA carrying a fluorescent dye is added to the DNA-nanoparticles and hybridization is studied.
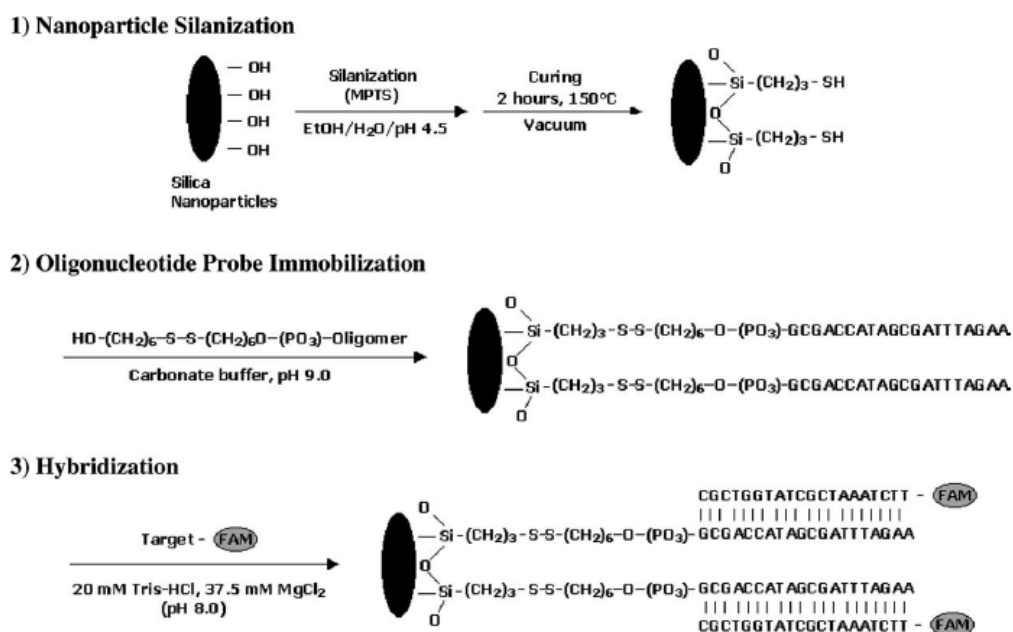
Figure 51: Principle of modification, immobilization and hybridization in the system [131].

In the ***Figure 52***, the results of the hybridization made with DNA-silica nanoparticles showed that significant signal was detected for the perfect target while no measurable signal was detected for a random sequence and buffer. As expected, no significant difference is seen between the perfect target sequence and the single-base mismatch sequence.
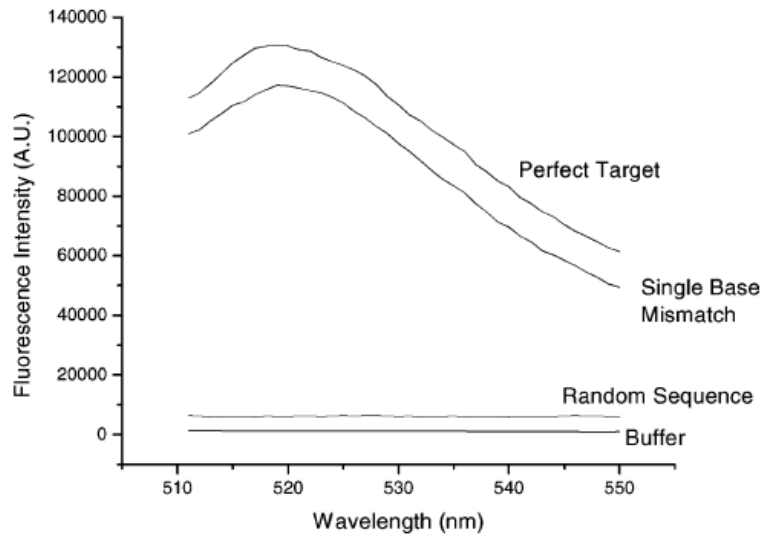
Figure 52: Results of hybridization in the system proposed by Tan et al [131].

3.2. Latex particles

Brown et al. first immobilized DNA onto nanoparticles in 1987 [132, 133]. They modified the method developed by Gilham in 1964 [ref] to immobilize oligonucleotides onto cellulose. In [132], the latex microparticles had an amino group at their surfaces. Then the immobilization was made via oligonucleotides containing an aldehyde or a carboxylic acid at their 5' end. An enzyme, T4 polynucleotide ligase, leads to DNA-beads grafting after functionalization of the oligonucleotides (***Figure 53***). As a detection method, a fluorescent dye was loaded in the microbeads, previously to the grafting of the DNA. Finally, a conventional fluorimeter was used for the DNA conjugates detection.
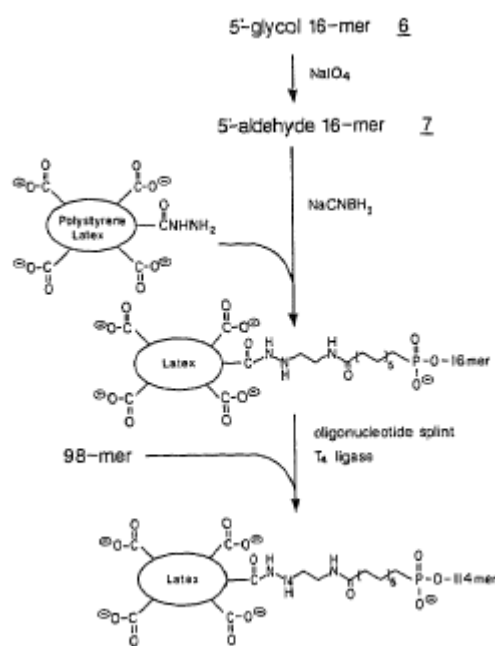
Figure 53: A two-step method for attachment of DNA to hydrazide latex spheres [132].

Another kind of DNA biosensors was produced by using latex particles for selective cleavage of mismatched DNA; this system was used for DNA diagnosis (***Figure 54***) [134]. In this work, the authors used a protein to detect sequence mismatches between a DNA probe and a target. The protein was MutS, which is a crucial element of the DNA mismatch repair system in many organisms such as E. Coli. They have then coupled MutS and anthraquinone to latex beads and checked if this system was able to detect mismatches in a biosensor. For the detection they used SYBR-gold, a dye able to detect double-stranded DNA but not single-stranded DNA. They were then able to see if the DNA was cleaved or not, and consequently if the sample had a mismatch or not.
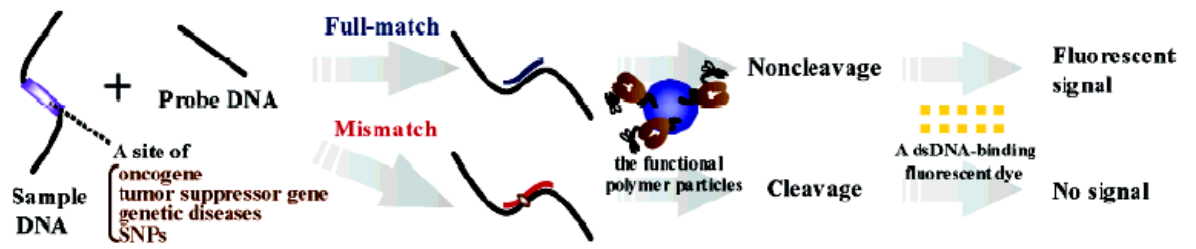
Figure 54: Representation of DNA detection mismatch using functional polymer latex particles [134].

Introduction to a new kind of biosensor

From the studies reported so far, we thought that use of polymer nanoparticles could be interesting for the development of a new kind of a DNA biosensor, because they can be used in liquid reactions. Moreover, an additional advantage of nanoparticles is that fluorescent dyes can be encapsulated inside (like demonstrated with QD's), and because they can be loaded with a high quantity of a dye, it is potentially a far more sensitive system than linking individual dye molecules. The intended functional polymer latex particles offer several distinct advantages compared to other devices. Firstly, they are easy to handle, they can be separated from solution by centrifugation and be collected. Secondly, because of their structure, it is possible to get a better modification yield. In all the literature reports, the system designed was not designed to return the DNA sample after hybridization measurements, which is sometimes important when the quantity of the sample is really low and it has to be used for several experiments.

The first attempt we made to produce a new DNA biosensor was by using thiolated polymer vesicles, where we wanted to graft the oligonucleotide via a disulfide bond (***Figure 55***). In this system, the oligonucleotide should be modified to have a thiol group at its 5' end. To this aim, a standard method was used to synthesize the ABA triblock copolymer; finally an end-group modification was performed.
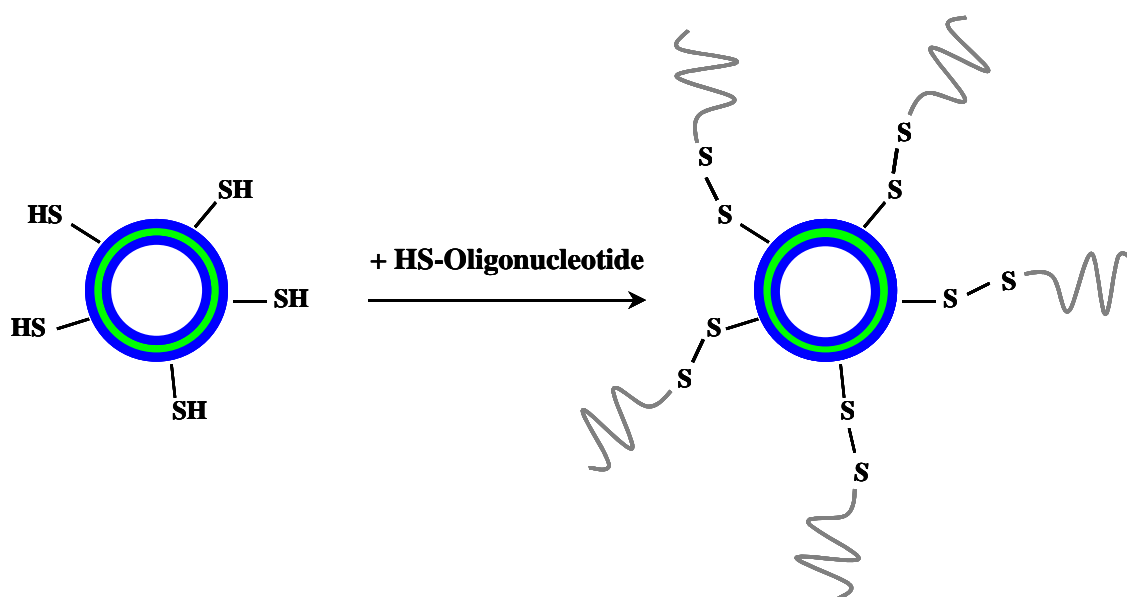
Figure 55: ABA triblock copolymer - DNA system.

First of all, we had to quantify the thiol available at the surface of the nanovesicles. For this experiment we used iodometric titration (***Figure 56***) [135].
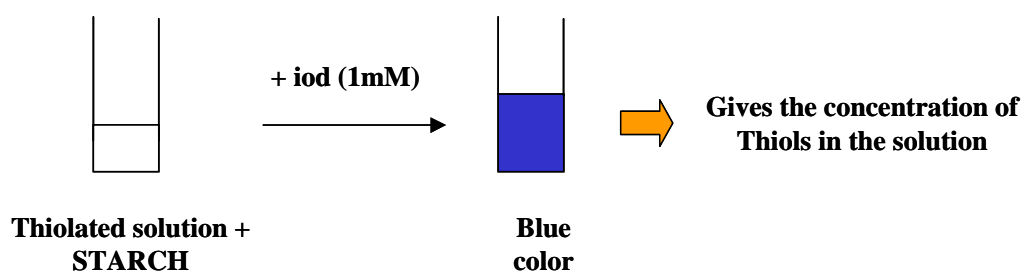
Figure 56: Scheme of the thiol quantification method.

In this method, potato starch is used as color indicator and added to the sample solution. Then a 1 mM aqueous iod solution makes the colorimetric quantification of thiols present in the sample. The reaction equation enables the calculation of thiol groups present in the sample (***Equation 1***).

$$2RSH + I_2 \longrightarrow Complex \longrightarrow RSSR + HI$$

$$\text{At the equivalence point:} \quad n(I_2) = 2 * n(SH)$$

Equation 1: Reaction equation of the iodometric reaction.

In *Figure 57*, the results of the thiol quantification are presented. For the sample CF11 containing SH groups we have a good agreement between the theoretical numbers of SH groups and the number calculated from the experiment. For theoretical calculation of SH groups in the polymer we take advantage of the fact that in one polymer chain we have two SH groups, one at each end. Then by knowing the polymer concentration used in the sample and the molecular weight of the polymer, we can achieve the number of moles of SH in the polymer. For that we assumed a stretched conformation of the polymer molecules within the vesicle membrane. Moreover, the SH groups inside the vesicles are not sensitive to the test because the reactants cannot go trough the membrane.

We can also see that in the sample containing no thiol groups we do not have any reaction occurring, which means no color change during the color quantification. Finally, with this method we were able to quantify the thiol content in our samples with an error of +/- 5 %.
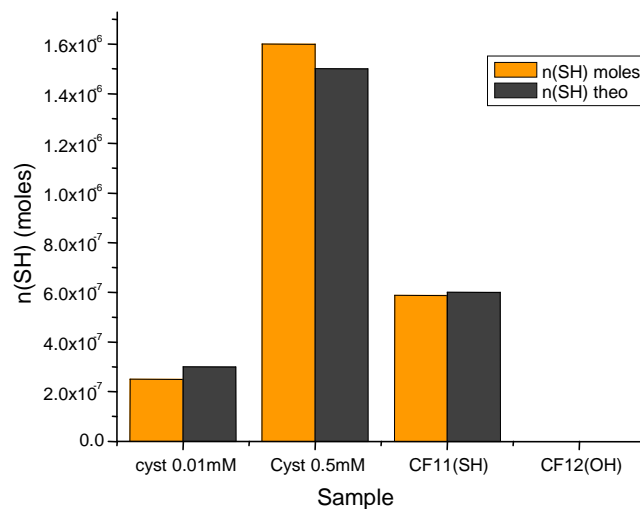
Figure 57: Results of thiol quantification.

After quantifying the thiol content on the vesicles, we tried to graft the oligonucleotides. For that we had to modify the oligonucleotide 5' end to get a thiolated oligonucleotide. We tried different methods to achieve the modification. The first one was using cystamine, imidazole and EDC (*Figure 58*) [136].
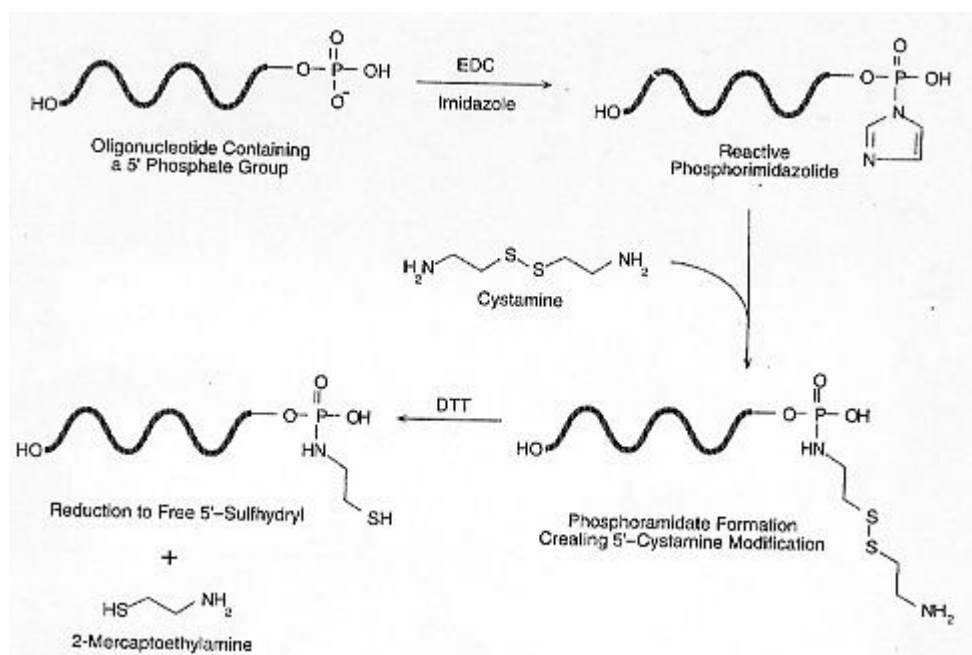
Figure 58: Oligonucleotide labeling with cystamine, EDC / imidazole method.

This method was successfully applied by different groups to create a thiol group at the 5' end of a DNA. Here, the thiol group was linked to the phosphate via a phosphoramidate bond. We modified the procedure and did not use DTT at the end, because the oligonucleotide is more stable with a disulfide bond than with a free thiol group. After purification of the oligonucleotide, MALDI-TOF was made to check if the modification was successful. Modification of the oligonucleotide was seen, but the oligonucleotide peak was quite small (*Figure 59*). On this spectrum, the peaks below 1000 correspond to the matrix and impurities.
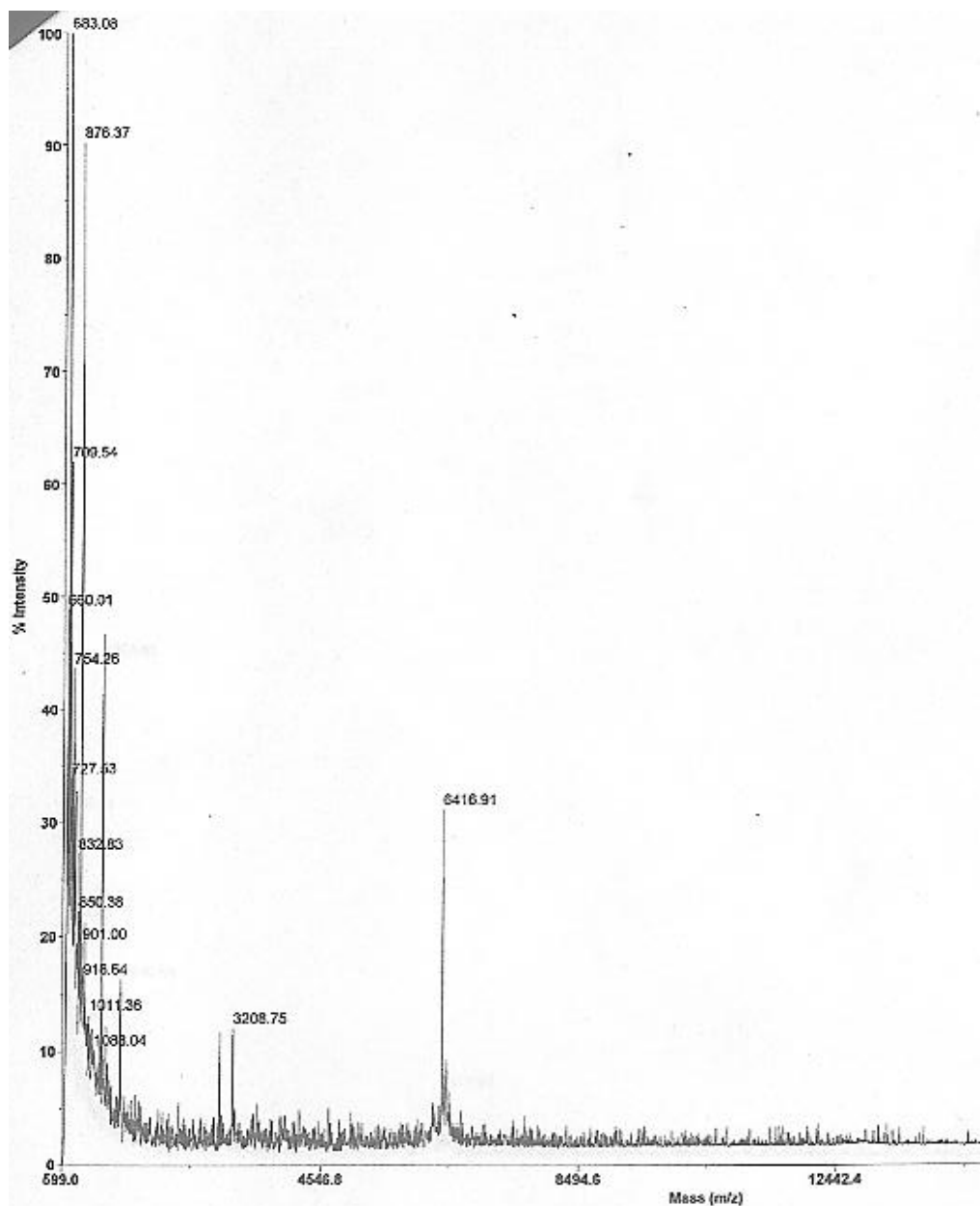
Figure 59: MALDI-TOF spectrum of thiol-modified DNA via cystamine, imidazole and EDC method.

We tried to estimate the quantity of DNA in the sample by UV measurements, but the concentration was too low to allow detection.

We then decided to use another method for the modification. This time, we used bacteriophage T4 polynucleotide kinase and ATPγS, we had the transfer of a thiolated phosphate onto the OH 5' end of the oligonucleotide (*Figure 60*).
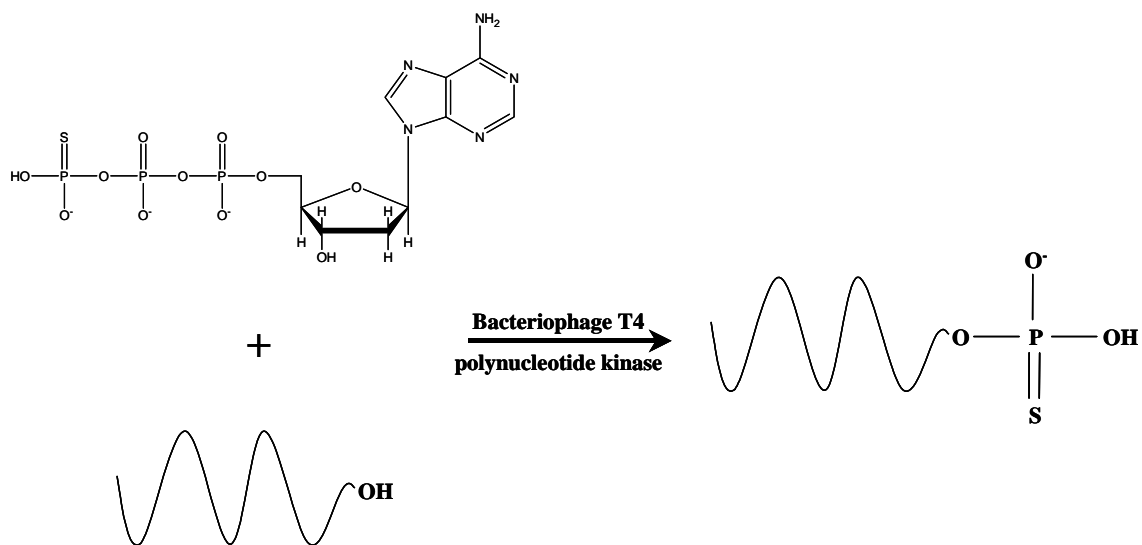
Figure 60: Oligonucleotide with bacteriophage T4 polynucleotide kinase.

The modification and the following purification of an oligonucleotide with this method are well known [137]. After purification MALDI-TOF spectra were made (*Figure 61*). We could not see the modification, but a UV measurement was done on the sample in order to estimate the concentration of modified DNA. To this aim, OD was measured at 260nm, and we found that the yield of the reaction was around 10 %.
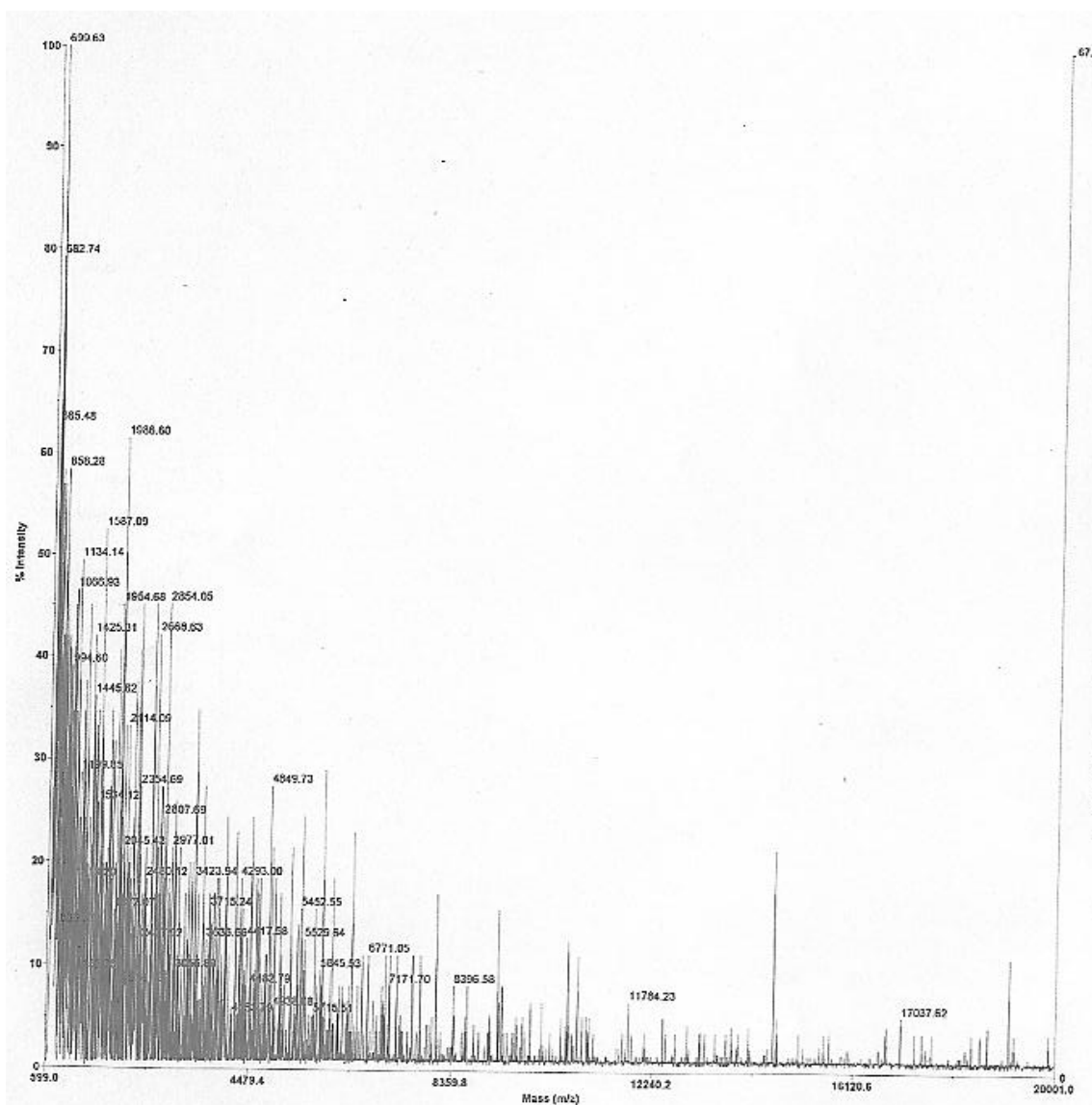
Figure 61: A MALDI-TOF spectrum of thiolated oligonucleotide modified by the enzymatic method.

The modification was successful, but once again the quantity of the modified oligonucleotide was very low. Alternatively, we tried to graft a commercial oligonucleotide carrying a spacer and a thiol at its 5' end to the thiolated vesicles.

For the formation of the disulphide bond, we used the procedure from Bernkop-Schnürch et al. [135, 138]. The pH of the vesicle solution was increased to 5.8, the DNA was then added, and the resulting solution was incubated at 37°C for various time periods with constant shaking. To check if the reaction was completed; MALDI-TOF, agarose gel and thiol

quantification were used, but no positive result was seen (***Figure 62***). In the figure we can see the peak from the thiolated oligonucleotide alone at 6603 Da; we can also see at around 2000 Da the peaks coming from the polymer (circle in ***Figure 62***).
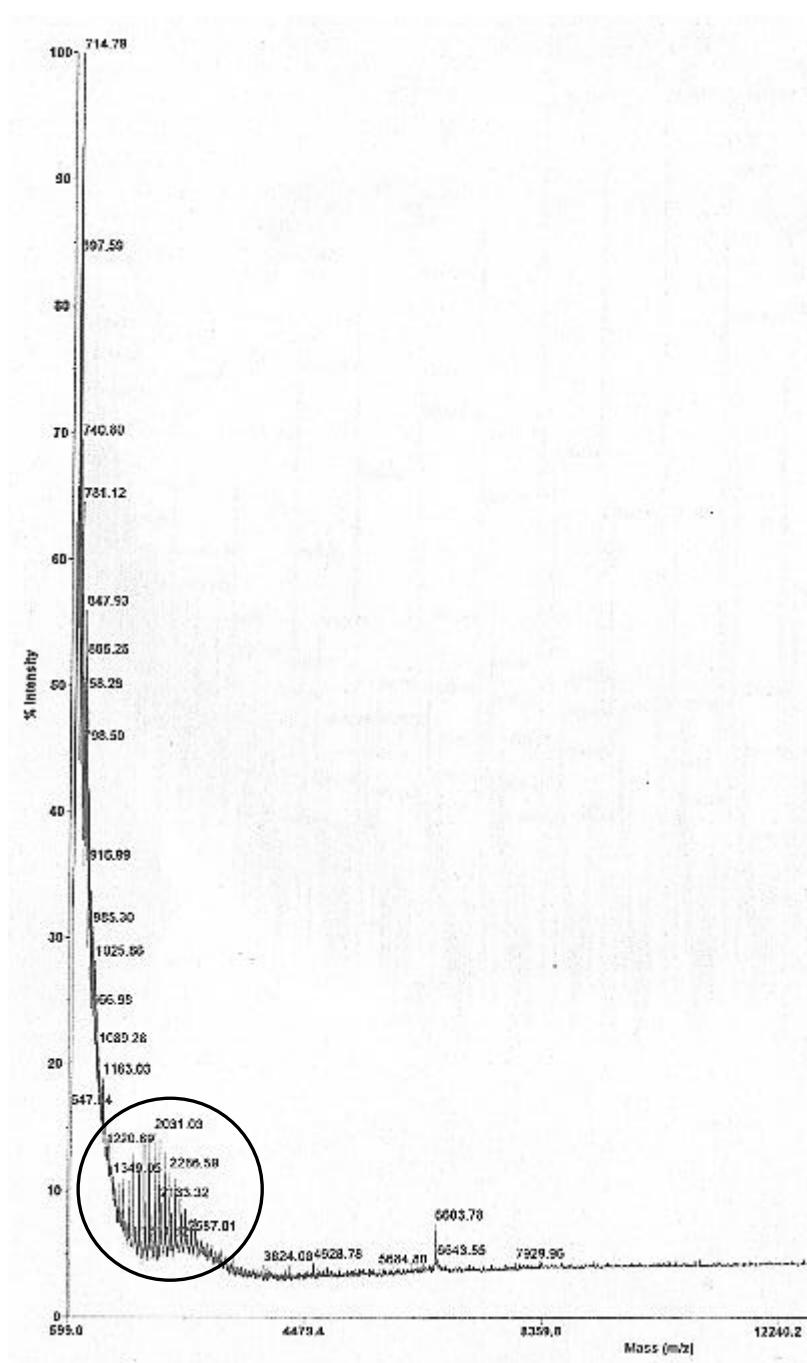
Figure 62: MALDI-TOF spectra of ABA triblock copolymer vesicles coupled to thiolated polymer.

This might result from problems encountered during sample degassing to prevent thiol-thiol interactions between two vesicles, but also from difficulties to achieve the disulfide bond between the vesicles and the oligonucleotides.

Finally, after all these unsuccessful trials to graft the polymer with the oligonucleotide, we realized that our system was not appropriate for biosensor development. Moreover, as explained before, because of the low density of the material (the vesicles density is nearly equal to 1 mg/cm^3), vesicles cannot be pelleted. All these difficulties led us to the change of the system.

We decided instead to use latex core-shell particles. Such nanoparticles have many advantages, as described previously. The structure of a core-shell particle is shown in *Figure 63*. These particles consist of a central core structure made by the polymerization of one monomer. Then a second polymer is synthesized around the core to form the shell. The two polymers used can have different behavior towards water, for example one can be hydrophobic and the other hydrophilic [139].
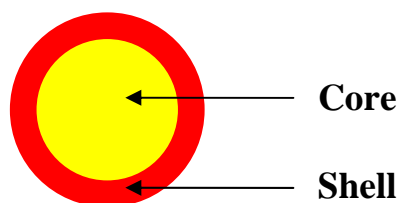
Core

Shell

Figure 63: Schematic representation of a core- shell particle

We used the two-step emulsion polymerization [140, 141] to synthesize core-shell nanoparticles (*Figure 64*). The poly(St-MMA-AEMA-DVB) shell provides us with the amino functionalization of the particles.

surfactant

PDMS core

Cross-linked shell

polymer nanocontainers

polymerization

polymerization

precipitation or/and ultrafiltration

M1: octamethyltetracyclosiloxane

M2:methylmethacrylate, styrene, divinylbenzene (crosslinking agent)

Step 1

Step 2

Step 3
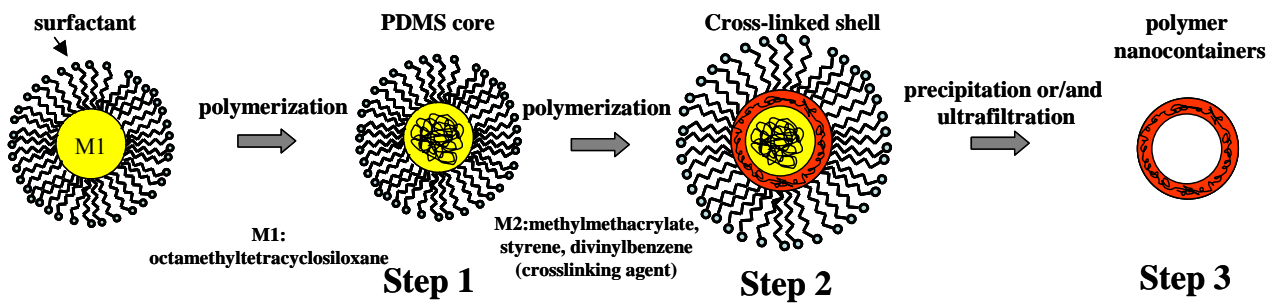
Figure 64: Representation of the two-step emulsion polymerization.

There are many advantages of the two-step emulsion polymerization. This procedure allows control of the size of the particles (from 100 to 900 nm), the thickness and number of shells, the amphiphilic properties, the network density and also the spherical architecture [142]. With this procedure we are also able to control the amino functionalization degree of the shell.

Core-shell particles can be easily pelletable, because of their high density. In this case the particles are not functionalized with thiol groups but with amino groups. Indeed, we wanted to develop a system where the particles can be centrifuged; they are then separated as a pellet form the solution. The grafting is then done via a phosphoamide bond (*Figure 65*). The oligonucleotide is bond to the nanoparticles via its 5' end, and more particularly via the γ-phosphate.
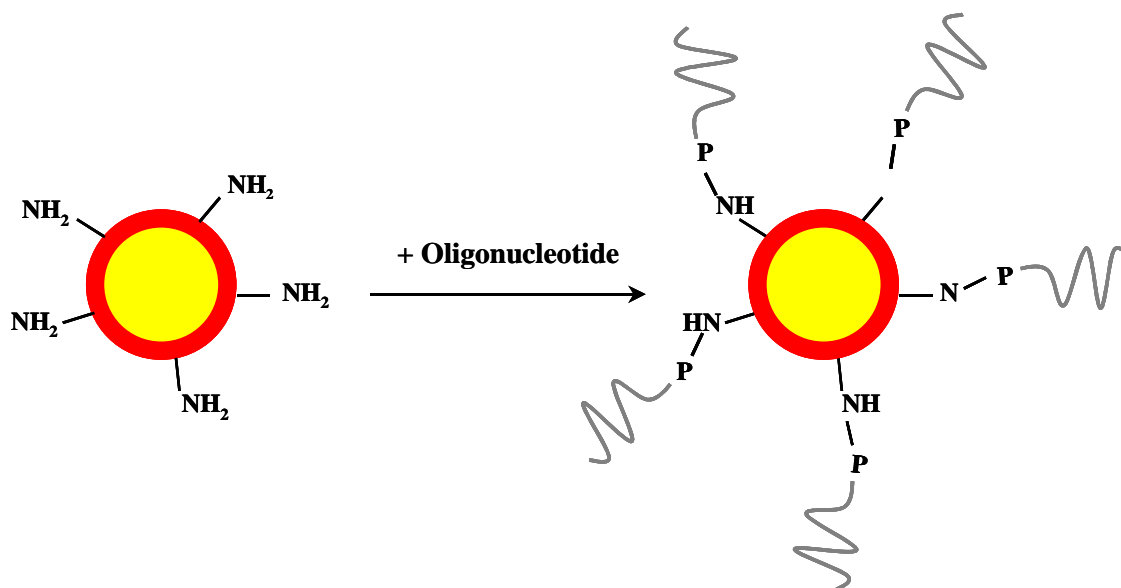
Figure 65: Nanoparticles-based DNA-biosensor.

In this work, we describe the preparative method for the functional polymer latex particles, the characterization of the covalent binding of DNA to those nanoparticles, and the hybridization efficiency of the detection system. We also study the effect of the oligonucleotide length on the hybridization process. Indeed, some studies were made on the steric factors that influence hybridization on solid supports. We wanted to see if in solution the same effect might occur [143].

In order to study the hybridization process, we used two different approaches based on fluorescence assays. The first one employs oligonucleotides labeled with Cy5 dye at the 3' end, and FCS as detection method. We chose the FCS, because it provides information on the hybridization process, and more particularly the hybridization kinetics at the surface of the core-shell particles within one measurement. Moreover, some groups proved that DNA hybridization could be studied with this setup [144-147].

In the second approach, a DNA intercalator: SYBR® Green is used, which is 10000 times more fluorescent when bound to double stranded DNA than when it interacts with single stranded DNA. For this measurement we used a thermocycler setup to measure, during several time cycles, the fluorescence variations of the hybridization and dehybridization of DNA in our sample. We therefore directly obtain information whether hybridization is occurring or not in our system, we can also determine the melting temperature (Tm) of our

system. Consequently, we can learn if the particles destabilize the DNA hybridization process or not.

Results and discussion

1. Oligonucleotides used

In order to get information on the effect of the nanoparticles on the hybridization process, we decided to use different length of oligonucleotides. We then added a polyT tail at the 5' end of the oligonucleotides (***Figure 66***), because several studies showed that a spacer between particles and the molecule grafted would overcome the steric hindrance at the particle surface [26, 30].

In the ***Figure 66***, the sequences of 80 and 125 nucleotides are the same except the number of thymines (in red). In the 80-nucleotide there is 5 T's and for the longer one, we have 50 T's. The DNA of 20 nucleotides was used as a control without T.

20 nt: GAG TAT TCA ACA TTT CCG TGT

80 nt: TTT TTG ACC TGC AGG CAT GCA AGC TTG GCA CTG GCC GTC GTT TTA CAA CGT CGT GAC TGG GAA AAC CCT GGC GTT ACC CA

125 nt: TTT TTT TTT TTT TTT TTT TTT TTT TTT TTT TTT TTT TTT TTT TTT TTT TTG ACC TGC AGG CAT GCA AGC TTG GCA CTG GCC GTC GTT TTA CAA CGT CGT GAC TGG GAA AAC CCT GGC GTT ACC CA

Figure 66: Oligonucleotide sequences used for a DNA biosensor. *Sequences are given from 5' to 3' end.*

2. Characterization of functional polymer latex particles

Functional polymer nanoparticles composed of a PDMS core and a shell of PS, PMMA, DVB and amino functional comonomer (AEMA) were chosen as support. The proposed method for their synthesis is the two-step emulsion polymerization via core-shell particles, which is often employed to obtain stable functional polymer nanoparticles. This technique allows the particle optimization by varying their size, shell thickness, cross-linking density and is therefore suited for scaling up the production of different types of

nanoparticles. Even more, this type of synthesis allows also the incorporation of functional groups (like amino groups) on the periphery of the polymer nanoparticles. For that, direct polymerization of suitable functional comonomers was performed. Eventually, such functional polymer nanoparticles consist of a polydimethylsiloxane core with 180 nm diameter, surrounded by an aminofunctionalized shell of 20 nm thickness (*Table 3*, *Figure 67*). They possess spherical shapes, and are very monodisperse in size. Additionally, they do not exhibit auto fluorescence. Due to their aminofunctionalized shells, the nanoparticles have high surface reactivity and can be easily grafted via a covalent bond with DNA strands.

Particles	Diameter (nm) by DLS/TEM	Core diameter (nm)	Shell thickness (nm)
Aminofunctionalized	230/200	180	20

Table 3: Characteristics of core-shell particles
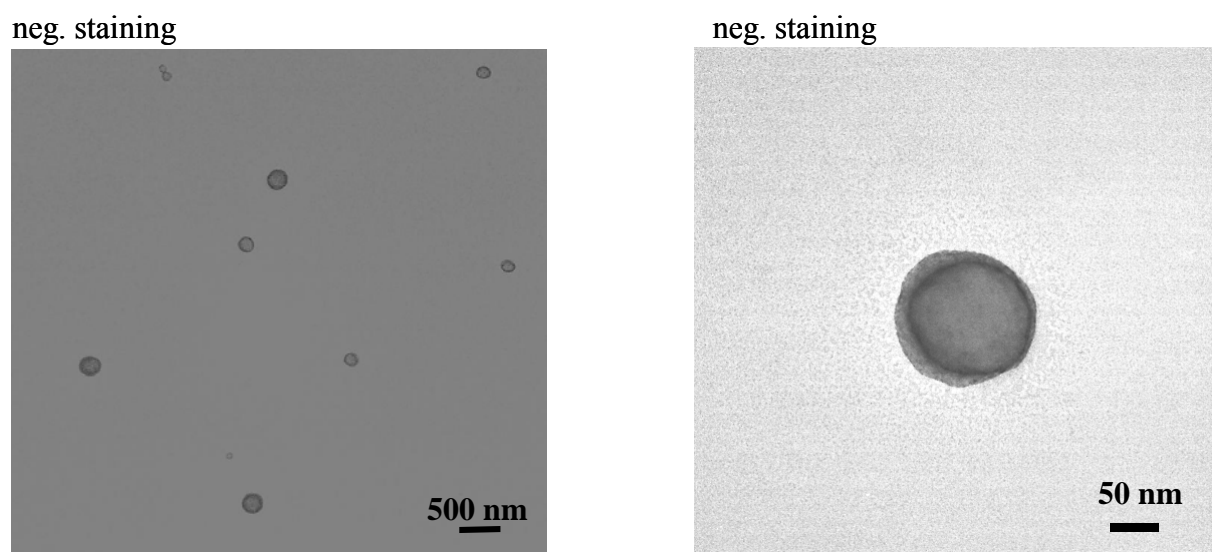
Figure 67: Transmission electron microscopy pictures of core-shell particles.

3. Quantification of amino groups at the core-shell particles' surface

The amino group quantification was performed by the fluorescamin method. For this method, a standard curve is made with different concentration of aminoethylmethacrylate. The fluorescence, obtained when amino groups are present, in each sample is measured at 477 nm (***Figure 68***).
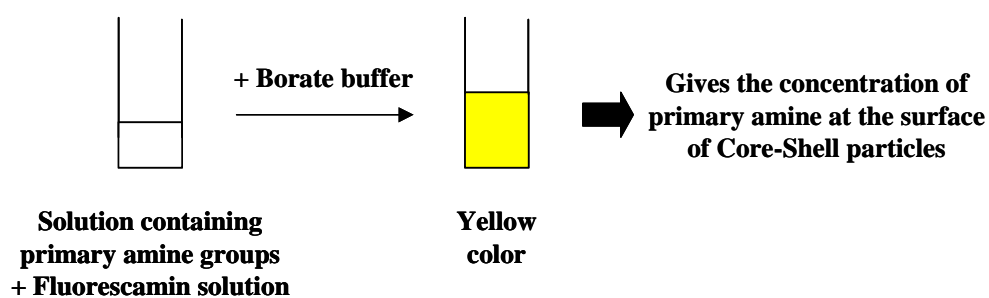
Figure 68: Fluorescamin method for primary amine quantification.

From different intensities obtained, a calibration curve is made. With this curve it was possible to determine the quantity of amino groups present at the surface of our particles (***Figure 69***).
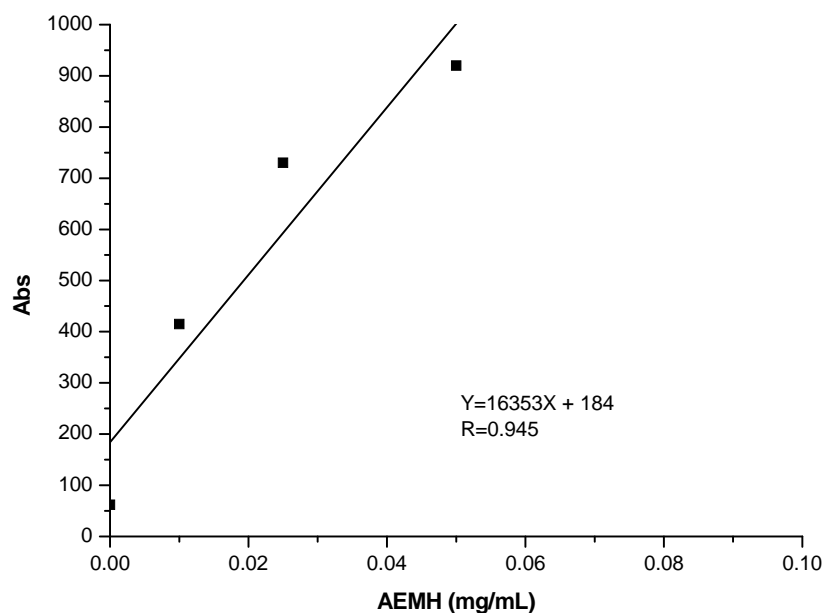
Figure 69: Fluorescamin method standard curve.

According to the standard amino group quantification, the used nanoparticles had on their surface 66 μmol of amino groups/g dry particles.

4. Characterization of DNA-carrying latex particles

4.1. Infra-Red Spectrometry

In order to prove the covalent immobilization of DNA molecules on polymer latex particles, the nature of chemical group on the surface of particles was investigated by FTIR spectra to detect the presence of the newly created phosphoamide bonds. The measurements were performed with the three lengths of DNA strands (20, 80 and 125 nt). The nanoparticles before grafting exhibited one weak absorption band at 1604 cm^{-1}, associated with a primary amine bond NH$_2$ (***Figure 70*** a). After grafting, the spectra showed a medium, newly appeared, absorption band at 1492 cm^{-1}. This peak was assigned to the secondary amine bond

NH; moreover this peak was associated with the disappearance of the band previously located at 1604 cm^{-1} (*Figure 70* b). This peak's disappearance does not mean that all the amino groups reacted, but their number is perhaps not high enough for the lower detection limit of the machine. Combining these results with those obtained from P^{32} experiments, we are able to prove that the DNA strand was covalently bound to the polymer latex particle via a phosphoamide bond.
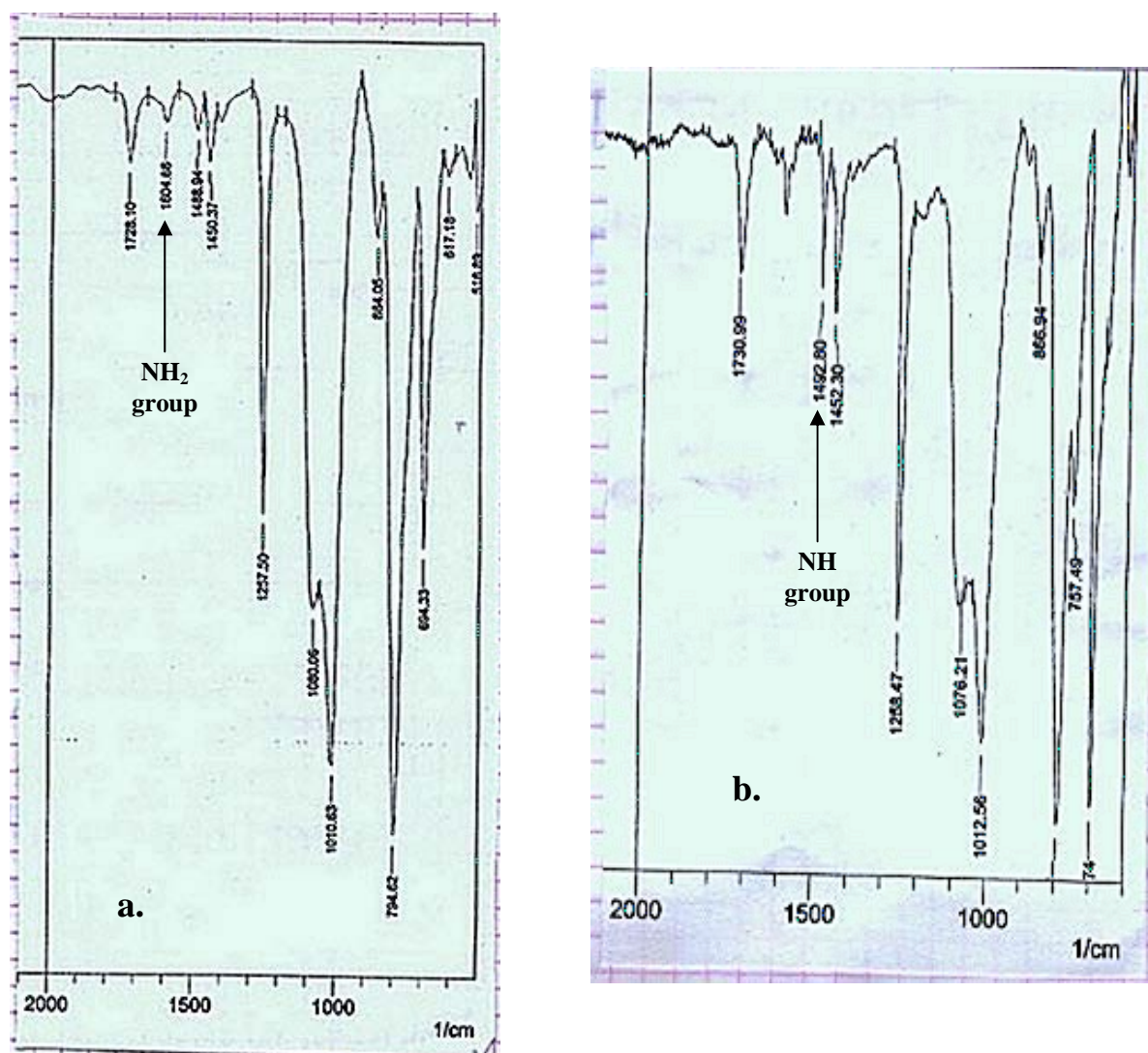
Figure 70: Infrared spectra of aminofunctionalized polymer latex particles: a/before grafting, b/after grafting.

4.2. Agarose gel

The 1.8 % agarose gel ensured that the grafting was achieved as seen in *Figure 71*.The migrations of the ssDNA are well visualized and allow us to have the position of the oligonucleotide alone (comb3, *Figure 71* and comb 2, *Figure 72*). In the combs containing the particles, where a coupling agent was present during the reaction, we can see that DNA is not migrating. This corresponds to the grafting of DNA to the particles, resulting in an increase of the DNA mass, which is then unable to migrate. Some fluorescence was found in the negative controls, which comes from the non-covalent binding occurring at the surface of the particles.

For the grafting experiments, we first changed the time of incubation to find the best conditions. For this purpose, the reaction was run for 1 to 24 hours at 50°C. This was done with the strand of 20nt. As shown in *Figure 71*, the DNA remains in the comb only after 24 hours of the reaction. Then we decided to make all our experiments with the incubation time of 24 hours.
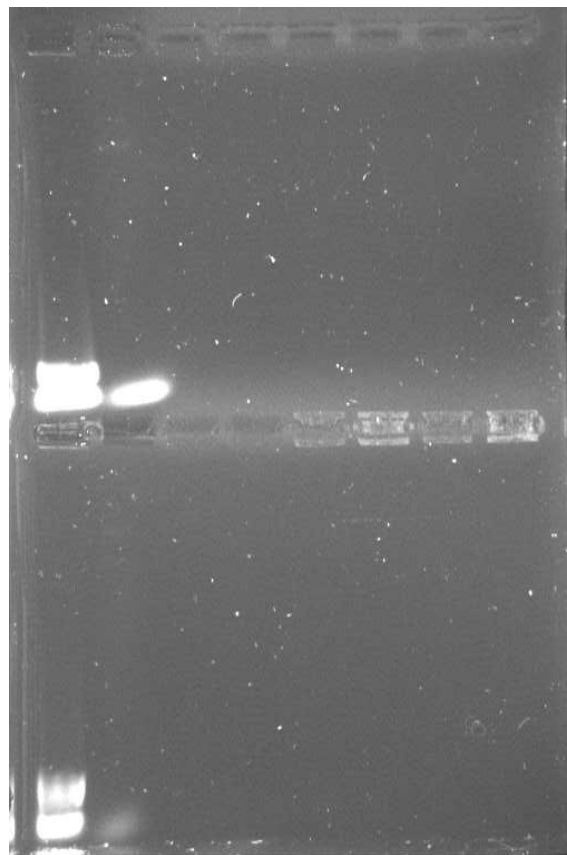
Figure 71: Agarose gel of 20nt DNA reacting with core-shell particles for different periods of time. From left to right, upper lane: (1) Molecular weight marker, (2) 20nt DNA,

(3,5) CS with DNA without EDC after 3 hours reaction, (4,6) 20nt-CS particles after 3 hours, (7) CS with DNA without EDC after 6 hours reaction, (8) 20nt-CS particles after 6 hours. Bottom line: (1) Molecular weight marker, (2) 20nt DNA, (3) CS with DNA without EDC after 6 hours reaction, (4) 20nt-CS particles after 6 hours, (5,7) CS with DNA without EDC after 24 hours reaction, (6,8) 20nt-CS particles after 24 hours

In **Figure 72**, agarose gels from all the DNA-core-shell particles are shown. The combs 8 and 9 showing the 80 nucleotides sequence are not really bright due to dilution problems. On the other hand, the negative controls on combs 5 and 15 show fewer signals than in the corresponding positive controls (4 and 14).
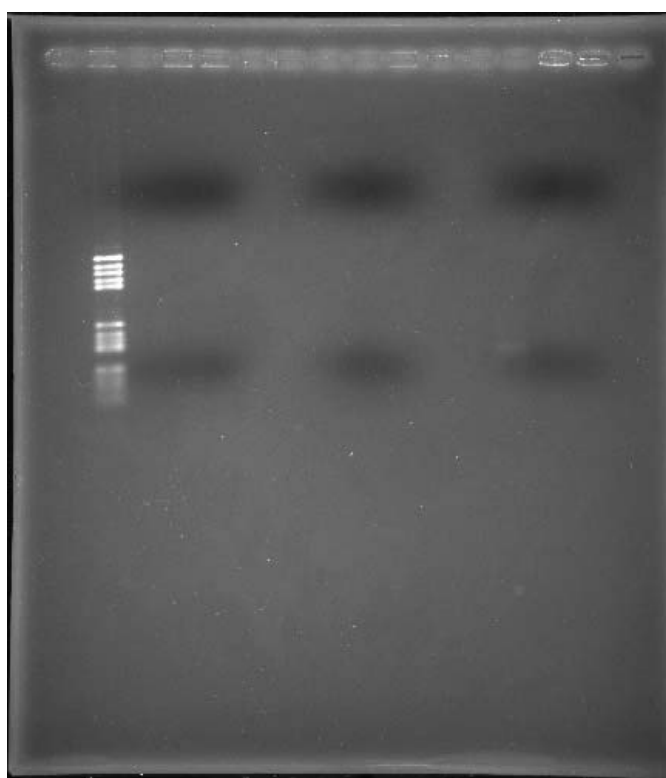
Figure 72: 1.8 % agarose gel in 1X TBE buffer. *Combs content (starting from the left) are: 2. Molecular weight markers, 3. 20nt oligonucleotide, 4. CS-DNA 20 with EDC, 5. CS-DNA 20 without EDC, 8. 80nt oligonucleotide, 9. CS-DNA 80 with EDC, 9. CS-DNA 80 without EDC, 13. 125nt oligonucleotide, 14. CS-DNA 125 with EDC, 15. CS-DNA 125 without EDC.*

In **Figure 73**, we can see clearly the covalent binding of the 80nt DNA onto the core-shell particles. Like in the gel above, we see some signal of the negative control band, coming from non-specific interactions between the particles and the DNA.
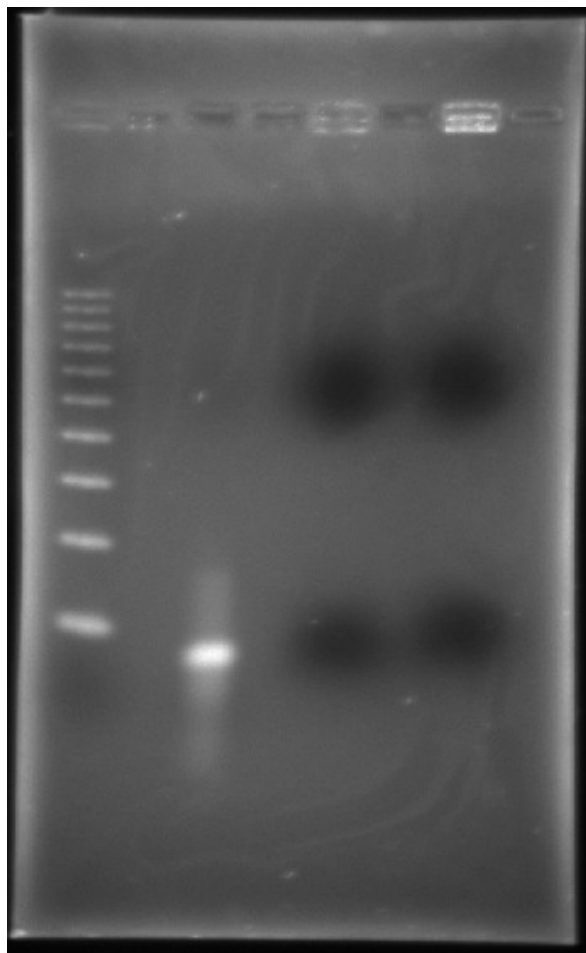
Figure 73: 1.8 % agarose gel of core-shell particles grafted with 80nucleotides DNA.
Combs content is (1) Molecular weight marker, (3) 80 nucleotides, (5) negative control, (7)
80nt grafted to CS particles.

The quantification of the binding was explored via radioactivity measurement in order to obtain the yield of the grafting reaction and to prove the covalent binding of the DNA on core-shell particles.

5. *Quantification of DNA grafted onto core-shell particles*

This experiment was made in order to quantify the grafting efficiency of ssDNA onto the core-shell particles. Basically, the same reaction as previously described was performed, but this time, ^{32}P oligonucleotides were used.

The protocol for radioactive labeling was followed with T4 polynucleotide kinase and ATP-γ-^{32}P. Ethanol/ammonium acetate precipitation was made to purify the obtained oligonucleotides and quantification of radioactivity was on a beta counter. The grafting on core-shell particles was performed, and after washing, the radioactivity remaining on the particles was quantified. A negative control was made like in the 'cold' assay to get the amount of the non-specific binding of the oligonucleotides onto the particles. This experiment was performed for the 20, 80 and 125 nt oligonucleotides.

The measurement of the radioactivity is given in counts per molecules (CPM). In *Figure 74* and *Figure 75*, the sample names S1 to S5 correspond to the supernatant obtained after each centrifugation (washing steps).

Sample name	Description
S1	Supernatant after 1st washing
S2	Supernatant after 2nd washing
S3	Supernatant after 3rd washing
S4	Supernatant after 4th washing
S5	Supernatant after 5th washing

Table 4: Specification of the supernatant obtained during DNA grafting onto CS particles.

For each DNA sequence, a negative control was made without the coupling agent, in order to quantify the non-specific binding onto the particles. From both figures, it is clear that the washing steps allowed us to get rid of the main part of unreacted oligonucleotides. We can also see that in both cases the quantity of non-specific binding is really low (insert *Figure 75*). Moreover, in the case of the 125 nucleotides sequence, the amount of DNA attached to the particles is comparable with the amount obtained in the case of the 80 nucleotides sequence. This means that the polyT tail does not affect the grafting process. The amount of bound DNA is smaller in the case of the 20 nucleotides sequence, because in this case less DNA was used for grafting.
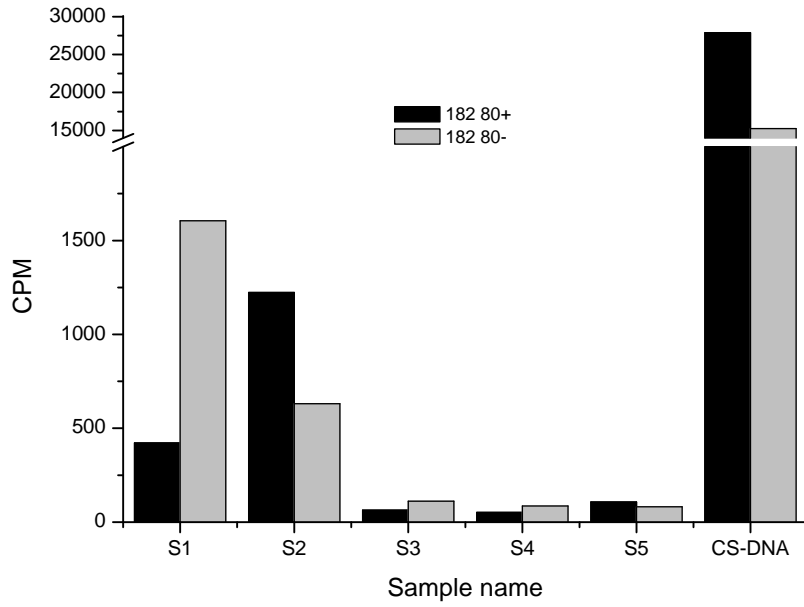
Figure 74: Radioactivity measurement of the core-shell particles grafted with the 80nt oligonucleotides. Radioactivity was measured after each washing.
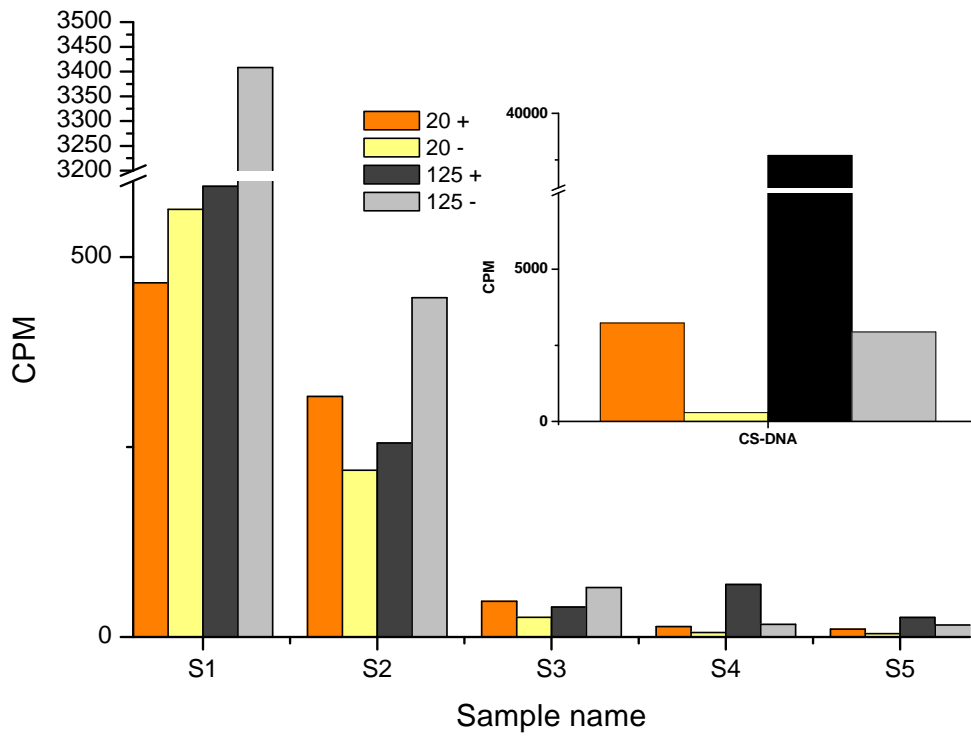
Figure 75: Results of radioactivity measurements with 20 and 125 nucleotides DNA.

To obtain the standard curve (***Figure 76***) we took different quantities of DNA after phosphorylation with P^{32} and we measured the radioactivity. We plotted the CPM versus the quantity of DNA in the sample. With this graph we were then able to quantify the DNA grafted on the particles. In fact, when we measured the radioactivity from the sample after grafting, we could go back to the quantity of DNA present in the sample. Finally this DNA quantity allowed us to calculate the yield of the grafting reaction.
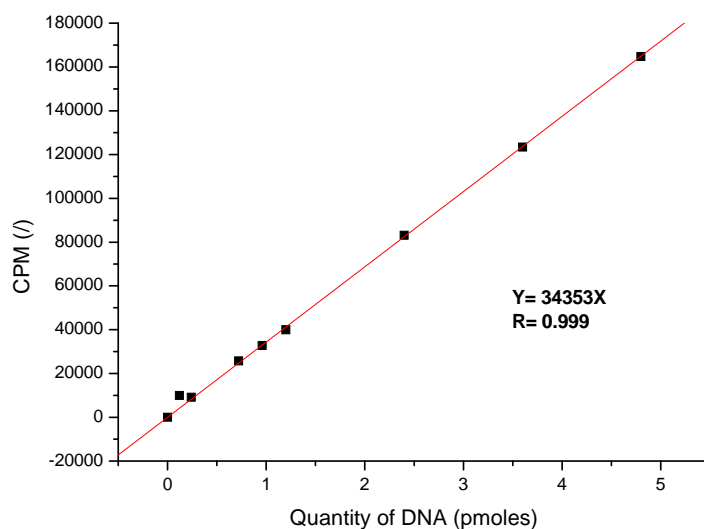
Figure 76: radioactivity standard measurement to quantify the ^{32}P present at the end of the reaction for the 80 nucleotides oligonucleotide.

From the radioactive counting results, 2.6 % of non-specific binding on the core-shell particles was found in the case of the 80nt oligonucleotide. The yield of the reaction for the particles treated with a coupling agent is then of 3 %. This yield is not so high but corresponds to yields commonly found in literature [131].

6.   *Hybridization of DNA particles with complementary strands*

The first measurements made by LSM showed that the surface properties of the shell provoke aggregation of the core-shell particles due to the presence of amino groups (***Figure***

77). Indeed, it is possible that half of the groups are protonated and the other half not. In this situation, different parameters as particle concentration, pH, salt concentration or addition of other blocking agent in the solution have to be investigated. For example, at basic pH, the core-shell particle surface should lose their cationic character due to the deprotonation of amino groups.

Finally, the influence of salt concentration was also examined. In fact, the particles behavior suggests that electrostatic interactions are the driving forces in the solubilization due to the charge screening effect, which inhibits the attractive electrostatic interactions. We tried different salt concentrations in the buffer. We used NaCl concentrations from 0 to 1 M. We found that the best buffer to decrease the aggregation phenomenon was 30 mM Hepes, 150 mM $MgCl_2$ and 1 M NaCl. This was seen in the pictures obtained from LSM, where the size of the particle aggregates decreased dramatically (*Figure 77*).
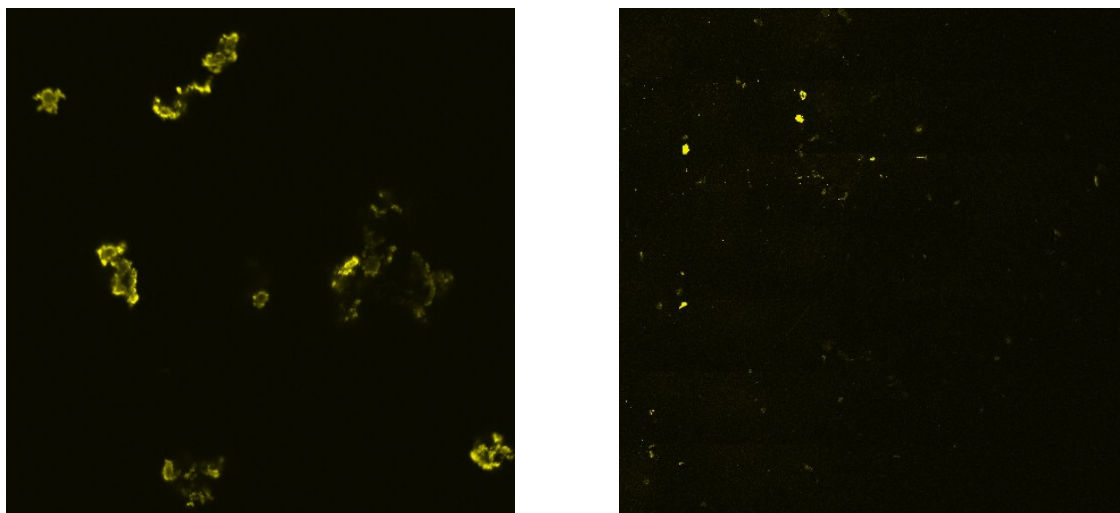
Figure 77: LSM pictures of DNA core-shell particles; a/ in 30 mM Hepes, 5 mM MgCl₂; b/ in 30 mM Hepes, 15 0mM MgCl₂, 100 mM NaCl.

Afterwards we decided to use this buffer in every hybridization experiment. The choice of this buffer was also validated by hybridization measurements where we used PerfectHyb buffer (*Figure 78*). With this buffer no hybridization was measured. For the rest of the experiments, we measured the fluorescence intensity versus the temperature. On the graph we have plot the fluorescence intensity over temperature 1st derivative, versus temperature: -d(RFU/dT).
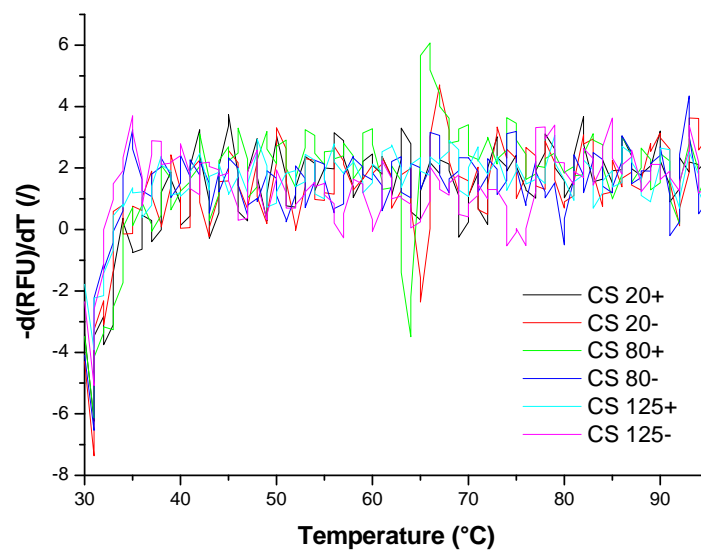
Figure 78: Hybridization of CS-DNA in PerfectHyb buffer.

In order to have a closer look at DNA hybridization in our system, we used SYBR Green dye and a thermocycler setup. SYBR Green was used because its fluorescence increases about 10000 times when bound to double stranded DNA than when it interacts with single-stranded DNA. This property gives us the possibility to determine the Tm of the DNA-carrying latex particles with the two different complementary strands. In parallel, FCS measurements were done; in this case we used a modified complementary strand carrying a Cy5 molecule at the end of the chain.

First of all, we calibrated the thermocycler experiment by measuring the fluorescence of the oligonucleotides with their complementary DNA. We then got the detection limit of the system, given in *Table 5*. We had then to use these quantities for the following measurements.

Oligonucleotide used (nt)	Quantity minimum for good DNA detection (ng)	Tm calculated (°C)
20	40	~ 66
80	1000	~ 75
125	1000	~ 75

Table 5: Characteristics of oligonucleotides with their complementary strand.

In addition, we were interested in looking at the influence of the core-shell particles on the fluorescence measured. For that we did the same experiment as before, but we added some CS particles to the solution. The results were really interesting because the CS particles have a minor influence on the hybridization of the oligonucleotides with the complementary strands of 20 bp (***Figure 79***).
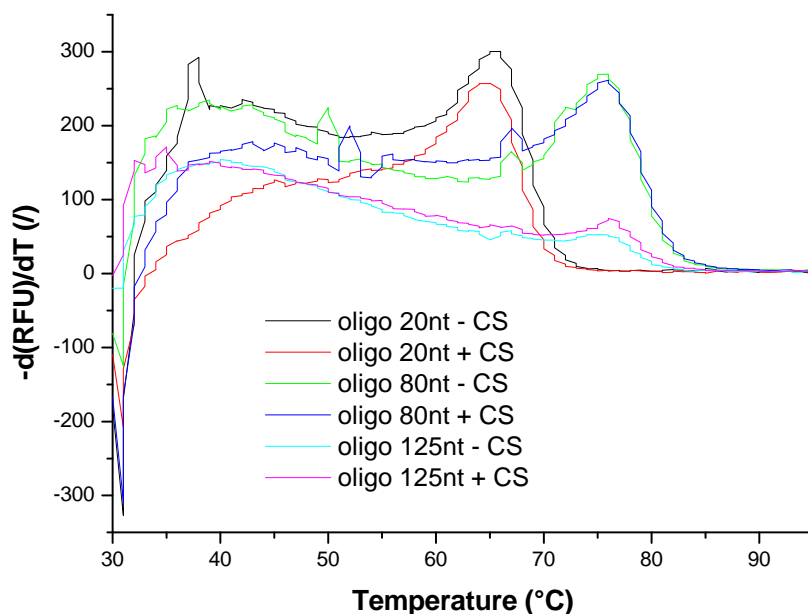
Figure 79: Influence of core-shell particles on DNA hybridization. The hybridization was performed with a 20nt complementary strand.

In the case of the hybridization with the 30nt complementary strand, we have no hybridization with the oligonucleotide of 20 bases, which is normal because these two sequences are not complementary (**Figure 80**). In the case of the 80 and 125 oligonucleotides with the 30nt complementary, the effect of the CS is more important than with the 20nt complementary but this will not be problematic for the rest of the study.
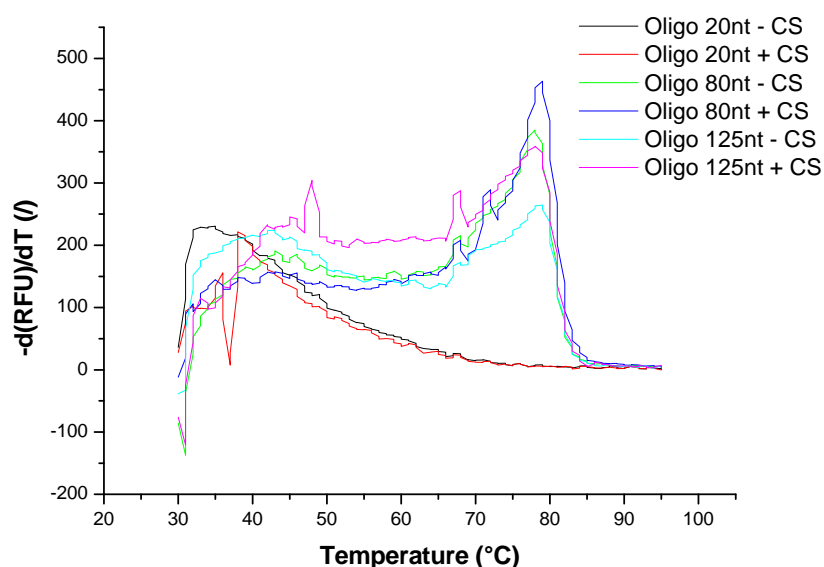
Figure 80: Influence of Core-shell particles on DNA hybridization with the 30nt complementary strand.

The first result we got for the fluorescence measurement in presence of CS particles, answered the question on secondary structures formed in our system. In fact by measuring the fluorescence of CS-DNA without a complementary strand, we got only fluorescence background. This is very important because it proved that there is no hairpin formed in our system.

In **Figure 81** are shown the results of the measurement of our CS-DNA particles with a complementary strand; we used as negative control the CS particles reacted with DNA

without the coupling agent. For CS-DNA 20 and 80, we see that there is hybridization occurring even in the negative control, meaning that some DNA still sticks to the particles.

a.
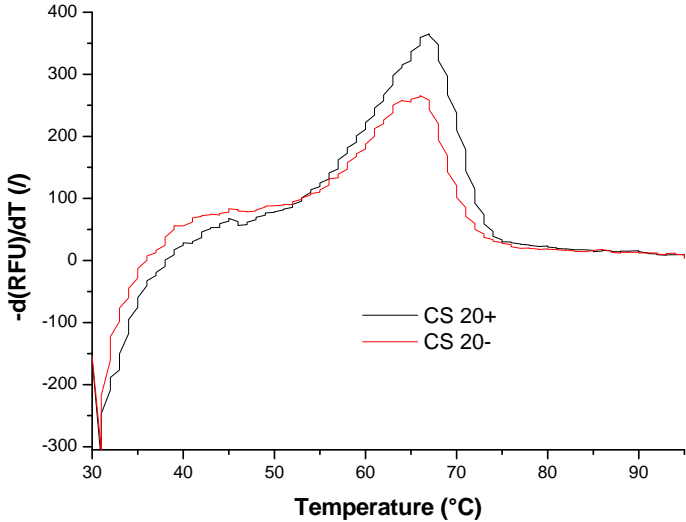
b.
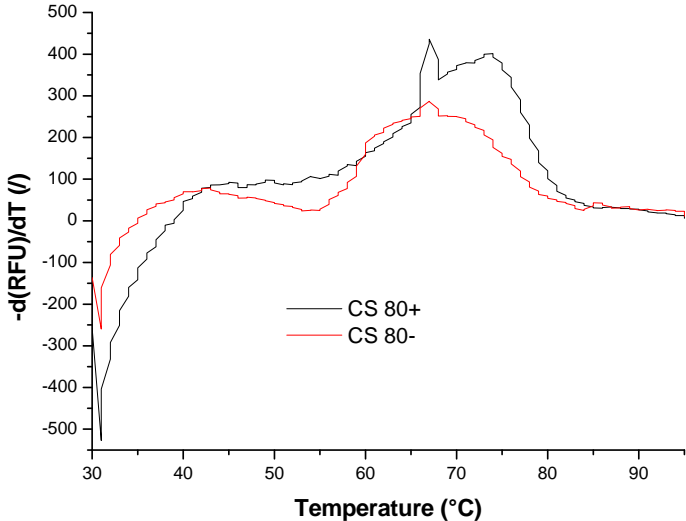
Figure 81: Hybridization of CS-DNA particles with the 20nt complementary strand, a/ oligonucleotide 20, b/ oligonucleotide 80.

Interestingly, this phenomenon does not occur for CS-DNA 125, meaning that there is less interactions between the DNA and the CS in this case. This could be related to better washing of the sample, but the samples were all washed at the same time by the same procedure. A more realistic explanation could be that the 50T tail at the 5' end of the oligonucleotide plays an important role.
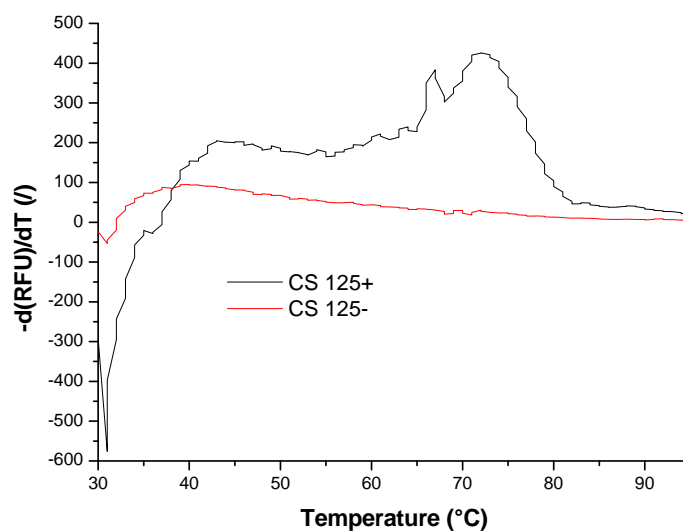
Figure 82: Hybridization of CS-DNA 125 particles with the 20nt complementary strand.

We have studied then the hybridization of all our samples with the 30nt complementary strand (*Figure 83*). The measurement made with the oligonucleotide 20 was again a negative control because this oligonucleotide and the 30nt complementary strand do not match (*Figure 83*).
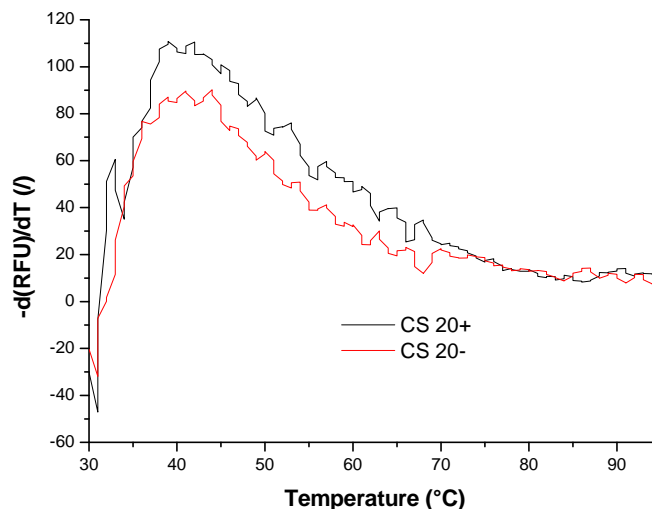
Figure 83: Hybridization of CS-DNA 20 particles with 30nt complementary strand.

Figure 84 presents the result of CS-DNA 80 and 125 hybridized with the 30nt complementary strand. In this figure the fluorescence intensity is higher than in the case of hybridization with the 20nt complementary DNA because the double strand contains 10bp more and consequently more SYBR Green interacts with it. The same results are obtained as previously. Indeed, for the CS-DNA 80 we still have high fluorescence for the negative control (*Figure 84*a). The result obtain with the CS-DNA 125 is similar to the previous one, and confirms the role of the polyT tail. We assume that polyT tail is able to move the strand away from the surface, leading then to a decrease of electrostatic interactions between the particles and the DNA (*Figure 84*b).

a.
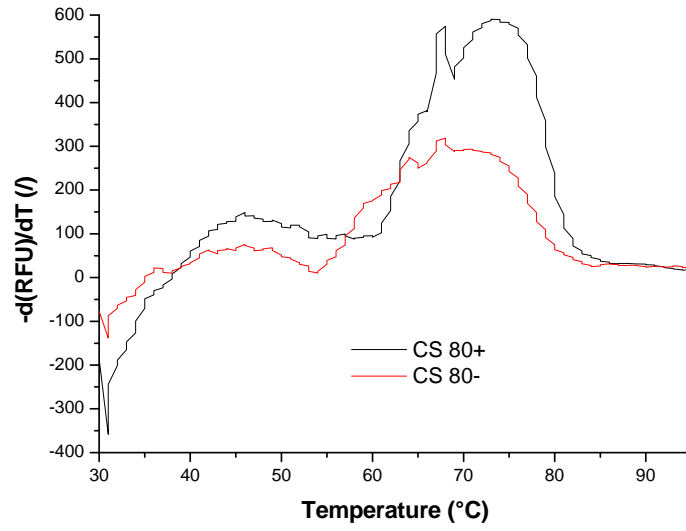
b.
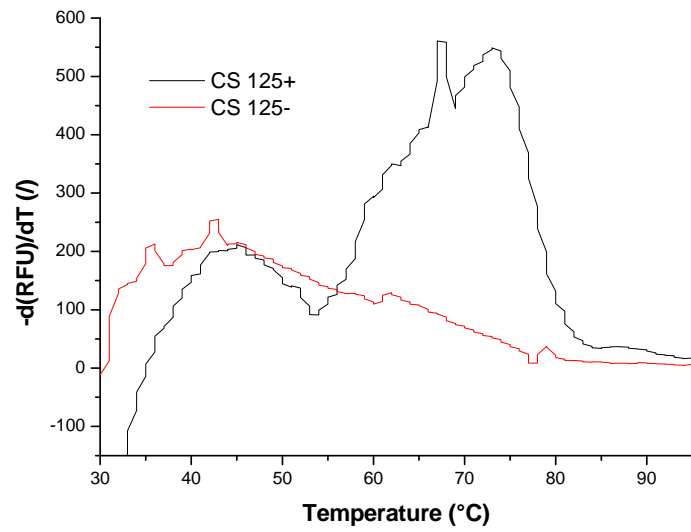
Figure 84: Hybridization of CS-DNA particles with 30nt complementary strand, a/ CS-DNA 80, b/ CS-DNA 125.

Because of the aggregation problems, we have decided to have a closer look at them. It is known that the addition of salmon sperm DNA, or BSA, or even Denhardt's solution could block electrostatic interactions among core-shell latex particles and prevent aggregation. Indeed, Denhardt's solution (composition: 0.02% BSA / 0.02% Ficoll / 0.02% polyvinylpyrrolidone) is widely used to decrease the non-specific binding on nitrocellulose membranes used for Western Blots. The results of SYBR Green measurements with BSA and salmon sperm DNA were completely the opposite of what was expected. In fact, we thought that one of those molecules would decrease the non-specific binding of DNA to the core-shell particles, but it was exactly the opposite, and we got much more fluorescence in our sample in presence of BSA or salmon sperm DNA. This result was higher with salmon sperm DNA that bound strongly the nanoparticles and gave a really high fluorescence. In *Figure 85* the effect of Denhardt's solution is shown on CS-DNA particles with the 20nt complementary strand; we see a decrease in fluorescence intensity.

a.
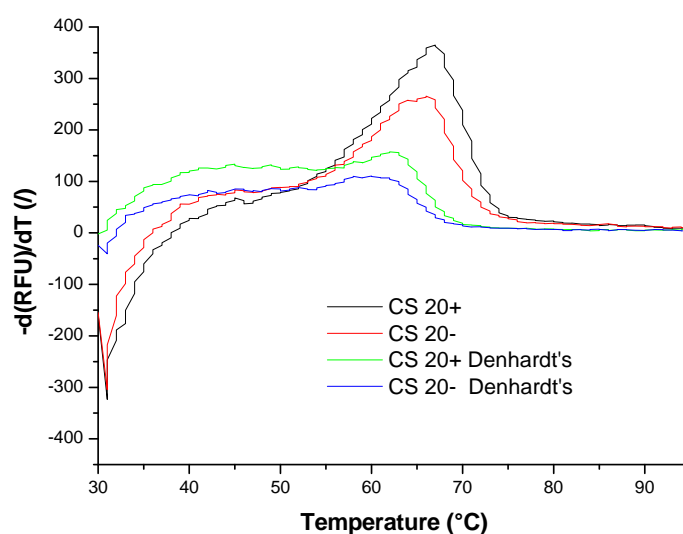
b.
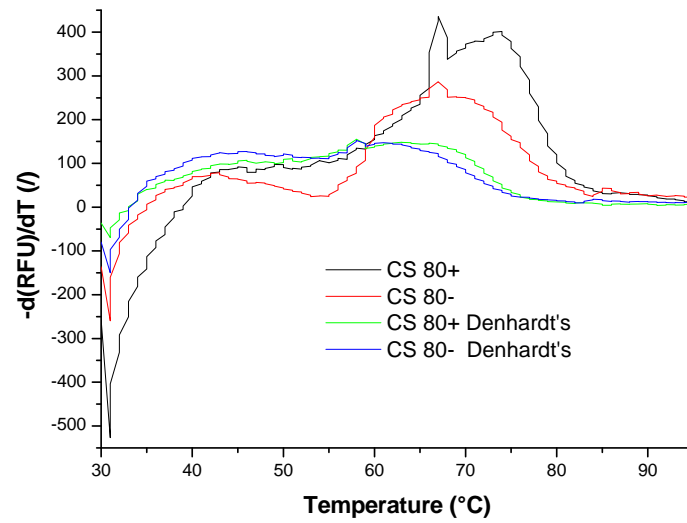
c.
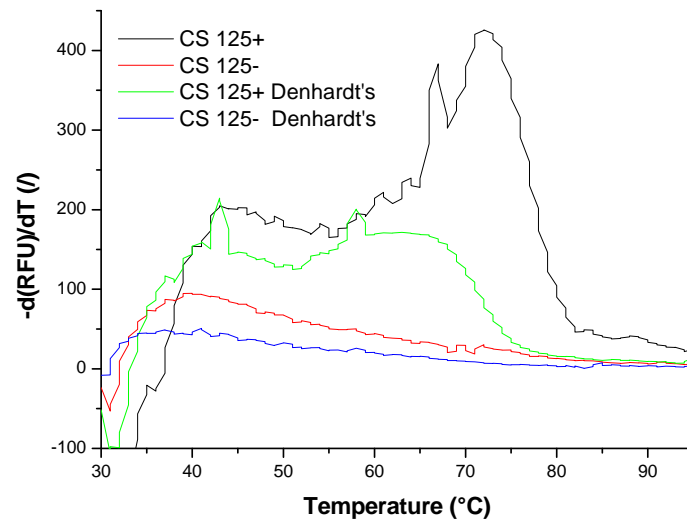
Figure 85: Hybridization of the CS-DNA particles with the 20nt complementary strand with or without Denhardt's, a/ oligonucleotide 20, b/ oligonucleotide 80, c/ oligonucleotide 125.

In *Figure 86* are given the fluorescence intensities for our system in the presence of the 30nt complementary strand. In part a, we have no fluorescence because we have no matching between the DNA sequences. For b and c, we got exactly the same results as with the 20nt complementary strand. The decrease of fluorescence is due to the components of Denhardt's solution, which destabilize our system a lot. In fact, these molecules are screening the charges around our particles and DNA; they prevent interactions between the different DNA strands. Finally we will not use Denhardt's solution for the rest of the study.

a.
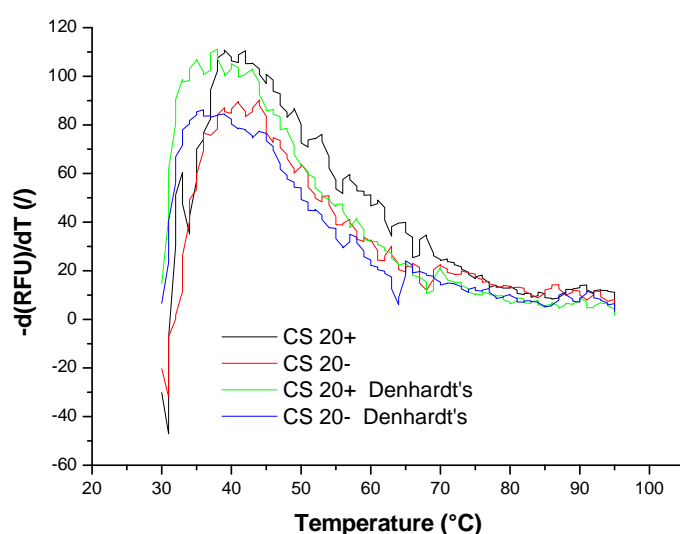
b.
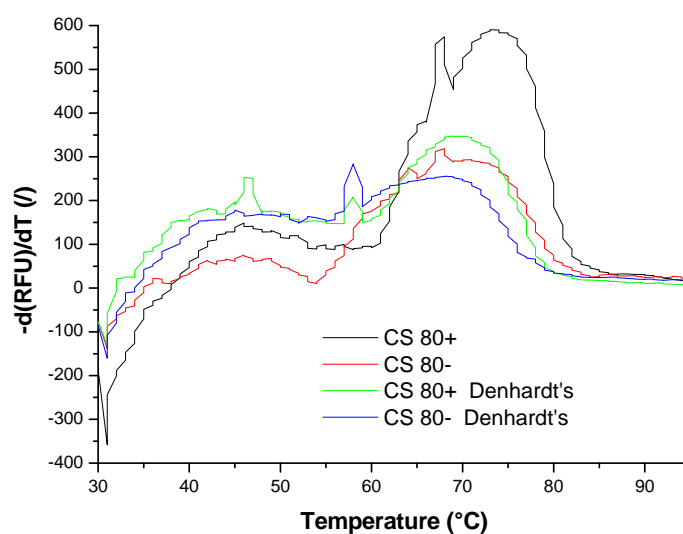
c.
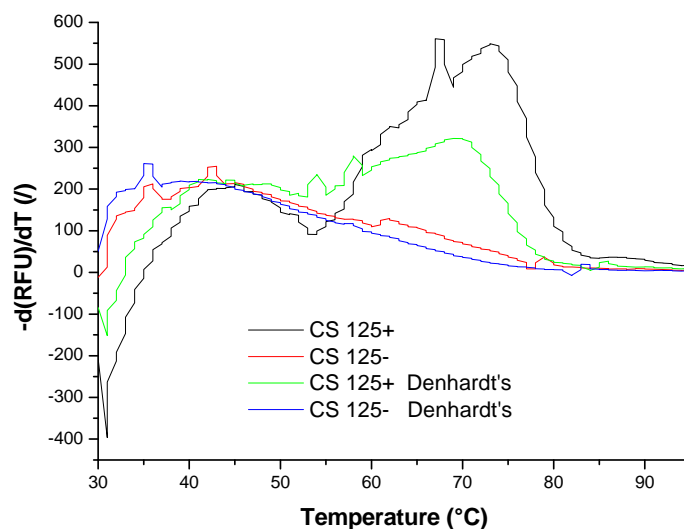
Figure 86: Hybridization of the CS-DNA particles with the 30nt complementary strand with or without Denhardt's, a/ oligonucleotide 20, b/ oligonucleotide 80, c/ oligonucleotide 125.

We could obtain the Tm of the entire different DNA grafted on the core-shell particles. In **Table 6** are shown the Tm of the CS-DNA particles, the obtained temperatures were compared to the melting point of the oligonucleotides alone. We found that the temperatures are similar, meaning that the CS particles do not disturb the hybridization process.

CS-DNA particles	Tm (°C)	Tm of oligonucleotide alone (°C)
20	~ 66	~ 66
80	~ 70	~ 75
125	~ 72	~ 75

Table 6: Melting point of core-shell–DNA particles calculated from the SYBR Green measurement.

Finally, we used FCS to detect the hybridization of the complementary DNA onto the core-shell-DNA particles. We made FCS measurements we made measurements without heating the system and other experiments with heating the system to 95°C to minimize the non-specific binding of DNA. From these measurements we found that the diffusion time of Cy5 alone was between 40 and 50 μs, which correspond to reference values. We also measured the DNA-Cy5 complementary strand; the diffusion time values are between 140 and 180 μs, which correspond to a strand of 20 nucleotides long. In both cases the diffusion time was measured before and after heating. Finally, we have measured the diffusion time of the whole system, which means nanoparticles incubated with DNA-Cy5 complementary strand. Two samples were used, the negative control without DNA bound on the nanoparticles, and the second sample was the DNA-nanoparticles. For these measurements only the oligonucleotide of 80 bases was grafted on the beads. In the case where we had no heating before the measurement, we obtained diffusion times between 150 and 430 μs, which correspond to diffusion times of the complementary DNA.

After heating the samples, we got completely different results. For the negative control, we got the same results as before, meaning that no non-specific binding was occurring in the sample. But for the sample where the beads were grafted with oligonucleotides, we got hybridization of the complementary strand. In fact, we got three different diffusion times, each of them corresponding to a defined population. First we had a diffusion time of 250 μs, which corresponds to DNA-Cy5 alone. The second diffusion time was 44 ms, which correspond to big aggregates still present in our sample. Finally, the last result was a diffusion times between 10 and 17 ms, which correspond to nanoparticles around 200 nm in diameter, and consequently to the hybridization of the DNA-Cy5 onto the CS particles. Such dimensions agree very well with the sizes of particles present in our system. The three different diffusion times observed come from the different sample regions, on which the FCS measurements were done. The quantity of hybridization was not really high, but this is in agreement with the grafting yield, which was not so high, around 5% of the DNA added in the reaction solution.

Conclusions DNA biosensor

We wanted to design a new kind of DNA biosensor by using polymeric nanoparticles as support. We showed that for our purpose the use of thiolated ABA triblock copolymer was not efficient. We then synthesized well-defined core-shell particles bearing amino groups on the shell. By using different analytical techniques, like DLS, TEM or colorimetric methods, we fully characterized the particles and quantified the numbers of amino groups at their surface. We also achieved the DNA grafting to core-shell particles, and proved it by agarose gel, radioactivity measurement and IR spectra.

Finally with different fluorescence measurement, we were able to prove that the use of a high salt concentration in the buffer decreased the aggregation in our system. With the SYBR Green measurements we proved that BSA, Salmon sperm DNA and even Denhardt's solution do not really play a role for the non-specific binding of DNA onto the nanoparticles. By FCS and SYBR Green measurements we proved that hybridization was occurring in our system and that the polyT tail on the oligonucleotide is important for hybridization.

Moreover, additional work should be done on our system. Firstly, we should try to decrease the non-specific binding of DNA on the core-shell particles with, for example, grafting some PEG on the shell. We could also try to obtain higher grafting efficiency, by heating the DNA at 95°C for 5 minutes before the grafting reaction to decrease the non-specific hybridization of the oligonucleotides. We should use again FCS measurements to try to measure the hybridization kinetics in our system. Finally, we could try to recover the target added to the DNA biosensor. We would have then proved that our system could be usable for DNA detection as well as DNA separation.

General conclusion and outlooks

Biological functionalization of membrane surface as well as compartmentalization are important processes in Nature. Our goal was to mimic these processes. To this aim, we decided to work on protein-polymer and DNA-polymer hybrids. In other words we took advantage of the various tailoring possibilities offered by polymer molecules to design and develop new tools.

Concerning the protein-polymer hybrid, we were able to show that a membrane protein that catalyses a vectorial transport could be incorporated in polymer membranes, and remain active. We also proved that the polymer itself induces the activity of the protein, and even sometimes gives a higher activity than lipidic environment. This offers the possibility to tailor the membrane with respect to the needs of the protein. Consequently, individual systems could be developed and investigated for every membrane protein.

This study opens the way to incorporation of other catalyzing membrane proteins and studies in polymeric membranes. For example, membrane proteins like F0F1-H$^+$ ATPase could be reconstituted and studied. We could also think about co-reconstitution of two, or even more proteins, leading to coupled reaction sequences and to artificial metabolic pathways. By doing so we could take advantages of the polymer as stabilizing and activating environment on one hand, and proteins, which give the biological function on the other hand.

In the case of the DNA-polymer hybrid, we created and developed a new system able to detect DNA hybridization. For this study we used core-shell nanoparticles, with well-defined physical and chemical properties. We were able to show the feasibility of DNA hybridization, but we still have to prove that our system can be pelleted.

Moreover our system can be tuned with any molecule able to react with an amine group. Then we could be able to graft RNA on our nanoparticles. Consequently this new kind of biosensor could be also used as tool for molecular biology or even nucleic acid-drugs interactions. Indeed nucleic acid-polymer hybrids could be an interesting alternative to usual method used to extract and recover DNA or RNA. They could also be useful in the "hit to lead" research because direct interactions between drugs and nucleic acids could be easily recorded.

Finally, with these two different studies we showed that ABA triblock copolymers are not only a synthetic material. They are able to interact and adapt to their environment. Moreover, associated to biological molecules, this material opens the way to many different fields and to many different applications.

Materials and Methods

Commercials products

E.Coli polar lipid extract and POPC were provided by Aventi Polar Lipids.

The detergent DDM Anagrade was provided by Anatrace.

The fluorescent probe SYBR green I® was purchased in Invitrogen.

The ACMA dye, BSA, Decyl-ubiquinone, β-NADH reduced disodium salt, EDC-HCl, MeIm, HEPES, Sodium Hydroxide were purchased from Sigma.

D4, St, MMA, DVB and DBSA were purchased from Fluka. AEMA and KPS were obtained from Aldrich. All the monomers were used without further purification.

The Sheared salmon sperm DNA was from Eppendorf. The BCA protein assay kit was purchased from Pierce. The Bio-Beads® SM-2 absorbent were from Bio-Rad.

All oligonucleotides (ssDNA) were purchased from Thermo Electron Corporation with an HPLC grade. The P^{32} phosphate was from Amersham Biosciences.

DNA molecular weight marker was purchased in Bio-Rad. We have used the 100bp EZ load DNA ladder.

The protein molecular weight standard was from New England Biolabs. We used the prestained protein marker from 6 to 175 kDa.

For the DNA modification we have used T4 polynucleotide ligase from NEB.

Centricons were purchased from Millipore and we were using the YM-10.

The fluorimeter and the spectrometer were from Perkin-Elmer. The UV/Vis spectrometer was a Lambda 35, the fluorimeter was the LS 55.

Infra-red spectra were recorded on Schimadzu FTIR 8300 Fourier-transform spectrophotometer with sample in solid using a Golden Gate ATR accessory.

The detection system for agarose gels was a Gel Doc XR (Biorad, Switzerland).

Complex I experiments

1. PMOXA-PDMS-PMOXA triblock copolymer synthesis and characteristics

1.1. Polymer used

Polymer	Molecular Weight (Da)	B/A
A15B62A15	7500	1.8
A21B69A21	9000	1.43
A9B106A9		5.12
A65B165A65		

A: PMOXA, B: PDMS

Table 7: characteristics of the polymers used for the Complex I experiments.

1.2. Polymer characteristics

NMR and GPC were applied to determine the Mn and the polydispersity of the polymers. In Table X are given all the Mn, formula and terminal modifications of the polymers used.

2. Protein purification

The NADH: ubiquinone oxidoreductase (Complex I) was isolated from an overproducing strain [148, 149] and kindly provided by Professor Thorsten Friedrich. The protein was stored at -80°C in 50 mM MES/NaOH pH=6, 50 mM NaCl, 5mM $MgCl_2$ and 0.1% DDM. When needed the NADH/ferricyanide activity of the protein was measured by the following protocol. The measure was made at 410 nm by following the ferricyanide reduction by the NADH. The solution was containing 300μl of vesicles or proteovesicles, 185μl of Tris/HCl pH=6 buffer and 5μl of 0.1M ferricyanide solution. The enzymatic activity

was recorded after the addition of 10μl of 10mM NADH. As reference sample, the same measure was made with "free" protein, 5μl of Complex I was mixed with the assay buffer

3. Complex I reconstitution in triblock copolymer vesicles

Complex I was reconstituted by using bio-beads SM-2; these beads absorb detergent (o-POE, DDM…) and are usually used for the crystallization of proteins and facilitate the formation of proteoliposomes [64, 65, 68]. The reconstitution of Complex I into proteovesicles was inspired by a method of Rigaud and by a method used in the group of Weiss H [39, 150].

Before using the bio-beads washings are needed, we have performed three washings with methanol and three washings with the buffer used for the reconstitution of the protein.

The polymer and detergent (DDM) were mixed in buffer solution and stirred overnight. The protein was then added to this mixture and stirred for 3 to 6 hours at 4°C. The bio-beads addition was then performed in three times with 12 hours between each addition. At the end the bio-beads were pelleted. The supernatant was then used for gel permeation chromatography to remove all the non-incorporated protein. Finally a concentration of the sample was made with centricon.

4. Titration of Complex I activity

In this experiment we have the ability of the protein to oxidize the NADH. Complex I was added, between 50 and 100 μg, to the lipids or polymer solution with different ratios (w/w) from 0.01 to 1, incubation was performed. The volume was then adjusted to 1ml by addition of buffer and 50μM of decyl-ubiquinone. A final incubation was made for 5 minutes at RT then the change of the absorbance at 340nm was recorded after the addition of 50μM of NADH. For all the experiment with lipids the conditions were kept the same [81] with incubation time of 20 minutes in ice. For the polymer we have decided to work with different time and incubation temperature (0°C and 25°C).

ABA thiolated triblock copolymer-DNA experiments

1. Formation of vesicles with thiolated polymer

For the vesicles formation, the standard method developed in our laboratory was used. 50 mg of thiolated polymer was dissolved in 250mg of ethanol; to yield a clear, homogeneous solution. Then this solution was dropped slowly in 4.7 ml of PBS buffer. The same method was used to prepare some non-thiolated vesicles. In this case the polymer used did not carry thiol groups at its end.

2. Quantification of thiols

To perform this quantification, an iodometric titration method was used. As negative control a non-thiolated polymer vesicles were used. The vesicles solutions were made as explained previously, and the pH was adjusted to 2-3 to prevent the disulfide bond formation. The solutions were diluted 6 times, and 3 ml of these diluted solutions were used for quantification. First 150μl of potato starch (10% solution) were added, and a 1mM iod solution was added until the blue coloration appears and stays stable. The volume of iod added was calculated and the moles number of thiol group present was obtained. In the negative control we got no coloration change at all.

3. Oligonucleotide thiolation

This modification is a chemical modification of the 5' end of the oligonucleotide. For the reaction 2 mg of EDC were put in an eppendorf, then 11.25 nmoles of DNA were used. Then 5 μl of 0.25M cystamine in 0.1 M imidazole were added quickly. The sample was vortexed, then centrifuged for 5 minutes at maximum speed. Finally 20 μl of a 0.1 M imidazole solution pH= 6 was added and the solution was reacted for 30 minutes at room

temperature. For purification, the sample was passed on a Sephadex G-25 column, with 10 mM sodium phosphate, 10mM NaCl, 0.2M EDTA as buffer.

4. Oligonucleotide enzymatic modification

In this case the oligonucleotide modification was achieved via the T4 polynucleotide kinase enzyme. We used this enzyme to transfer on the 5' end of the oligonucleotide a phosphate carrying a thiol group. To this aim 11.4 µl of water, 10 pmoles of ATPγS, 10 pmoles of DNA and 2 µl of T4 polynucleotide kinase buffer were put in an eppendorf. Persistent tapping on the tube made the mixing of reagents. Then 10units of T4 polynucleotide kinase were added to the previous solution. The solution was mixed again and was let to incubate for 1 hour at 37°C. Finally the enzyme was inactivated by heating the solution for 10 minutes at 68°C.

5. Purification of modified oligonucleotides

For the purification of the oligonucleotide we used the sodium acetate- ethanol precipitation. Sodium acetate, 1/10 of the oligonucleotide solution volume, is added to the modified oligonucleotide solution. Then 2.5 times of the volume is added of ethanol. This solution is cooled down to –20°C for 30 minutes to 1 hour, a centrifugation at 13000 rpm is then made for 15 minutes. The supernatant is taken away and the same volume of 70% ethanol is added to the pellet. The solution is again centrifuged at 13000 rpm for 5 minutes. Once again the supernatant is taken away and the pellet is dried. Finally the pellet is resuspended in the minimum volume of TE buffer.

6. Grafting of DNA on the thiolated nanovesicles

For this experiment, the pH of thiolated vesicles was put to 6.8. Then the 1 ml of thiolated vesicles (600 nmoles) were put in a vial with 56.3 nmoles of SH modified oligonucleotide. This solution was incubated at 37°C for various times. Every hour 800 µl of

the starting solution were taken out. For each aliquot, 50 µl were used for agarose gel and 750 µl were used for iodometric titration.

7. *Maldi-Tof experiments*

In our case, the matrix used was the mixture of 600 µl of solution A and 300 µl of solution B.

- ✓ Solution A: a spatule of dihydroxyacetophenone in 1 ml of a 50 % acetonitrile solution.
- ✓ Solution B: 92 mg of ammonium tartrate in 1 ml of water.

For the Maldi-Tof experiments, the DNA solutions were first desalted by putting 1 to 2 µl of solution onto a filter, standing upon a water-containing beaker. The desalting process was made for 20 minutes. Finally 1 µl of desalted DNA and 1 µl of matrix were mixed on the Maldi-Tof plate, and the sample was dried. The measure was performed on a Voyager-DE PRO.

Core-shell particles experiments

1. *Buffers*

The following buffers were prepared and used for each experiment with core-shell particles DNA functionalized:

- ➤ Washing buffer: 0.4N NaOH, 0.25% SDS heated at 50°C.
- ➤ Hybridization buffer: 30mM HEPES, 150mM $MgCl_2$, 1M NaCl.
- ➤ Running buffer for agarose gel: 1X TBE.

2. Oligonucleotides

The sequences of the oligonucleotides used in this study are shown in the following *Table 8*.

Name	Sequence (5' to 3')	Length (nucleotides)
20	GAG TAT TCA ACA TTT CCG TGT	20
80	TTT TTG ACC TGC AGG CAT GCA AGC TTG CA CTG GCC GTC GTT TTA CAA CGT GAC TGG GAA AAC CCT GGC GTT ACC CA	80
125	TTT TTT TTT TTT TTT TTT TTT TTT TTT TTT TTT TTT TTT TTT TTT GAC CTG CAG GCA TGC AAG CTT GGC ACT GGC CGT CGT TTT ACA ACG TGA CTG GGA AAA CCC TGG CGT TAC CCA	125
Comp 20_1	ACA CGG AAA TGT TGA ATA CTC	20
Comp 20_2	AAC GAC GGC CAG TGC CAA GC	20
Comp 30	TCA CGT TGT AAA ACG GCC AGT GCC AAG	30

Table 8: Oligonucleotides used.

For the radioactivity experiments, oligonucleotides were purchased with a hydroxylated 5' end and for all others experiments they had a phosphorylated 5' end.

3. Preparation of Polymer Latex Particle

PDMS core and a shell of Poly(St-MMA-AEMA-DVB) were synthesized by two-step emulsion polymerization via core-shell particle. So, the polymerization of PDMS was conducted using 20 g of water, 5 g of M1 and an amount of DBSA equivalent at 1.5 wt% of the monomer. The distilled water and the surfactant were added at room temperature into a three-necked flask magnetically stirred about 400 rpm and purged of oxygen by bubbling argon during a few minutes. When the temperature of the mixture reaches 80°C, the monomer is added dropwise. After the polymerization proceeded, it was neutralized with NaOH 0.1N. In a second step, the crosslinked shell is synthesized via seeded polymerization of St-MMA-AEMA-DVB (M2) on the seed PDMS particle by using KPS as initiator and without additional surfactant. A selected amount of PDMS latex (10 ml), water (10 ml) and KPS (2.5 wt% of monomers) were first loaded into the flask purged of oxygen by bubbling argon for a few minutes. When the temperature reaches 80°C, the monomer mixture (5 g) is added dropwise at a low rate of about 10 ml/h and the polymerization was proceeding during 4 h. Further purification was performed by reprecipitation in methanol, repeated centrifugations (20 minutes, 4000 rpm) and resuspension in distillated water.

The quantification of the surface density of amino group present on the particles was based on fluorescamin reaction with the primary amino groups. The characterization of the polymer latex particles was achieved via NMR, DLS and TEM.

4. Particle Size by Dynamic Light Scattering

Particle size characterization was performed with dynamic light scattering experiments using a commercial goniometer (ALV-Langen) equipped with He-Ne laser (λ=633 nm) and at scattering angles between 30° and 150°. An ALV-5000 correlator calculates the photon intensity autocorrelation function $g^2(t)$.

5. Particle Morphology by Transmission Electron Microscopy

Particle morphology was examined by transmission electron microscopy (TEM-Hitachi H-7000). The polymer latex particle was thinned with distilled water and treated with a sonicator 0.5 % uranyl acetate is used as stain to enhance the contrast of core-shell particles.

6. Amino Group Quantification by Fluorescence Spectroscopy

The fluorescence spectroscopy measurements were carried out using a luminescence spectrometer LS55 (Perkin Elmer). The surface density of amino group was based on fluorescamin reaction with the primary amino groups. Standard solutions of functional monomer AEMA were prepared in the range of 0.01-0.10 mg/ml. Then, 0.1 ml of standard was added to 2.9 ml of borate buffer solution (0.1M-pH 9.5), followed by 1 ml of solution of fluorescamin in acetone (0.3 mg/ml). Before the measurements, 1 ml of the mixture was taken and added to 2 ml of borate buffer. The excitation wavelength was 393 nm and the emission wavelength was measured at 477 nm.

7. DNA grafting onto the Core-Shell particles

Core-Shell particles were dispersed in 30mM Hepes at 1% (w/v) overnight. The grafting with DNA was achieved by adding to 1ml of Core-Shell solution different amounts of ssDNA solution. To start the coupling, 600µl of a (0.1M MeIm, 0.1M EDC) solution is added while only 0.1M MeIm is used in the negative controls. The grafting was carried out at 50°C for 24h. The particles were then microcentrifuged at 13400 rpm for 45 minutes. The pellet was washed with the washing buffer and then microcentrifuged three times more with washing between every centrifugation. The last washing of the pellet was done with distillated water. In a last step, the Core-Shell particles were redispersed in the specific buffer used in the following hybridization experiment.

To ensure us that the grafting was achieved IR measurements and agarose gels were performed with the particles obtained.

8. *Radioactivity labeling and grafting*

A standard protocol was used for the radioactive phosphorylation of the 5' end of oligonucleotides. Here oligonucleotide (10fmoles) is mixed with ATP-γ-^{32}P (50μCi), 10X bacteriophage T4 polynucleotide kinase buffer (2μl) and water (11.5μl). Then T4 polynucleotide kinase (~10 units) is added to the previous mixture. This solution is incubated for1 hour at 37°C. To inactivate the enzyme the solution is heated for 10 minutes at 68°C. Then the tube is put in ice, and purification of the oligonucleotide is made. Here we have used the ammonium acetate/ ethanol method [137]. Finally the modified oligonucleotide is resuspended in the minimum volume of buffer. Quantification of radioactivity was made with 2ml of scintillation buffer and 2μl of radioactive material. After this quantification, the modified DNAs are used for the grafting to core-shell particles.

9. *Quantification of DNA on core-shell particles*

To achieve the quantification of DNA grafted onto core-shell particles, we have used the radioactive oligonucleotides prepared previously. We have used various increasing volume of radioactive DNA. We have taken between 0.1 μl and 10 μl of DNA and measured the CPM present in each sample. Then plotting the quantity of DNA versus CPM makes a standard curve.

10. *Visualization of Core-Shell-grafted-DNA particles with agarose gel*

A 1.8% agarose gel was made to visualize if the grafting is completed. 20 μl of sample with loading buffer were poured onto the gel. Running conditions were 1 hour at 100 mV. Bathing the gel in an ethidium bromide solution for 30 min allowed us to visualize the DNA.

11. Fluorecence detection of the complementary strand onto core-shell-DNA particles

11.1. <u>FCS measurements</u>

The FCS measurements were made on a Leika LSM 510-ConfCor2. We have taken a ratio of 0.75 of CS- DNA to the complementary DNA. The complementary strand used here was Comp 30, and we have made the FCS experiments only with the 80nt oligonucleotide. The experiment was made by adding CS- DNA particles to the complementary strand, then the solution was heated at 95°C for 5 minutes and finally we let the solution cooling down to ~70°C at room temperature. Then the measure was performed with 1µl of this solution

11.2. <u>SYBR green measurements</u>

The experiments were made on a thermocycler from Biorad. The machine was not making any DNA amplification but it was just detecting the presence of double stranded DNA to obtain the Tm of our system. The fluorescence emission was measured at 520 nm. The total volume used in the wells was 40 µl and was obtained by addition of hybridization buffer to the solution of complementary DNA and Core-Shell particles, and SYBR Green. In this volume the complementary strand was added with a ratio of 0.75 between Core-Shell-DNA particles and the target sequence. Various parameters were tested in these experiments.

Abbreviations

ACMA: 9-amino-6-chloro-2-methoxyacridine

AEMA: Aminoethylmethacrylate hydrochloride

BCA: Bicinchoninic acid

BSA: Albumin from Bovine Serum

Bp: Base pair

CMC: Critical Micellar Concentration

CPM: Count per molecule

Cy3: Fluorecent cyanine 3

Cy5: Fluorecent cyanine 5

DBSA: 4-dodecylbenzenesulfonic acid

DLS: Dynamic Light Scattering

DDM: n-Dodecyl-β-D-Maltopyranoside

DNA: Deoxyribonucleic acid

cDNA: complementary DNA

ssDNA: Single strand DNA

D4: Octamethyltetracyclosiloxane

DTT: Dithiothreitol

DVB: divinylbenzene

EDC-HCl: *N*-Ethyl-*N'*-(3-dimethylaminopropyl) carbodiimide hydrochloride

EPR: Electron paramagnetic resonance

FCS: Fluorescence Correlation Spectroscopy

GPC: Gel Permeation Chromatography

IR: Infra-Red

KPS: Potassium persulfate

LSM: Confocal Laser scanning microscopy

MALDI-TOF: Matrix-assisted laser desorption/ionization-Time of flight

MCH: 6-Mercapto-1-hexanol

MeIm: 2-Methylimidazole

Mn: Molecular weight

MMA: Methylmethacrylate

β-NADH: $\beta-$Nicotinamide adenine dinucleotide

NMR: Neutron Magnetic Resonance

Nt: nucleotide

OD: Optical Density

PDMS: Polydimethylsiloxane

o-POE: n-Octyl-oligo-oxyethylene

POPC: 1-Palmitoyl-2-Oleoyl-*sn*-Glycero-3-Phosphocholine

Poly(St-MMA-AEMA-DVB: Poly(Styrene-Methylmethacrylate-Aminoethylmethacrylate-Divinylbenzene)

PMOXA: Polymethyloxazoline

QD: Quantum dots

RNA: Ribonucleic acid

RT-PCR: Real Time-Polymerase Chain Reaction

SDS: Sodium Dodecyl Sulphate

St: styrene

TE: Tris- EDTA

TBE: Tris Borate- EDTA buffer

TEM: Transmission Electron Microscopy

TLC: Thin Layer Chromatography

Tm: melting point

ZnS: Zinc sulphide

Appendix

Confocal Laser scanning microscopy (LSCM):

The Confocal microscopy differs from traditional widefield optical microscopy. For the research scientist, there are several advantages to using a confocal microscope to obtain data compared with conventional optical microscopy. One of the hallmark features of this process is the ability to obtain serial optical sections with a confocal microscope. Using digital image processing techniques, these serial images can be re-assembled to form 3D representations of the structures being studied. By applying various antibodies conjugated with fluorescent markers, the relative distributions of epitopes of interest can be studied. With the advancement of the methods and devices available, double and triple labeling techniques are now commonplace. Images are taken point-by-point and reconstructed with a computer, rather than projected trough an eyepiece.

In a laser scanning confocal microscope a laser beam passes a light source aperture and then is focused by an objective lens into a small focal volume within a fluorescent specimen (*Figure 87*). A mixture of emitted fluorescent light as well as reflected laser light from the illuminated spot is then recollected by the objective lens. A beam splitter separates the light mixture by allowing only the laser light to pass through and reflecting the fluorescent light into the detection apparatus. After passing a pinhole the fluorescent light is detected by a photo-detection device transforming the light signal into an electrical one, which is recorded by a computer.

As seen on *Figure 87* the detector aperture obstructs the so-called out-of-focus light: fluorescent light not originating from the focal plane of the objective lens. The result of such technique is sharper images compared to conventional microscopy techniques. The detected light of each volume scanned represent one pixel on the resulting image. As the laser scans over the plan of interest a whole image is obtained pixel-by-pixel and line-by-line. The assembly of the successive focal planes obtains the 3D image.
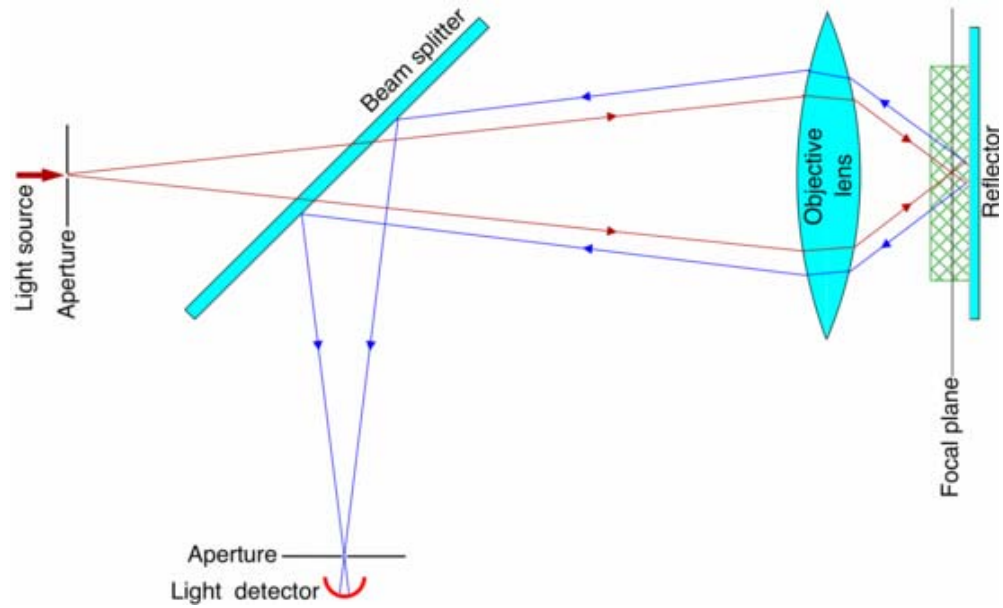
Figure 87: Confocal Laser Scanning Microscopy principle [151].

In addition, confocal microscopy provides the capacity for direct, non-invasive serial optical sectioning of intact, thick living specimens with minimum sample preparation. As this microscopy depends on fluorescence, the sample usually needs to be treated with fluorescence dye to make things visible. Anyway the dye concentration can be very low so that the disturbance for the biological system is kept to a minimum. Green fluorescence protein has been used to this purpose.

Fluorescence Correlation Spectroscopy (FCS):

Fluorescence Correlation Spectroscopy (FCS) is a type of spectroscopy based on the measurement of fluorescence insity and the analysis of it fluctuations, which can be due to the diffusion of the observed fluorophore in the excitation volume or to changes in the fluorescence quantum yield arising from chemical reactions. Measurements are usually made on only a few molecules at a time, of the order of 10 milliseconds, which is achieved by illuminating tiny volumes (around 1 femtoliter), available by employing two-photon excitation or confocal optics.

The classical setup of FCS is shown below (***Figure 88***). This system is quite similar to the LSCM technique presented before. In fact, the exciting radiation provided by a laser beam is directed onto a micorscope objective via adichroic mirror and focused on the sample. The fluorescent light form the sample is collected by the same objective and passed through the dichroic and the emission filter. The pinhole in the image plan blocks any fluorescence light not originateing from the focal region.
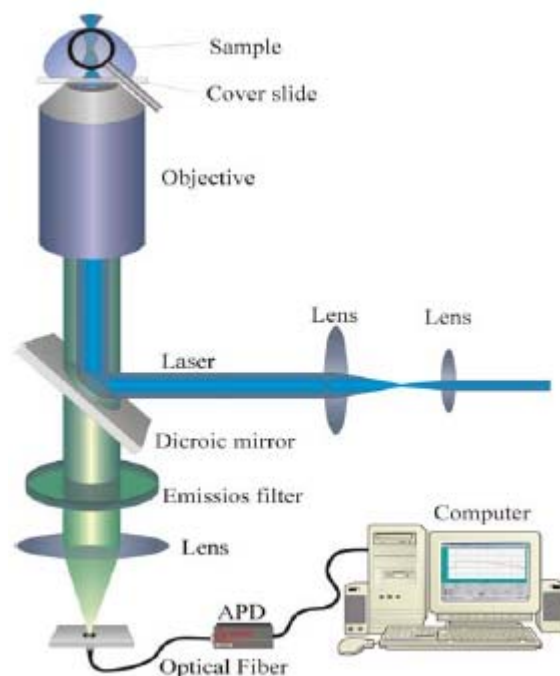
Figure 88: Schematical drawing of an FCS setup. *Taken from Schwille.*

The sample carrier depends on the applications. For test measurements, a simple cover slide on which a drop is placed will be sufficient. More elaborate measurements can be done in special sealed chambers or deep-well slides.

The FCS has various applications like:

- ✓ Concentration and aggregation measurements.
- ✓ Mobility and molecular interactions determination.
- ✓ Association/Dissociation and enzyme kinetics monitoring.

Fluorescence Correlation Spectroscopy in a versatile technique for both in vitro and in vivo applications. Based on light irradiation only, it is minimally invasive and thus extremely useful for investigating biological systems.

Real-Time Polymerase Chain Reaction (RT-PCR):

In molecular biology this technique is used to simultaneously quantify and amplify a specific part of a given DNA molecule. This technique is used to determine whether or not a specific sequence is present in the sample; and if it is present, the number of copies in the sample. The procedure follows the general patterns of the polymerase chain reaction, but the DNA is quantified after each round of amplification. Two common methods of quantification are the use of fluorescent dyes that intercalate with double-strand DNA, and modified DNA oligonucleotides probes that fluoresce when hybridized with a complementary DNA.

Real-time PCR have the advantage that it is not necessary to measure the concentrations of mRNA or DNA in a sample before exposing it to real-time polymerase chain reaction.

There are numerous potential applications for the technique of real-time PCR, like knowing how the genetic expression of a particular gene changes over time, or in response to changes in environmental conditions. It can be also used to detect the changes in gene expression of a tissue after pharmacological agent administration.

References

1. Moulay, S., *Polymer history in short.* Actualite Chimique, 1999(12): p. 31-43.
2. Seymour, R.B., *Polymers Are Everywhere.* Journal Of Chemical Education, 1988. **65**(4): p. 327-334.
3. http://www.steve.gb.com/science/molecules.html.
4. http://www.whatislife.com/glossary/p.htm.
5. http://www.nanoword.net/library/def/bldefsa.htm.
6. *http://academic.brooklyn.cuny.edu/biology/bio4fv/page/molecular.*
7. http://img.sparknotes.com/figures/A/a981208a1abd542364d5a13c08702881/lipid.gif.
8. http://physioweb.med.uvm.edu/diffusion/frap/membranes/images/phospholipida.gif.
9. Hirano, K., H. Fukuda, and S.L. Regen, *Polymerizable Ion-Paired Amphiphiles.* Langmuir, 1991. **7**(6): p. 1045-1047.
10. Antonietti, M. and S. Forster, *Vesicles and liposomes: A self-assembly principle beyond lipids.* Advanced Materials, 2003. **15**(16): p. 1323-1333.
11. Israelachvili, J.N., *Intermolecular and surface forces.* 1991.
12. Lasic, D.D., *Doxorubicin in sterically stabilized liposomes.* Nature, 1996. **380**(6574): p. 561-562.
13. Lasic, D.D., *Recent developments in medical applications of liposomes: sterically stabilized liposomes in cancer therapy and gene delivery in vivo.* Journal Of Controlled Release, 1997. **48**(2-3): p. 203-222.
14. Lasic, D.D., *Poly(ethylene oxide) coated liposomes: Theory and practice.* Abstracts Of Papers Of The American Chemical Society, 1997. **213**: p. 58-POLY.
15. Lasic, D.D., *Novel applications of liposomes.* Trends In Biotechnology, 1998. **16**(7): p. 307-321.
16. Hillmyer, M.A. and F.S. Bates, *Synthesis and characterization of model polyalkane-poly(ethylene oxide) block copolymers.* Macromolecules, 1996. **29**(22): p. 6994-7002.
17. Whitesides, G.M., J.P. Mathias, and C.T. Seto, *Molecular Self-Assembly And Nanochemistry - A Chemical Strategy For The Synthesis Of Nanostructures.* Science, 1991. **254**(5036): p. 1312-1319.
18. Soo, P.L. and A. Eisenberg, *Preparation of block copolymer vesicles in solution.* Journal Of Polymer Science Part B-Polymer Physics, 2004. **42**(6): p. 923-938.
19. Yu, G.E. and A. Eisenberg, *Multiple morphologies formed from an amphiphilic ABC triblock copolymer in solution.* Macromolecules, 1998. **31**(16): p. 5546-5549.
20. Kita-Tokarczyk, K., et al., *Block copolymer vesicles - using concepts from polymer chemistry to mimic biomembranes.* Polymer, 2005. **46**(11): p. 3540-3563.
21. Shenhar, R., N. T.B., and V.M. Rotello, *Self-assembly and self-organization*, in *Introduction to nanoscale science and technology*, M. Di Ventra, S. Evoy, and J.R.J. Heflin, Editors. 2004, Kluwer Academic Publishers. p. 41-74.
22. Nardin, C. and W.G. Meier, *Polymerizable amphiphilic block copolymers: From nanostructured hydrogels to nanoreactors and ultrathin films.* Chimia, 2001. **55**(3): p. 142-146.
23. Davis, S.S., *Biomedical applications of nanotechnology - Implications for drug targeting and gene therapy.* Trends In Biotechnology, 1997. **15**(6): p. 217-224.
24. Davis, S.S. and L. Illum, *Polymeric Microspheres As Drug Carriers.* Biomaterials, 1988. **9**(1): p. 111-115.
25. Josephson, L., et al., *High-efficiency intracellular magnetic labeling with novel superparamagnetic-tat peptide conjugates.* Bioconjugate Chemistry, 1999. **10**(2): p. 186-191.

26.	Smirnov, V.N., et al., *Carrier-Directed Targeting Of Liposomes And Erythrocytes To Denuded Areas Of Vessel Wall.* Proceedings Of The National Academy Of Sciences Of The United States Of America, 1986. **83**(17): p. 6603-6607.

27.	Torchilin, V., *Immobilization of specific proteins on liposome surface: systems for drug targeting*, in *Liposomes technology*, G. GRegoriadis, Editor. 1984, CRC Press. p. 75-94.

28.	Torchilin, V.P., *Drug targeting.* European Journal Of Pharmaceutical Sciences, 2000. **11**: p. S81-S91.

29.	Torchilin, V.P., et al., *Targeted Accumulation Of Polyethylene Glycol-Coated Immunoliposomes In Infarcted Rabbit Myocardium.* Faseb Journal, 1992. **6**(9): p. 2716-2719.

30.	Chazov, E.I., et al., *Endothelial Cell-Culture On Fibrillar Collagen - Model To Study Platelet-Adhesion And Liposome Targeting To Inter-Cellular Collagen Matrix.* Proceedings Of The National Academy Of Sciences Of The United States Of America-Biological Sciences, 1981. **78**(9): p. 5603-5607.

31.	Galaev, I.Y. and B. Mattiasson, *'Smart' polymers and what they could do in biotechnology and medicine.* Trends In Biotechnology, 1999. **17**(8): p. 335-340.

32.	Silvander, M., N. Bergstrand, and K. Edwards, *Linkage identity is a major factor in determining the effect of PEG-ylated surfactants on permeability of phosphatidylcholine liposomes.* Chemistry And Physics Of Lipids, 2003. **126**(1): p. 77-83.

33.	Vriezema, D.M., et al., *Vesicles and polymerized vesicles from thiophene-containing rod-coil block copolymers.* Angewandte Chemie-International Edition, 2003. **42**(7): p. 772-776.

34.	Torchilin, V.P., et al., *Polymerization Of Liposome-Encapsulated Hydrophilic Monomers.* Makromolekulare Chemie-Rapid Communications, 1987. **8**(9): p. 457-460.

35.	Torchilin, V.P., et al., *Poly(ethylene glycol)-coated anti-cardiac myosin immunoliposomes: Factors influencing targeted accumulation in the infarcted myocardium.* Biochimica Et Biophysica Acta-Biomembranes, 1996. **1279**(1): p. 75-83.

36.	Ringsdorf, H., B. Schlarb, and J. Venzmer, *Molecular Architecture And Function Of Polymeric Oriented Systems - Models For The Study Of Organization, Surface Recognition, And Dynamics Of Biomembranes.* Angewandte Chemie-International Edition In English, 1988. **27**(1): p. 113-158.

37.	Choi, H.J., H. Lee, and C.D. Montemagno, *Toward hybrid proteo-polymeric vesicles generating a photoinduced proton gradient for biofuel cells.* Nanotechnology, 2005. **16**(9): p. 1589-1597.

38.	Choi, H.J. and C.D. Montemagno, *Artificial organelle: ATP synthesis from cellular mimetic polymersomes.* Nano Letters, 2005. **5**(12): p. 2538-2542.

39.	Graff, A., et al., *Virus-assisted loading of polymer nanocontainer.* Proceedings Of The National Academy Of Sciences Of The United States Of America, 2002. **99**(8): p. 5064-5068.

40.	Nallani, M., et al., *A nanocompartment system (synthosome) designed for biotechnological applications.* Journal Of Biotechnology, 2006. **123**(1): p. 50-59.

41.	Ranquin, A., et al., *Therapeutic nanoreactors: Combining chemistry and biology in a novel triblock copolymer drug delivery system.* Nano Letters, 2005. **5**(11): p. 2220-2224.

42.	Stoenescu, R., A. Graff, and W. Meier, *Asymmetric ABC-triblock copolymer membranes induce a directed insertion of membrane proteins.* Macromolecular Bioscience, 2004. **4**(10): p. 930-935.

43. Haefele, T., K. Kita-Tokarczyk, and W. Meier, *Phase behavior of mixed Langmuir monolayers from amphiphilic block copolymers and an antimicrobial peptide.* Langmuir, 2006. **22**(3): p. 1164-1172.

44. Sauer, M., et al., *Ion-carrier controlled precipitation of calcium phosphate in giant ABA triblock copolymer vesicles.* Chemical Communications, 2001(23): p. 2452-2453.

45. Dumas, F., M.C. Lebrun, and J.F. Tocanne, *Is the protein/lipid hydrophobic matching principle relevant to membrane organization and functions?* Febs Letters, 1999. **458**(3): p. 271-277.

46. Geimer, J. and D. Beckert, *Study of radical pairs generated by photoreduction of anthraquinone-2,6-disulfonic acid with thymine by Fourier transform electron paramagnetic resonance.* Chemical Physics Letters, 1998. **288**(2-4): p. 449-458.

47. Sazanov, L.A., et al., *A role for native lipids in the stabilization and two-dimensional crystallization of the Escherichia coli NADH-ubiquinone oxidoreductase (complex I).* Journal of Biological Chemistry, 2003. **278**(21): p. 19483-19491.

48. Sinegina, L., et al., *Activation of isolated NADH: ubiquinone reductase I (complex I) from Escherichia coli by detergent and phospholipids. Recovery of ubiquinone reductase activity and changes in EPR signals of iron-sulfur clusters.* Biochemistry, 2005. **44**(23): p. 8500-8506.

49. Turro, N.J. and I.V. Khudyakov, *Time-Resolved Electron-Spin-Resonance And Laser Flash Spectroscopy Investigation Of The Photoreduction Of Anthraquinone-2,6-Disulfonic Acid, Disodium Salt By Sodium-Sulfite In Aerosol Ot Reverse Micelles.* Journal Of Physical Chemistry, 1995. **99**(19): p. 7654-7662.

50. Wunderbaldinger, P., L. Josephson, and R. Weissleder, *Tat peptide directs enhanced clearance and hepatic permeability of magnetic nanoparticles.* Bioconjugate Chemistry, 2002. **13**(2): p. 264-268.

51. Zhao, M., et al., *Differential conjugation of tat peptide to superparamagnetic nanoparticles and its effect on cellular uptake.* Bioconjugate Chemistry, 2002. **13**(4): p. 840-844.

52. Cao, Y.C., et al., *A two-color-change, nanoparticle-based method for DNA detection.* Talanta, 2005. **67**(3): p. 449-455.

53. Chen, Y., J. Aveyard, and R. Wilson, *Gold and silver nanoparticles functionalized with known numbers of oligonucleotides per particle for DNA detection.* Chemical Communications, 2004(24): p. 2804-2805.

54. Hinz, M., et al., *Polymer support for exonucleolytic sequencing.* Journal Of Biotechnology, 2001. **86**(3): p. 281-288.

55. Lytton-Jean, A.K.R. and C.A. Mirkin, *A thermodynamic investigation into the binding properties of DNA functionalized gold nanoparticle probes and molecular fluorophore probes.* Journal Of The American Chemical Society, 2005. **127**(37): p. 12754-12755.

56. Park, S.J., T.A. Taton, and C.A. Mirkin, *Array-based electrical detection of DNA with nanoparticle probes.* Science, 2002. **295**(5559): p. 1503-1506.

57. Membrane Structure, c., *Molecular biology of the cell.*

58. http://www.accessexcellence.org/RC/VL/GG/images/Fig_11.21.gif.

59. Daghastanli, K.R.P., et al., *Lipid composition-dependent incorporation of multiple membrane proteins into liposomes.* Colloids And Surfaces B-Biointerfaces, 2004. **36**(3-4): p. 127-137.

60. Parmar, M.M., K. Edwards, and T.D. Madden, *Incorporation of bacterial membrane proteins into liposomes: factors influencing protein reconstitution.* Biochimica Et Biophysica Acta-Biomembranes, 1999. **1421**(1): p. 77-90.

61. Eytan, G.D., M.J. Matheson, and E. Racker, *Incorporation Of Mitochondrial-Membrane Proteins Into Liposomes Containing Acidic Phospholipids.* Journal Of Biological Chemistry, 1976. **251**(21): p. 6831-6837.

62. Knol, J., K. Sjollema, and B. Poolman, *Detergent-mediated reconstitution of membrane proteins.* Biochemistry, 1998. **37**(46): p. 16410-16415.

63. Madden, T.D., *Protein Reconstitution - Methodologies And Applications.* International Journal Of Biochemistry, 1988. **20**(9): p. 889-895.

64. Rigaud, J.L., B. Pitard, and D. Levy, *Reconstitution Of Membrane-Proteins Into Liposomes - Application To Energy-Transducing Membrane-Proteins.* Biochimica Et Biophysica Acta-Bioenergetics, 1995. **1231**(3): p. 223-246.

65. Rigaud, J.L., et al., *Use of detergents in two-dimensional crystallization of membrane proteins.* Biochimica Et Biophysica Acta-Biomembranes, 2000. **1508**(1-2): p. 112-128.

66. Abeywardena, M.Y., T.M. Allen, and J.S. Charnock, *Lipid-Protein Interactions Of Reconstituted Membrane-Associated Adenosine-Triphosphatases - Use Of A Gel-Filtration Procedure To Examine Phospholipid-Activity Relationships.* Biochimica Et Biophysica Acta, 1983. **729**(1): p. 62-74.

67. Racker, E., et al., *Reconstitution, A Way Of Biochemical-Research - Some New Approaches To Membrane-Bound Enzymes.* Archives Of Biochemistry And Biophysics, 1979. **198**(2): p. 470-477.

68. Rigaud, J.L., et al., *Detergent removal by non-polar polystyrene beads - Applications to membrane protein reconstitution and two-dimensional crystallization.* European Biophysics Journal With Biophysics Letters, 1998. **27**(4): p. 305-319.

69. Nardin, C., et al., *Nanoreactors based on (polymerized) ABA-triblock copolymer vesicles.* Chemical Communications, 2000(15): p. 1433-1434.

70. Nardin, C., et al., *Polymerized ABA triblock copolymer vesicles.* Langmuir, 2000. **16**(3): p. 1035-1041.

71. Vijayan, K., et al., *Interactions of membrane-active peptides with thick, neutral, nonzwitterionic bilayers.* Journal Of Physical Chemistry B, 2005. **109**(30): p. 14356-14364.

72. Nardin, C., et al., *Amphiphilic block copolymer nanocontainers as bioreactors.* European Physical Journal E, 2001. **4**(4): p. 403-410.

73. Ho, D., et al., *Fabrication of biomolecule-copolymer hybrid nanovesicles as energy conversion systems.* Nanotechnology, 2005. **16**(12): p. 3120-3132.

74. Choi, H.J. and C.D. Montemagno, *Biosynthesis within a bubble architecture.* Nanotechnology, 2006. **17**(9): p. 2198-2202.

75. Xi, J.Z., et al., *Lessons learned from engineering biologically active hybrid nano/micro devices.* Advanced Functional Materials, 2005. **15**(8): p. 1233-1240.

76. Leif, H., et al., *Isolation And Characterization Of The Proton-Translocating Nadh-Ubiquinone Oxidoreductase From Escherichia-Coli.* European Journal Of Biochemistry, 1995. **230**(2): p. 538-548.

77. Krebs, W., et al., *Na+ translocation by the NADH: ubiquinone oxidoreductase (complex I) from Klebsiella pneumoniae.* Molecular Microbiology, 1999. **33**(3): p. 590-598.

78. Anraku, Y. and R.B. Gennis, *The Aerobic Respiratory-Chain Of Escherichia-Coli.* Trends In Biochemical Sciences, 1987. **12**(7): p. 262-266.

79. myweb.uiowa.edu.

80. Sharpley, M.S., et al., *Interactions between phospholipids and NADH: ubiquinone oxidoreductase (complex I) from bovine mitochondria.* Biochemistry, 2006. **45**(1): p. 241-248.

81.   Friedrich, T. and B. Bottcher, *The gross structure of the respiratory complex I: A Lego-System (vol 1608, pg 1, 2004).* Biochimica Et Biophysica Acta-Bioenergetics, 2004. **1657**(1): p. 71-71.

82.   http://www.biologie.uni-hamburg.de/b-online/library/crofts/bioph354/images/nad2.gif.

83.   http://www.ceri.com/mito.gif.

84.   Stolpe, S. and T. Friedrich, *The Escherichia coli NADH: ubiquinone oxidoreductase (complex I) is a primary proton pump but may be capable of secondary sodium antiport.* Journal Of Biological Chemistry, 2004. **279**(18): p. 18377-18383.

85.   Lee, A.G., *How lipids interact with an intrinsic membrane protein: the case of the calcium pump.* Biochimica et Biophysica acta, 1998. **1376**: p. 381-390.

86.   Lee, A.G., *How lipids affect the activities of integral membrane proteins.* Biochimica et Biophysica acta, 2004. **1666**: p. 62-87.

87.   Keusgen, M., *Biosensors: new approaches in drug discovery.* Naturwissenschaften, 2002. **89**(10): p. 433-444.

88.   http://biomed.brown.edu/Courses/BI108/BI108_2003_Groups/Diabetes_Technology/glucosereaction.JPG.

89.   http://www.esi-group.com/SimulationSoftware/CFD_ACE/images/sensor1_lg.jpg.

90.   *www.canon.com/technology/future/07.html*.

91.   http://chem.ch.huji.ac.il/~eugeniik/sandiego04s.jpg.

92.   Wang, J., *From DNA biosensors to gene chips.* Nucleic Acids Research, 2000. **28**(16): p. 3011-3016.

93.   http://en.wikipedia.org/wiki/DNA_microarray.

94.   Brown, P.O. and D. Botstein, *Exploring the new world of the genome with DNA microarrays.* Nature Genetics, 1999. **21**: p. 33-37.

95.   http://www.pharmadd.com/archives/Sep.

96.   Vercoutere, W. and M. Akeson, *Biosensors for DNA sequence detection.* Current Opinion In Chemical Biology, 2002. **6**(6): p. 816-822.

97.   Katz, E. and I. Willner, *Probing biomolecular interactions at conductive and semiconductive surfaces by impedance spectroscopy: Routes to impedimetric immunosensors, DNA-Sensors, and enzyme biosensors.* Electroanalysis, 2003. **15**(11): p. 913-947.

98.   Wang, J., *Nanomaterial-based amplified transduction of biomolecular interactions.* Small, 2005. **1**(11): p. 1036-1043.

99.   Drummond, T.G., M.G. Hill, and J.K. Barton, *Electrochemical DNA sensors.* Nature Biotechnology, 2003. **21**(10): p. 1192-1199.

100.   Murphy, L., *Biosensors and bioelectrochemistry.* Current Opinion In Chemical Biology, 2006. **10**(2): p. 177-184.

101.   www.chim.unifi.it/ana/dnael.htm.

102.   McGlennen, R.C., *Miniaturization technologies for molecular diagnostics.* Clinical Chemistry, 2001. **47**(3): p. 393-402.

103.   Steel, A.B., T.M. Herne, and M.J. Tarlov, *Electrochemical quantitation of DNA immobilized on gold.* Analytical Chemistry, 1998. **70**(22): p. 4670-4677.

104.   Mirkin, C.A., et al., *DNA-induced assembly of gold nanoparticles: A method for rationally organizing colloidal particles into ordered macroscopic materials.* Abstracts Of Papers Of The American Chemical Society, 1996. **212**: p. 249-INOR.

105.   Qin, W.J. and L.Y.L. Yung, *Nanoparticle-DNA conjugates bearing a specific number of short DNA strands by enzymatic manipulation of nanoparticle-bound DNA.* Langmuir, 2005. **21**(24): p. 11330-11334.

106. Sato, K., K. Hosokawa, and M. Maeda, *Rapid aggregation of gold nanoparticles induced by non-cross-linking DNA hybridization.* Journal Of The American Chemical Society, 2003. **125**(27): p. 8102-8103.

107. Thaxton, C.S., D.G. Georganopoulou, and C.A. Mirkin, *Gold nanoparticle probes for the detection of nucleic acid targets.* Clinica Chimica Acta, 2006. **363**(1-2): p. 120-126.

108. Li, C.Z., Y.L. Liu, and J.H.T. Luong, *Impedance sensing of DNA binding drugs using gold substrates modified with gold nanoparticles.* Analytical Chemistry, 2005. **77**(2): p. 478-485.

109. Gibbs, J.M., et al., *Polymer-DNA hybrids as electrochemical probes for the detection of DNA.* Journal Of The American Chemical Society, 2005. **127**(4): p. 1170-1178.

110. Li, C.Z., et al., *Protein-DNA interaction: impedance study of MutS binding to a DNA mismatch.* Chemical Communications, 2004(5): p. 574-575.

111. LizMarzan, L.M., M. Giersig, and P. Mulvaney, *Synthesis of nanosized gold-silica core-shell particles.* Langmuir, 1996. **12**(18): p. 4329-4335.

112. Strother, T., et al., *Synthesis and characterization of DNA-modified silicon (111) surfaces.* Journal Of The American Chemical Society, 2000. **122**(6): p. 1205-1209.

113. Strother, T., R.J. Hamers, and L.M. Smith, *Covalent attachment of oligodeoxyribonucleotides to amine-modified Si (001) surfaces.* Nucleic Acids Research, 2000. **28**(18): p. 3535-3541.

114. http://probes.invitrogen.com/media/publications/600.pdf.

115. Dubertret, B., *Quantum dots - DNA detectives.* Nature Materials, 2005. **4**(11): p. 797-798.

116. Gerion, D., et al., *Synthesis and properties of biocompatible water-soluble silica-coated CdSe/ZnS semiconductor quantum dots.* Journal Of Physical Chemistry B, 2001. **105**(37): p. 8861-8871.

117. Lacoste, T.D., et al., *Super resolution molecular ruler using single quantum dots.* Biophysical Journal, 2000. **78**(1): p. 402A-402A.

118. Michalet, X., et al., *Quantum dots for live cells, in vivo imaging, and diagnostics.* Science, 2005. **307**(5709): p. 538-544.

119. http://www.nrl.navy.mil/Review02/images/materialFig9.gif.

120. Bruchez, M., et al., *Semiconductor nanocrystals as fluorescent biological labels.* Science, 1998. **281**(5385): p. 2013-2016.

121. Chan, W.C.W. and S.M. Nie, *Quantum dot bioconjugates for ultrasensitive nonisotopic detection.* Science, 1998. **281**(5385): p. 2016-2018.

122. Mitchell, G.P., C.A. Mirkin, and R.L. Letsinger, *Programmed assembly of DNA functionalized quantum dots.* Journal Of The American Chemical Society, 1999. **121**(35): p. 8122-8123.

123. Gerion, D., et al., *Sorting fluorescent nanocrystals with DNA.* Journal Of The American Chemical Society, 2002. **124**(24): p. 7070-7074.

124. Parak, W.J., et al., *Conjugation of DNA to silanized colloidal semiconductor nanocrystalline quantum dots.* Chemistry Of Materials, 2002. **14**(5): p. 2113-2119.

125. Stsiapura, V., et al., *Functionalized nanocrystal-tagged fluorescent polymer beads: synthesis, physicochemical characterization, and immunolabeling application.* Analytical Biochemistry, 2004. **334**(2): p. 257-265.

126. Han, M.Y., et al., *Quantum-dot-tagged microbeads for multiplexed optical coding of biomolecules.* Nature Biotechnology, 2001. **19**(7): p. 631-635.

127. Taylor, J.R., M.M. Fang, and S. Nie, *Probing specific sequences on single DNA molecules with bioconjugated fluorescent nanoparticles.* Analitycal chemistry, 2000. **72**: p. 1979.

128. Caruso, F., *Avdance materials*, 2001(13): p. 11.
129. Zhang, S., et al., *Fabrication of core-shell latex spheres with CdS/polyelectrolyte composite monolayers.* Colloids and surfaces A, 2005.
130. Tan, W., et al., *bionanotehcnology based on silica nanoparticles.* medicinal research reviews, 2004. **24**(5): p. 621.
131. Hilliard, L.R., X.J. Zhao, and W.H. Tan, *Immobilization of oligonucleotides onto silica nanoparticles for DNA hybridization studies.* Analytica Chimica Acta, 2002. **470**(1): p. 51-56.
132. Kremsky, J.N., et al., *Immobilization Of Dna Via Oligonucleotides Containing An Aldehyde Or Carboxylic-Acid Group At The 5' Terminus.* Nucleic Acids Research, 1987. **15**(7): p. 2891-2909.
133. Wolf, S.F., et al., *Rapid Hybridization Kinetics Of Dna Attached To Submicron Latex-Particles.* Nucleic Acids Research, 1987. **15**(7): p. 2911-2926.
134. Oba, S., et al., *Development of polymer latex particles for selective cleavage of mismatched DNA and their application for DNA diagnosis.* Bioconjugate Chemistry, 2005. **16**(3): p. 551-558.
135. Bernkop-Schnurch, A. and S. Steininger, *Synthesis and characterisation of mucoadhesive thiolated polymers.* International Journal Of Pharmaceutics, 2000. **194**(2): p. 239-247.
136. *bioconjugate techniques.* Vol. 17. 1996.
137. Sambrook and Russell, *Molecular cloning: a laboratory manual.* Vol. 2. 2001.
138. Bernkop-Schnurch, A., V. Schwarz, and S. Steininger, *Polymers with thiol groups: A new generation of mucoadhesive polymers?* Pharmaceutical Research, 1999. **16**(6): p. 876-881.
139. Yun, Y., H.Q. Li, and E. Ruckenstein, *Hydrophobic core/hydrophilic shell amphiphilic particles.* Journal Of Colloid And Interface Science, 2001. **238**(2): p. 414-419.
140. Jungmann, N., et al., *Synthesis of amphiphilic poly(organosiloxane) nanospheres with different core-shell architectures.* Macromolecules, 2002. **35**(18): p. 6851-6857.
141. Kong, X.Z. and E. Ruckenstein, *Core-shell latex particles consisting of polysiloxane-poly(styrene-methyl methacrylate-acrylic acid): Preparation and pore generation.* Journal Of Applied Polymer Science, 1999. **73**(11): p. 2235-2245.
142. Lee, S. and A. Rudin, *Control Of Core Shell Latex Morphology.* Acs Symposium Series, 1992. **492**: p. 234-254.
143. Schepinov, M.S., et al., *Selectively Cleavable Synthetic Oligodeoxyribonucleotides For The Reversible Immobilization Of Dna.* Bioorganicheskaya Khimiya, 1994. **20**(8-9): p. 955-966.
144. Foldes-Papp, Z., et al., *A new ultrasensitive way to circumvent PCR-based allele distinction: Direct probing of unamplified genomic DNA by solution-phase hybridization using two-color fluorescence cross-correlation spectroscopy.* Experimental And Molecular Pathology, 2005. **78**(3): p. 177-189.
145. Kinjo, M. and R. Rigler, *Ultrasensitive Hybridization Analysis Using Fluorescence Correlation Spectroscopy.* Nucleic Acids Research, 1995. **23**(10): p. 1795-1799.
146. Rigler, R., *Fluorescence Correlations, Single-Molecule Detection And Large Number Screening - Applications In Biotechnology.* Journal Of Biotechnology, 1995. **41**(2-3): p. 177-186.
147. Kim, J., et al., *The initial step of DNA hairpin folding: a kinetic analysis using fluorescence correlation spectroscopy.* Nucleic Acids Research, 2006. **34**(9): p. 2516-2527.

148. Friedrich, T., *The NADH: ubiquinone oxidoreductase (complex I) from Escherichia coli.* Biochimica Et Biophysica Acta-Bioenergetics, 1998. **1364**(2): p. 134-146.

149. Spehr, V., et al., *Overexpression of the Escherichia coli nuo-operon and isolation of the overproduced NADH: ubiquinone oxidoreductase (Complex I).* Biochemistry, 1999. **38**(49): p. 16261-16267.

150. Linke, P., et al., *Dimeric Ubiquinol - Cytochrome-C Reductase Of Neurospora Mitochondria Contains One Cooperative Ubiquinone-Reduction Center.* European Journal Of Biochemistry, 1986. **158**(3): p. 615-621.

151. http://en.wikipedia.org/wiki/Confocal_laser_scanning_microscopy.